INELASTIC BEHAVIOUR OF STEEL BEAM-COLUMNS

BY

MORISCO, Ir.

A thesis submitted in partial fulfilment of the requirement for the award of Degree of Doctor of Philosophy in Civil Engineering (Structures)

DEPARTMENT OF CIVIL ENGINEERING

THE CITY UNIVERSITY

LONDON

October, 1986

TO MY FAMILY

C O N T E N T S

LIST OF FIGURES

LIST OF TABLES

ACKNOWLEDGEMENT

The work reported in this thesis was carried out under the supervision and constant guidance of Dr. K.S. Virdi, to whom the author is deeply grateful for his encouragement and valuable advice throughout the duration of the work.

Thanks are due to the staff members of the Civil Engineering Structures Laboratory for their help in carrying out the tests.

The author would like to take this opportunity of expressing his deep sense of gratitude to the Government of Indonesia, for sponsoring the author's research at this University, through [redacted]

Thanks are also due to the City University Computer Unit, for generously making available all the facilities.

ABSTRACT

This thesis describes the development of an inelastic stability analysis for restrained pin-ended steel beam-columns having an axial load, biaxial end moments and lateral loads in X and Y directions along the length. The lateral loads may be a combination of several distributed and concentrated loads. The beam-column cross-sections are uniform along the length, and may be doubly or singly symmetric. Ultimate loads can be obtained by increasing some or all components of the loads. The analysis can be made with or without considering residual stresses and torsion effects. The analysis essentially consists of obtaining equilibrium shape corresponding to increasing values of the principal variables up to the peak of the applied load versus deflection curves. The Newton-Raphson method is employed for the iteration in the analysis. Solutions of the integration of stress resultants are obtained with the Gaussian quadrature formulae.

Experiments of eight full-scale steel beam-columns loaded uniaxially and biaxially are reported and used to check the validity of the analytical method. The slenderness ratios of the beam-columns tested were 78 and 117. These values were chosen to cover the intermediate and the slender beam-columns. The discrepancy between the observed and calculated strength remains an average of 93% with a standard deviation of 8%.

The theoretical model was applied to generate interaction curves for pin-ended steel beam-columns with concentrated and linearly distributed loads. The results were compared with BS 5400:Part3. Further, the theory was also used to study the effects of residual stresses and torsion on the calculated collapse loads. It was found that residual stresses could reduce the beam-column strength by up to 15%, whereas reduction as much as 35% was found due to the torsional effects on beam-columns with slenderness ratio 60.

NOTATION

The following notations have been used in the text. Any deviation or addition has been defined locally.

A = area of cross-section

a = distance of an elemental area from the centre of twist

a_c = distance of the centre of the compression flange to the centre of twist

a_t = distance of the centre of the tension flange to the centre of twist

b = flange width

C_{fc} = stiffness of the compression flange

C_{ft} = stiffness of the tension flange

D = distance between centre line of flanges

d = depth of section

d_i = distance of any point (ξ_i, η_i) to the neutral axis

d_n = distance of the centroid to the neutral axis

E = elastic modulus

G = elastic shear modulus

H = weighting coefficient of the Gaussian quadrature

I = moment of inertia

I_p = polar moment of inertia

I_w = warping rigidity

I_x = moment of inertia about X axis

I_y = moment of inertia about Y axis

I_{yc} = moment of inertia of the compression flange about Y axis

I_{yt} = moment of inertia of the tension flange about Y axis

I_{ξ} = moment of inertia about ξ axis

I_{η} = moment of inertia about η axis

$\bar{K}$ = Wagner effect = $\int a^2 dA$

K_{xl} = stifness of major axis restraining beam at L

K_{xo} = stiffness of major axis restraining beam at O

K_{yl} = stiffness of minor axis restraining beam at L

K_{yo} = stiffness of minor axis restraining beam at O

K_T = St. Venant torsion constant

L,l = length of beam-column

M = moment

M_D = moment resistance

M_{Dxc} = major axis moment resistance of the member, with respect to the extreme fibre

M_{Dyc} = minor axis moment resistance of the member, with respect to the extreme fibre

M_{fc} = minor axis moment of the compression flange

M_{ft} = minor axis moment of the tension flange

M_p = plastic moment

M_r = ultimate moment with residual stresses considered

M_{rxl} = major axis restraining moment at L

M_{rxo} = major axis restraining moment at O

M_{ryl} = minor axis restraining moment at L

M_{ryo} = minor axis restraining moment at O

M_{tn} = ultimate moment with torsion effect neglected

M_{txl} = total major axis moment at L

M_{txo} = total major axis moment at O

M_{tyl} = total minor axis moment at L

M_{tyo} = total minor axis moment at O

M_u = ultimate moment

M_x = major axis moment

M_{xl} = major axis moment at L

M_{xo} = major axis moment at O

M_y = minor axis moment

M_y = yield moment

M_{yl} = minor axis moment at L

M_{yo} = minor axis moment at O

M_z = torsional moment

M_ξ = moment about ξ axis

$M_{\xi ex}$ = external moment about ξ axis

$M_{\xi in}$ = internal moment about ξ axis

M_η = moment about η axis

$M_{\eta ex}$ = external moment about η axis

$M_{\eta in}$ = internal moment about η axis

M_ζ = moment about ζ axis

$M_{\zeta ex}$ = external moment about ζ axis

$M_{\zeta in}$ = internal moment about ζ axis

N = axial force, normal force

np = number of point loads

nl = number of point loads in the left side of the section

P = axial force

P_D = axial force resistance

P_x = point load at the X direction

P_y = point load at the Y direction

P_y = yield axial force

R_{xo} = minor axis reaction force at O

R_{yo} = major axis reaction force at O

r = radius of gyration

S = elastic section modulus

S_y = yield stress

s = length of typical element

t_f = flange thickness

t_w = web thickness

u = minor axis displacement

u_c = minor axis displacement of the centroid

u_{ct} = minor axis displacement of the compression flange caused by the twist

u_{fc} = minor axis displacement of the compression flange

u_{ft} = minor axis displacement of the tension flange

u_{tt} = minor axis displacement of the tension flange caused by the twist

V_{fc} = shear of the compression flange

V_{ft} = shear of the tension flange

v = major axis displacement

v_c = major axis displacement of the centroid

w = displacement component

X_ξ = stiffness of the section about ξ axis

x_o = X coordinate of shear centre

Y_η = stiffness of the section about η axis

y_o = Y coordinate of shear centre

Z = elastic section modulus

Z = error magnitude

Z_p = plastic section modulus

z_i = distance of station 'i' from end O

z_{pi} = distance of point load 'i' from end O

α = inclination of neutral axis with respect to the ξ axis

β = end moment ratio

ϵ = strain

ϵ_i = strain of elemental area 'i'

ϵ_o = strain of the centroid

ϵ_{wi} = warping straint of an elemental area 'i'

θ = angle of twist

σ = stress

σ_{rc} = compressive residual stress

σ_{rt} = tension residual stress

φ_{xl} = rotation about X axis at L

φ_{xo} = rotation about X axis at O

φ_{yl} = rotation about Y axis at L

φ_{yo} = rotation about Y axis at O

ω_i = distance of elemental area a_i from the centroid

ϕ = curvature

ϕ_{fc} = curvature about η axis of the compression flange

ϕ_{ft} = curvature about η axis of the tension flange

ϕ_w = flange curvature about η axis caused by warping

ϕ_t = total curvature

ϕ_ξ = curvature about ξ axis

ϕ_η = curvature about η axis

$< a >$ = a if $a>0$, and 0 if $a<0$

1. INTRODUCTION

1.1. GENERAL

Whether the structure be man-made or created by nature, the column is a key element in resisting collapse under gravity loading, in buildings, bridges, plants and trees. When the axial compression load is combined with bending, then the members can be specified as beam-columns. The bending may result from lateral loading, applied end moments, or eccentric application of axial load. Since compression members in actual structures such as trusses and frames have unavoidable bending moments along the members due to the eccentricity of axial force, initial deflection or restraint from adjacent members, no column with purely axial load actually exists. Thus, all compression members could be treated and designed as beam-columns.

1.2. OUTLINE OF PREVIOUS WORK ON BEAM-COLUMNS

A review of literature on axially loaded column is available in several textbooks, and is not repeated here. The present review relates primarily to beam-columns.

Von Karman [1] was the first to recognize the fact that the deflected axis of any column could be represented by a portion of the deflection curve of an axially loaded column. Based on this concept he gave a general and exact

theory for the determination of the in-plane buckling loads of rectangular steel columns with small and equal eccentricities of loading at each end.

Westergaard and Osgood [2], in 1928, simplified Von Karman's solution of eccentrically loaded compression members by assuming the deflected centreline of the column to be a sinusoidal curve. Based on this simplification and an actual stress-strain relationship, they discussed analytically the behaviour of eccentrically loaded columns and initially curved columns. It was found from their computations that this simplification on the deflected shape of a column resulted only in a slight deviation from the more accurate solution and the simplified approach gave values which lie on the safe side. However, the analytical expressions obtained by Westergaard and Osgood are still so complex that numerical results can be evaluated only through a graphical procedure.

Realizing that the complexity of Westergaard and Osgood's [2] solution was caused by the nonlinearity of the actual stress-strain relationship, Jezek [3] proposed his theory by idealizing the material as elastic-perfectly plastic. Further, Jezek established the equilibrium only at midheight of the beam-column. The solution based upon these assumptions leads to analytical expressions for the ultimate load-carying capacity of eccentrically loaded in-plane beam-

columns or rectangular cross-sections. It was found by Jezek that, in general, the values of the maximum strength computed from his approximate equations were higher than the values determined from the exact solution using the real stress-strain curve. But, for all practical purposes, Jezek's approximate equations give satisfactory results.

All the work discussed above was done without considering torsion. Wagner [4] was the first to investigate torsional buckling of open thin walled sections. But Wagner based his theory upon the arbitrary assumption that the centre of rotation during buckling coincides with the centre of shear, which, in general, was not found in practice. The results of Wagner's analysis are therefore not exact.

Goodier [5,6,7] extended the governing differential equations to include beam-column under biaxial bending with identical loading conditions at each end. Goodier's equations were simplified by the assumption that the twisting and displacements of any cross section of the beam-column were small compared to the eccentricities of the loading. Discussions of the theory were given by Bleich [8], and Timoshenko and Gere [9].

Neal [10], following Goodier's work, in 1950 studied the phenomenon of lateral buckling in deep mild steel beams of rectangular cross-section. The study was carried out from both a theoretical and an experimental point of view. Neal obtained numerical solutions for a beam simply supported at the ends, carrying a central load passing through the centroid of the cross-section, and a cantilever carrying a single concentrated load. The solutions were obtained by using finite difference approximations for the first and second derivatives of the angle of twist. Later, Wittrick [11] extended the method to include strain hardening.

Goodier's simplified equations have been solved exactly by Culver [12,13] and approximately by Thurlimann [14], Dabrowski [15] and Prawel and Lee [16]. The numerical results of Thurlimann and Dabrowski are all within 1% of the exact values given by Culver. The result of Prawel and Lee, however, differ significantly, in certain cases, from the exact values. Errors as large as 25% for the deflections and 7% for the total stress have been obtained. Dabrowski considered the problem of biaxial bending from an energy standpoint and utilized the Rayleigh-Ritz method to obtain a solution. Thurlimann, on the other hand, dealt directly with the equations of biaxial bending and obtained a solution using results from the problem of in-plane bending. Considering the close agreement between the result of the

approximate solutions of Thurlimann and Dabrowski and the exact solution, for the pupose of design calculations, the approximate solutions seem to be more advantageous than the exact solution. The approximate solutions may be performed on a desk calculator whereas the exact solution requires a digital computer to obtain numerical results in a reasonable amount of time. However, until the accuracy of the approximate solutions is established for a wide range of problems, use of the exact solution seems warranted.

Chwalla was the first to work on the restrained elastic-plastic column. The work has been reported by Bleich [8]. Chwalla presented a procedure to calculate equilibrium configurations for columns under eccentric axial loads. The method was applied to a three-bay column, the centre bay acted on by external moments applied at the ends of this bay. Numerical results were given for special cases and could be adopted as a check on any future simplified method for investigation of the same or related problem.

More research was undertaken by Bijlaard, Fishermann and Winter [17]. They developed a solution to the problem of elastically restrained columns by limiting the study to members that did not fail by local or lateral-torsional instability. Experimental work was carried out on eighteen columns, half on square bars and the others on I-sections. To investigate the influence of residual

stresses, half of the specimens were annealed. The columns were tested with fixed degrees of elastic restraint and with various eccentricities. Ultimate loads were determined as well as loads which caused first local yielding. Two computational methods for restrained column of any cross-sectional shape, bent in symmetrical single curvature were presented. The first one was an exact method and the other was based on certain assumptions. Agreement between experiment and theory was satisfactory. Later the extension of the methods to deal with unsymmetrical bending was developed by Bijlaard [18]. Cases with unequal end eccentricities and unequal end restraints could be solved with the methods.

Further and rather more extensive work was carried out in the University of Cambridge by Baker and his associates [19] who worked for the Steel Structures Research Committee to investigate the plastic behaviour of structures for the design method development. In the experiment, symmetrical single and double curvature cases were investigated. The influence of various end conditions were examined. Firstly the plastic theory applied to columns of rectangular cross-section was discussed. Even a rectangular section had little direct practical use, the discussion was really important to serve as an introduction to the more difficult problems involving I sections. Agreement between the experimental and theoretical results was very good, the

average error on the collapse loads was less than 5%. A great difference between observed and theoretical results occured in a case where a column had been bent in double curvature. The collapse load obtained when the effects of unloading were ignored was 12.3% too low. When the effects of unloading were included, the collapse load was 7.9% too high. The most likely explanation of the excessive value obtained when unloading was allowed for was the presence of imperfections, which would lead to asymmetric form of failure in the actual column. Further, some approximate methods of calculating collapse loads were also given.

Horne [20] was the first to derive for the curvature of an initially straight prismatic member of rectangular cross-section subjected to any combination of axial load and bending moment about a principal axis. The material was assumed to show elastic-perfectly plastic behaviour, with a finite drop of stress at yield. Using these results, expressions for the shape of elastic-plastic compression members at all stages of plasticty were derived. It was shown how solutions for the collapse loads of eccentrically loaded struts and of members with ends restrained in certain directions could be obtained without resorting to numerical procedures.

Horne [21,22] has also provided some design data. In 1964, theoretical solutions based on modification to an elastic analysis for beam-columns subjected to any ends moment ratio with both ends free to warp and simply supported about the strong and weak axis was published. The stability criteria were that plastic hinges may form at either end of the beam-column length. Governing equations for bending and torsion involving minor axis imperfections were reduced to a set of six non-linear equations. These were solved iteratively to give the maximum safe axial load in terms of major and minor axis slenderness ratios, the torsional parameter and the end moment ratio for which the above mentioned stability criteria were satisfied. The theory was based on equivalent moment approach which assumed that the behaviour of a beam-column under an axial load and two different end moment ratios about the strong axis was the same as a beam-column subjected to the same axial load and a uniform strong axis moment M_x where M_x was a function of the end moment ratio. The presence of residual stresses was not considered. Extensive sets of design charts were produced based on this approach.

In 1959 Galambos [23] provided solutions for the inelastic lateral torsional buckling of wide flange beam-columns under uniaxial uniform bending. Lateral torsional buckling of H-columns is complicated by the occurence of twisting and warping of the column cross-section.

Analytical solutions for inelastic lateral torsional buckling of columns are also difficult to obtain owing to the non-linearity of the governing differential equations. In Galambos's work the effect of residual stresses was considered. In the inelastic range, due to primary deflections in the presence of axial load, the bending and torsional stiffnesses of a beam-column vary along the length. To simplify the solution, the stiffness of the beam-column was assumed to be uniform along the length and equal to the magnitude at the beam-column end. An upper bound solution was thus achieved. It would have been possible to obtain a lower bound solution by evaluating the moment along the length of the column. However to evaluate these, recourse would have had to be taken to some form of numerical technique to establish the equilibrium shape of the beam column under a given loading. This equilibrium shape of the beam-column in the inelastic range may be determined by a number of iterative methods. In the United State the Column Deflection Curve [24] has been used to find equilibrium shapes in the plane of bending as would have been necessary in this case.

A further extension along the same lines was made by Ojalvo [24] who described how convenient nomographs could be developed for the design of columns with one end hinged and also for columns with equal applied end moments and equal rotational restraints. The type of column failure

considered was that of bending about one principal axis of the cross section. The plane of bending was also the plane of thrust, applied moments, and the restraining moments. Graphical methods of performing calculations with non-linear rotational restraints and unequal end eccentricities were also given.

More accurate solutions for inelastic lateral torsional buckling of beam-columns under major axis bending were then developed by Galambos and Fukumoto [25]. In this work they reported the solution for the one end moment case. The solution of the problem which consisted of two separate steps was one of trial and error. The first step consisted of calculating the coefficients appearing in the finite difference equations of lateral-torsional buckling for the yielded beam-column at evenly spaced points along the length of the member. The operations that were involved consisted of the solution of involved analytical expressions. The results of the first computational step were used to set up the simultaneous equations that furnished the buckling determinant. This determinant was solved in the second step by a larger and faster computer. Further, they [25] showed graphically the fact that lateral-torsional buckling could reduce the strengths of beam-column considerably. It was also shown that the loading case with one end moment only was less severe than the case with two equal end moments.

Another paper was presented by Johnston [26] in 1971. He analyzed the inelastic behaviour of concentrically loaded rectangular column with the aid of a digital computer. In the procedure adopted, small increments of strain caused by axial shortening and bending curvature were successively superimposed after bending began at tangent modulus load. The superimposition of each incremental strain distribution resulted from a corresponding deflection of the column. The incremental stress distribution should be such that equilibrium exists between the internal and the external bending moments and thrust.

Birnstiel and Michalos [27], following the related work of Johnston [26], presented a general procedure for determining the ultimate carrying capacity of columns loaded eccentrically with respect to their principal axes. The method was restricted to columns of wide flange sections made of elastic-perfectly plastic material without residual thermal strains. Warping strains due to nonuniform twist were considered. However, their procedure requires successive trials and corrections and needs considerable computational effort for a solution.

A few years later, Harstead, Birnstiel and Leu [28] improved the procedure mentioned above by introducing a systematic correction procedure. Since then, the laborious trial and correction could be reduced to a few cycles by

solving a system of linear equation for the corrections at each station along the columns. Birnstiel and his associates [29] also conducted experiments on isolated H-columns subjected to biaxial loading. The result of these tests and the effects of warping restraint at column ends on the ultimate load-carrying capacity of the column, and the effect of residual thermal strains on the behaviour of the column were examined and compared. The agreement between the numerical and experimental results appeared to be satisfactory. Harstead, Birnstiel and Leu [28] stated that Goodier's equations are not applicable at large loads to elastic problems such as those selected by Culver [12,13]. This is due to the fact that, as the value of rotation of the beam-column cross-section become large, the error in Goodier's approximation becomes considerable.

It has not been possible to obtain analytical solutions to the differential equations of bending of elasto-plastic compression members composed of the common structural sections. In part, this difficulty is caused by the inability to express curvature explicitly in terms of moment and thrust. Hauck and Lee [30] solved the problem by evaluating a series of elliptic integrals, i.e. the integration of the nonlinear differential equation was performed analytically. The process of analytical integration has been extended for H-section members bent about their major axes. This has been solved by idealizing

the member cross-section as being composed of a series of thin-walled elements.

As an extension to the case of elastically restrained beam-columns, Milner [31] appears to be the first to report the theoretical and experimental study of restrained and biaxially loaded H-section beam-columns. A computational procedure was developed to enable a theoretical study of restrained elastic-plastic columns. The governing differential equations of equilibrium were first expressed in terms of finite differences and a numerical integration procedure was adopted for the solution. His main purpose was to determine the significant parameters affecting the behaviour of the elastically restrained H-section beam-columns subjected to biaxial loading. Milner's results indicated that the effect of unloading after yielding occured in biaxially loaded beam-columns, was to raise the collapse load by a small increment. The effect of the order of load application upon the failure load was observed to be significant. Also, the effects of residual stresses were less when the loading was eccentric and decreased as the eccentricity increased so that this effect could be small for restrained beam-columns.

More development and solutions of elastically restrained beam-columns under biaxial bending and torsion using finite difference methods for numerical solutions were

reported by Vinnakota and his associates [32,33,34] in 1975. The method could be employed to solve the problem on columns loaded by equal or unequal end moments with symmetrical or unsymmetrical rotational restraints at ends. The influences of material yielding, residual strain as well as warping strains that resulted from the twisting of the cross-section of column, were included in the analysis. The equilibrium equations were formulated with respect to an arbitrary coordinate system and no reference was made to the shear centre, centroid, or principal axis. This way the shift in the shear centre and the shift and rotation of principal axes of the elastic core, as yielding of the cross-section progress was taken care of automatically. Further, the predicted ultimate loads and load deformation responses showed satisfactory agreement with the available test and analytical results.

Sharma and Gaylord [35] applied Jezek's concept to biaxially loaded beam-columns and assumed, as well, an elastic-perfectly plastic idealization for the material and sinusoidal variations for the lateral displacements and rotation of the cross-section of the deflected axis of the beam-column. The solution of the equations of equilibrium was simplified by only considering equilibrium at midheight of the beam-column between the applied force at the ends of the beam-column and the internal resistance of the midheight of the beam-column.

Employing a similar technique adopted by Fukumoto and Galambos [23], Lim and Lu [36] studied the occurence of inelastic lateral torsional buckling of laterally unsupported beam-columns restrained against weak axis bending and warping at the column ends. Both the tangent modulus and the reduced modulus solution were provided. The same technique was extended to cover the case of inelastic lateral torsional buckling problems in continuous beam-columns with warping and weak axis bending restraints at the joints.

A more approximate method of analysis for biaxially loaded restrained columns has been described by Santathadaporn and Chen [37]. The problems to be solved are limited to the case of symmetrical loading. The deflected shape of the column was assumed to be a sine function. The analytical procedure required calculation of the internal forces including torsional moments of the elastic-plastic cross-section. For this the column cross-section was divided into finite elements. The strain and stress at each element were computed as the average values at its centroid. Numerical integration was performed by summing up the effect of all the elements. The equations were expressed in a different form and were derived for the rate of change of forces as variables denoting infinitesimal increment. Similarly the rate of change of external forces at mid-span of the column were developed. Yielding and instability

effect were incorporated in the stiffness matrix [38] which can be interpreted as the tangent of the load deformation curve. The actual solution process was iterative and equilibrium was only satisfied at mid-height of the column.

The Newton-Raphson iterative approach was extended to solve the general case of asymmetrical biaxial bending of pin ended columns by Virdi [39,40]. The theory was developed in connection with studies on composite concrete columns. In the analysis, all twisting effects are ignored because of the large twisting rigidity of the solid cross-section. Thus the method is quite simplified and applicable to many biaxially loaded beam-columns of solid sections such as reinforced concrete or steel concrete composite sections as well as torsionally stiff bare steel beam-columns. In order to calculate the internal forces of a section, the section was divided into finite elements as was adopted by Harstead, Birnstiel and Leu [28]. Moment-thrust-curvature relationships were computed by summing up the effect of all the small elements and using an interpolation technique. In computing these relationships the exact nature of the stress-strain curve was accounted for by idealizing it as multilinear curve. Residual stresses could also be incorporated. A finite difference scheme was employed to determine the stable deflected shape. A set of trial deflections was assumed along the length and curvatures computed. Moment-thrust-curvature relations were then

computed for given axial load. To follow, external moments were calculated and compared with the internal moments. The solution process was iterative and the Newton-Raphson correction procedure was set up at this stage for obtaining the new deflected shape. Subsequent deflected shapes were obtained for increasing axial loads applied eccentrically. In a later development, Virdi improved the integration of stress resultants using Gaussian quadrature formuale [40].

In a more recent work Sen [41] presented an analytical method to solve the problem of determining the failure load of steel beam-columns. The problem investigated was that often encountered in practice of major axis asymmetrical bending with minor imperfections. The tests covered beam-columns of short to intermediate slenderness (45-74) on which high axial loads could be sustained and in effect explored the plastic hinge rotation capacity in this load range. The theoretical work covered torsional effects and asymmetric bending. A numerical solution based on central finite differences was adopted in the study and the method employed was Successive Over Relaxation. The method developed covered initial curvature, residual stress and a non linear stress-strain curve. However, the solution was for double symmetric I-section only.

A detailed description of available design methods has been published by Chen and Atsuta [42,43]. They presented precisely the basic theoretical principles, methods of analysis in obtaining the solutions of beam-columns, and the recent developments of theories of biaxially loaded beam-columns. It was shown how those theories could be used in the solution of practical design problems. Residual stress imperfections, and elastic-plastic behaviour were included in their methods. After presenting the basic theory systematically, from the most elementary to the most advanced stage of development, they proceeded directly to the solutions of particular problems. The various methods of solutions were presented. In most cases, numerical results were given in terms of tables, charts, and diagrams which furnished values of critical loads for various beam-column problems.

Later, more recent developments in design methods were presented by Lui and Chen [44]. A deterministic aproach was used to assess the strength of centrally loaded H-columns, taking into consideration the effects of residual stresses, initial out-of-straightness, and small end restraints. The column types used in the study included hot-rolled wide-flange shapes and flame-cut H-shapes. The deterministic column strength data were generated with the aid of a computer. These data were analysed and categorised, resulting in the development of a set of

restrained-end multiple column curves. These curves were then compared with the current column design curves to show the effect of small restraint on the maximum strength of columns. In addition, the new column curves were compared with the basic column curves [45], and effective length factors, expressed as a function of the magnitude of end restraint, were proposed.

Interaction between elastic buckling and plastic collapse has been studied by Ho [46]. Investigation was carried out on the failure of beam-columns subjected to axial compression, transverse loading, and unequal end moments. A formula was proposed to predict the failure load of such beam-columns. Derivation of the formula was based on the concept of interaction between the two modes of failure, i.e. elastic buckling and plastic collapse of the beam-column. The effects of initial deformation, residual stresses and the spread of plasticity in the beam-column were considered. Subsequent application of the formula to other more general cases showed that good agreement with results obtained either theoretically or experimentally could be achieved.

1.3. SUMMARY OF RESEARCH AND FORMULATION OF THE PROBLEM

The behaviour of beam-columns has been the subject of research for many years. A substantial amount of work, both experimental and theoretical, has been done on the problem of bare steel beam-columns. Usually, the deflected shape of the beam-column is assumed to be a sine function and the stability of the structure is checked at the midlength only. In the traditional approach, the development of the methods are based on the elastic limit of the structures. The recent development of the limit state approach to design has focused attention on simplifying design procedures and accuracy of the results obtained. It is possible to make an accurate analysis of the behaviour of steel beam-columns which includes the effect of torsion, residual stress and imperfections. However, the more accurate are the results expected, the more factors are needed to be considered and the more complicated problems to be solved. Thus, it seems to be impossible to get simplicity and accuracy at the same time. Since approximate solutions are more advantageous than the exact one, design rules are usually based on an appoximate analysis and certain effects may be covered by means of a safety factor. Obviously, accurate information about these effects is needed for this purpose. Although torsion effects have been considered in many design methods, relatively little information is available about its magnitude for design purposes.

In this study, a rigorous method of the ultimate load analysis of steel beam-columns has been developed. The solution may be obtained with or without considering the effects of torsion, residual stresses and imperfections on the beam strength. The effect of torsion on the steel beam-column ultimate load is explored by means of a parametric study. Before the relevant design data can be used with confidence, it is necessary to prove the validity of the theory through carefully selected experiments. The validity of the computer program is also proved by comparing the results with the available experimental and theoretical data. Design data and graphs are presented for future developments. The analytical procedure, in general is similar to the previous method used by Virdi [39,40] to study composite concrete columns with the notable difference being the inclusion of torsional effects in the present study. Thus, the actual deflected shapes of the beam-columns are determined by iteration and stability is examined at each nodal point.

1.4. SCOPE AND LAYOUT OF THE THESIS

The general objective of this thesis was to obtain an analytical method which could be employed to simulate actual tests for determination of the collapse load of bare steel beam-columns under biaxial bending.

In Chapter 2 the theory adopted to develop the proposed analytical method is outlined. The assumptions taken are described and the equations are derived.

Chapter 3 describes the computer program BECOL written to determine the ultimate load of monosymmetric I steel beam-columns, including the residual strain and torsional effects. In this chapter, the computation procedure is outlined.

Chapter 4 introduces the experimental work. In this part, details of the test programme, material tests, load paths followed during the tests, instrumentation, loading rig test procedures and test results are described.

Chapter 5 deals with the validity of the computer program. For this purpose, the validity is examined in the light of comparisons with the existing solutions of biaxial bending for beam-columns. Comparison between the theoretical and the experimental results is also presented in this chapter.

Application of the method is demonstrated to generate design data in Chapter 6. It is followed by discussion of the results obtained. Finally, conclusions drawn from the theoretical and experimental results are outlined in Chapter 7.

2. FAILURE LOAD THEORY

2.1. INTRODUCTION

The general approach in obtaining the failure load of a beam-column is to calculate the deflected shape under a small fraction of the design load. For equilibrium, the external forces and moments are balanced by the internal stress-resultants. Moment-thrust-curvature relations can be adopted to compute the internal stress-resultants. This requires information about steel stress-strain relations and any residual stresses in the cross-section.

Iteration for calculating the deflected shape which satisfies the equilibrium conditions may be done using Newton-Raphson method [47,48,49]. After the equilibrium conditions have been obtained, the computation may proceed with further loading increments. These steps are repeated until a deflected shape in equilibrium with the applied loading can no longer be obtained. The final load combination which satisfies the equilibrium condition may be specified as the ultimate load of the beam-column.

For a given cross-section under a constant thrust, the variation of moment with curvature is linear in the elastic range. In the inelastic range the relation becomes non-linear and is also affected by the presence of residual stresses.

The numerical integration method adopted here is similar to the one suggested by Virdi [47,48,49]. The cross-section is divided into a few rectangular blocks for computing the internal forces. Gauss quadrature formulae are used to obtain the integration involved. Residual stress can be easily accounted for.

2.2. ASSUMPTIONS

The major assumptions are as follows :

(a) Deflections are small, so that curvature can be represented by the second derivative of the deflections.

(b) The lateral loads act through the original centroidal axis of the beam-column.

(c) The cross sections are uniform over the length of the beam-column.

(d) The effect of shear stresses on the yielding of the section is negligible. Further, the shear stresses have no effect on deflections or in producing a combined stress yield condition.

(e) The shear modulus G is assumed to retain its full elastic value after yield has taken place.

(f) Local buckling of individual rectangular elements comprising the section, is ignored.

2.3. STEEL STRESS-STRAIN RELATIONS

Most previous studies reported in literature, have adopted an elastic-perfectly plastic bilinear curve. The effect of strain hardening has usually been ignored.

The theory developed here is based on a multi-linear stress-strain characteristic. Any experimental stress-strain curve can be idealised as a multi-linear curve with a desired degree of accuracy. This also enables the analysis for bilinear elastic perfectly plastic characteristics.

2.4. RESIDUAL STRESSES

The residual stresses are defined as those stresses that remain in structural member after the rolling or fabrication processes. To satisfy the conditions of equilibrium, the axial force and moments obtained by integrating the residual stresses acting on any cross-section must be zero. It is now recognised that in order to obtain a better understanding of inelastic beam-column behaviour it is necessary to consider residual stresses.

Residual stresses are introduced into a member due to cooling of different parts of the section after the hot rolling process. The portion of a member that cools most slowly develops residual tension that is balanced by

residual compression in other portions of the member. In the fabrication of metal structures, flat plates and straight beams are often formed or straightened at room temperatures into desired shapes. These cold-forming operations obviously cause inelastic deformations and residual stresses, since the steel retains its formed shape. The magnitude and distribution of residual stresses across the section are highly variable, depending on the shape and size of the section and manufacturing process.

The typical hot-rolled H shape has residual compression in its flange tips, and residual tension in the vicinity of the flange-web junction, which cools slowly. According to Brockenbrough and Johnston [50] residual stresses from cooling are approximately constant along the length of a column, whereas cold-straightening stresses frequently occur only at particular locations where the member has been straightened. For most columns, the maximum compressive stresses caused by cold straightening are of about the same magnitude as those caused by cooling, but Brockenbrough and Johnston have shown that residual stresses which result from cooling are more important from the stand point of column strength.

Two residual stress patterns are frequently considered in studying inelastic beam-column behaviour. The first pattern is shown in Fig. 2.1 and assumes linear

variation between points of extreme stress. The second pattern is shown in Fig. 2.2. The variation is parabolic with compressive stresses in the web. In using these patterns in moment-thrust-curvature relations, the residual stresses are first converted to residual strains. The strains due to the applied loads are superimposed on the residual strains. The net stresses in the section can now be determined using the net strain so obtained and the material stress-strain characteristic.

In the results presented in this thesis, the first residual stress pattern has been adopted. Based on the condition that residual stresses are self-equilibrating, the tensile residual stress σ_{rt} in the web can be obtained using :

$$\sigma_{rt} = \sigma_{rc} \left\{ \frac{b.t_f}{b.t_f + t_w.(d - 2t_f)} \right\} \quad ....(2.1)$$

where b = flange width

t_f = flange thickness

d = depth of the section

t_w = width of the web

σ_{rc} = compressive residual stress

σ_{rt} = tensile residual stress

2.5. INTERNAL STRESS-RESULTANTS

2.5.1. Internal Stress-Resultant Equations

Fig. 2.3. shows a beam-column with its applied loading. The loading consits of an axial force N, lateral forces P_x and P_y, and end-moments about the X and Y axes. The right hand screw rule has been adopted for positive moments. Fig. 2.4 shows the general displacements of a cross-section. Equilibrium has to be satisfied in the deflected state of the beam-column.

The cross-section is initially in position 1. Under the action of external forces, the cross-section moves to position 2, giving the u and v displacements shown. Displacements u, v, the twist and the coordinates of S, viz. x_o and y_o are all positive as shown. The quantities u, v and θ are small so that the geometry of small displacements applies.

The cross-section undergoes twisting during deformation. Thus, the member principal axes X and Y rotate through an angle θ, taking the orientation of axes ξ and η. The displacement components u_c and v_c of a point S at (x_o, y_o) relative to the centroid, become

$$u_c = u + \theta . y_o \qquad \text{.....(2.2)}$$

$$v_c = v - \theta . x_o \qquad \text{.....(2.3)}$$

Another geometric change which occurs during the beam-column displacement is the inclination of the ζ axis to the original Z axis caused by the slope du/dz and dv/dz. Thus twisting the beam-column together with u and v displacements means that forces computed in the X-Y-Z coordinate system differ from those computed for the $\xi - \eta - \zeta$ system.

Curvature of any such section may be determined with the finite difference methods, a technique for the reduction of continuum to a system with a finite number of degrees of freedom. The basis of the method is that the derivatives of functions at a point can be approximated by an algebraic expression consisting of the value of the function at that point and several nearby points. Detail of finite difference methods are available in several textbooks (see, for example, Collatz [51] and Vinnakota [52]). In this method, central differences will give more accurate results than backward or forward differences. For this reason, central differences will be adopted for the proposed analytical method. The first and the second derivatives of a function (Fig. 2.5) may be approximated with the following equations :

$$u_i' = -\frac{1}{2\Delta z}\,(u_{i+1} - u_{i-1})$$

$$u_i'' = \frac{1}{\Delta z^2}\,(u_{i+1} - 2u_i + u_{i-1}) \qquad \ldots(2.4)$$

Internal stress-resultant equations of elastic members have been discussed extensively in many textbooks [9]. By virtue of the assumption regarding plane sections, the elongation ϵ is proportional to the distance from the neutral axis. In the elastic case, the stress at any fibre is proportional to the strain. The moments M_ξ and M_η are approximated by the following equations :

$$M_\xi = - EI_\xi \frac{d^2v}{dz^2} = - EI_\xi . \phi_\xi \qquad .....(2.5)$$

$$M_\eta = - EI_\eta \frac{d^2u}{dz^2} = - EI_\eta . \phi_\eta \qquad .....(2.6)$$

where: E = elastic modulus

I_ξ = moment of inertia about ξ axis

I_η = moment of inertia about η axis

The twisting moment M_ζ, including pure torsion, Wagner-effect and warping is written in the form :

$$M_\zeta = GK_T \frac{d\theta}{dz} + \bar{K} \frac{d\theta}{dz} - EI_w \frac{d^3\theta}{dz^3} \qquad .....(2.7)$$

$$K_T = \sum \frac{t^3 s}{3} \qquad .....(2.8)$$

$$\bar{K} = \int \sigma . a^2 . dA \qquad .....(2.9)$$

where : G = shear modulus

t = thickness of typical element

s = length of typical element

σ = stress in a small element

a = distance of the element from the centre of twist

I_w = warping rigidity

θ = angle of rotation of the section

In studying failure load, inelastic behaviour of the material has to be considered. Since the assumption regarding plane sections is applied, then the elongation ϵ is proportional to the distance from the neutral axis. But it should be noted, the stress is not proportional to the strain in the inelastic range.

Accordingly the deteriorated stiffness about ξ axis may be expressed as :

$$X_\xi = \int_A (\sigma . \eta / \phi_\xi) \, dA \qquad \ldots\ldots(2.10)$$

where dA = a small area of the cross section

σ = stress of the small area dA

η = lever arm of dA to ξ axis

A = total area of the cross section

Similarly about the η axis the stiffness becomes :

$$Y_\eta = \int_A (\sigma . \xi / \phi_\eta) \, dA \qquad \ldots\ldots(2.11)$$

The Wagner effect term K in Equation (2.7) can be similarly computed from :

$$\bar{K} = \int_A \omega_i^2 \, dA \qquad \ldots\ldots(2.12)$$

where ω_i = distance from the dA to the centre of twist

If the stiffness of the compression and tension flange are denoted by C_{fc} and C_{ft}, then

$$C_{fc} = \int_A (\sigma . \xi / \phi_\eta) \, dA \qquad \ldots\ldots(2.13)$$

$$C_{ft} = \int_A (\sigma . \xi / \phi_\eta) \, dA \qquad \ldots\ldots(2.14)$$

where : A = areas of the tension and compression flange

The shear centre, S , of a monosymmetric I section (Fig.2.6) can be calculated with the following equations [53] :

$$\rho = \frac{I_{yc}}{I_{yc} + I_{yt}} \qquad \ldots\ldots(2.15)$$

$$a_c = \frac{I_{yt}}{I_{yc} + I_{yt}} . D = (1 - \rho) D \qquad \ldots\ldots(2.16)$$

$$a_t = \frac{I_{yc}}{I_{yc} + I_{yt}} . D = \rho . D \qquad \ldots\ldots(2.17)$$

where I_{yc} and I_{yt} are the section minor axis second moment of area of the compression and tension flange respectively. The values of ρ thus range from 0 for a tee-beam with flange in tension to 1 for a tee-beam with flange in compression. For an equal flanged beam, ρ is 0.5 .

The contribution of the twist θ to the flange deflections can be shown with the following equations :

$$u_{ct} = a_c . \theta \qquad \text{.....(2.18)}$$

$$u_{tt} = - a_t . \theta \qquad \text{.....(2.19)}$$

where : u_{ct} = minor axis displacement of the compression flange caused by the twist

u_{tt} = minor axis displacement of the tension flange caused by the twist

Curvature which is caused by the warping deflections at flanges generates strains in the flange-elements. These warping strains should be considered in the stress computation. Distribution of the strains can be seen in Fig. 2.7.

Taking the warping deflection into account, total displacements of the compression and tension flange, u_{fc} and u_{ft} are expressed as :

$$u_{fc} = u + \theta . a_c \qquad \text{.....(2.20)}$$

$$u_{ft} = u - \theta . a_t \qquad \text{.....(2.21)}$$

Based on Equations (2.20) and (2.21), the curvatures of compression and tension flanges, ϕ_{fc} and ϕ_{ft} can be determined by :

$$\phi_{fc} = \frac{d^2u}{dz^2} + a_c . \frac{d^2\theta}{dz^2} \qquad \text{.....(2.22)}$$

$$\phi_{ft} = \frac{d^2u}{dz^2} - a_t . \frac{d^2\theta}{dz^2} \qquad \text{.....(2.23)}$$

As mentioned previously, the stiffnesses of the compression and tension flange are C_{fc} and C_{ft} respectively. Then the flange bending mements, M_{fc} and M_{ft} may be obtained with the following equations :

$$M_{fc} = C_{fc} . \left(\frac{d^2u}{dz^2} + a_c . \frac{d^2\theta}{dz^2} \right) \qquad \text{.....(2.24)}$$

$$M_{ft} = C_{ft} . \left(\frac{d^2u}{dz^2} - a_t . \frac{d^2\theta}{dz^2} \right) \qquad \text{.....(2.25)}$$

The respective flange shear, V_{fc} and V_{ft}, after neglecting the certain product of small quantities become :

$$V_{fc} = \frac{dM_{fc}}{dz} \qquad \text{.....(2.26)}$$

$$V_{ft} = \frac{dM_{ft}}{dz} \qquad \text{.....(2.27)}$$

The resisting warping torque about C, M_{wf} is expressed as :

$$M_{wf} = V_{fc} \cdot a_c - V_{ft} \cdot a_t \qquad \text{.....(2.28)}$$

Combining Equations (2.5)-(2.6) with Equations (2.10)-(2.11), resisting bending moments may be obtained with the following equations :

$$M_{\xi} = \int_A \sigma . \eta . dA \qquad \text{.....(2.29)}$$

$$M_{\eta} = \int_A \sigma . \xi . dA \qquad \text{.....(2.30)}$$

From Equations (2.7)-(2.9) and Equations (2.13)-(2.30), twisting moment resistances can be computed as follows

$$M_{\zeta} = (GK_T - \bar{K}) + \left(\frac{dM_{fc}}{dz} . a_c - \frac{dM_{ft}}{dz} . a_t \right) \qquad \text{....(2.31)}$$

2.5.2. Moment-Thrust-Curvature Relations

There are nine variables involved in the moment-thrust-curvature relations when torsional effects are considered. The variables are : moments M_x, M_y and M_z, axial force N, primary curvature of the beam ϕ, secondary

curvature of the flanges due to warping ϕ_w, distance of the neutral axis to the origin d_n, inclination of the neutral axis α and angle of twist of the section θ.

For convenience, in the next derivation, moments M_x, M_y and M_z will be replaced by M_ξ, M_η and M_ζ respectively. With reference to Fig. 2.8., correlation between those variables may be written as :

$$M_\xi = M_x + M_y.\theta \qquad \text{.....(2.32)}$$

$$M_\eta = M_y - M_x.\theta \qquad \text{.....(2.33)}$$

$$M_\zeta = M_z \qquad \text{.....(2.34)}$$

There are four equations of equilibrium relating to those nine unknowns. Thus by assigning values to any five of the variables, the other four can be determined. The curvature ϕ and inclination of the neutral axis α may be obtained with the following equations :

$$\phi_t = \sqrt{\phi_\xi^2 + \phi^2} \qquad \text{.....(2.35)}$$

$$\alpha = \text{Tan}^{-1}(\phi_\eta/\phi_\xi) \qquad \text{.....(2.36)}$$

where : ϕ_ξ = curvature about ξ axis

ϕ_η = curvature about η axis

ϕ_t = total curvature

α = inclination of neutral axis with respect to the -axis.

With reference to Fig. 2.9. , the strain distribution across the section can be obtained from :

$$\epsilon_o = \phi_t \, d_n \qquad \text{.....(2.37)}$$

$$\text{and} \quad \epsilon_i = \epsilon_o \left(1 - \frac{d_i}{d_n}\right) \qquad \text{.....(2.38)}$$

where : ϵ_o = strain at the origin O

ϵ_i = strain at any point (ξ_i, η_i)

d_i = distance of any point (ξ_i, η_i) to the neutral axis

With reference to Fig. 2.7, strain due to warping may be obtained with the following equation :

$$\epsilon_{wi} = - \phi_w . \xi_i \qquad \text{.....(2.39)}$$

where : ϵ_{wi} = warping strain of an elemental area 'i'.

ϕ_w = flange curvature about η axis caused by warping

In order to calculate the internal stress-resultants of a section, the value of the strains obtained from Equation (2.38) should be modified by taking the residual and warping strains into account. By using the stress-strain characteristic of the material, the stress σ corresponding to the strain ϵ is determined. Thus, the internal stress resultants are :

$$N = \int_A \sigma \, dA \qquad \text{.....(2.40)}$$

$$M_\xi = \int_A \sigma \cdot \eta \, dA \qquad \text{.....(2.41)}$$

$$M_\eta = \int_A \sigma \cdot \xi \, dA \qquad \text{.....(2.42)}$$

2.5.3. Computational Method

To obtain the actual internal stress-resultants of a section, numerical integration procedure has to be applied. The section is usually devided into a grid of small elements. The strain and the stress in each element are determined using the procedure described above. Accordingly, Equations (2.40) - (2.42) may be approximated as follows :

$$N = \int_A \sigma \, dA = \sum_{n=1}^{i=n} \Delta a_i \cdot \sigma_i \qquad \text{.....(2.43)}$$

$$M_\xi = \int_A \sigma \cdot \eta \, dA = \sum_{i=1}^{i=n} \Delta a_i \cdot \sigma_i \cdot \eta_i \qquad \text{...(2.44)}$$

$$M_\eta = \int_A \sigma \cdot \xi \, dA = \sum_{i=1}^{i=n} \Delta a_i \cdot \sigma_i \cdot \xi_i \qquad \text{..(2.45)}$$

where a_i is the element area, η_i and ξ_i are the respective lever arms for ξ and η axes and n is the total number of elements.

This method has been adopted by Gesund [54], Virdi [39] and Sen [41]. An alternative method is to adopt the Gauss Quadrature Formulae which have been shown by Virdi [47,48,49] to be highly versatile and yet remarkably rapid.

According to the Gauss Quadrature Formulae, a definite integral between the limits -1 and +1 can be replaced by a weighted sum of the values of the integrand at certain specific points. Thus :

$$\int_{-1}^{1} f(\xi)\,.d\xi = \sum_{i=1}^{i=m} H_i.f(a_i) \qquad .....(2.46)$$

where H_i are the weighting coefficients, $\xi_i = a_i$ are specified Gauss points and m is the number of 'Gauss points' used in the integration. The higher the value of m, the greater is the accuracy achieved. It is pointed out that the integration is exact if $f(\xi)$ is a polynomial of degree up to (2m-1). Values of H_i and a_i are available in tabular form [55,56].

Similarly a double integral can be replaced by a double summation :

$$\int_{-1}^{1}\int_{-1}^{1} f(\xi,\eta)\,d\xi\,d\eta = \sum_{i=1}^{i=m}\sum_{j=1}^{j=m} H_i.H_j.f_{(a_i,b_j)} \qquad ...(2.47)$$

where H_i and H_j are the weighting coefficients and a_i and b_j are the coordinates of Gauss points where the function $f(\xi,\eta)$ is to be evaluated. The equation implies a square area between the limits -1 and +1 for two axes ξ and η.

However, any rectangular area can be successfully mapped onto the square area limits -1 and +1, as shown in Fig. 2.10. The converse mapping, from the so called natural coordinates(ξ,η) to the Cartesian coordinates (x,y) is readily performed through the following equations :

$$x=[(1-\xi)(1-\eta)\ (1+\xi)(1-\eta)\ (1-\xi)(1+\eta)\ (1+\xi)(1+\eta)]\begin{bmatrix} x_p \\ x_q \\ x_r \\ x_s \end{bmatrix} \qquad (2.48)$$

$$y=[(1-\xi)(1-\eta)\ (1+\xi)(1-\eta)\ (1-\xi)(1+\eta)\ (1+\xi)(1+\eta)]\begin{bmatrix} y_p \\ y_q \\ y_r \\ y_s \end{bmatrix} \qquad (2.49)$$

The elemental area $d\xi.d\eta$ gets transformed to dx.dy thus :

$$dx.dy = |J|\ d\xi.d\eta \qquad .....(2.50)$$

where,

$$[J] = \frac{1}{4}\begin{bmatrix} -(1-\eta) & (1-\eta) & -(1+\eta) & (1+\eta) \\ -(1-\xi) & -(1+\xi) & (1-\xi) & (1+\xi) \end{bmatrix}\begin{bmatrix} x_p & y_p \\ x_q & y_q \\ x_r & y_r \\ x_s & y_s \end{bmatrix} \qquad (2.51)$$

Thus an integral in Cartesian coordinates can be evaluated as follows :

$$\int_A g_{(x,y)}.dx.dy = \int_{-1}^{1}\int_{-1}^{1} g_{(x,y)}.|J|.d\xi.d\eta$$

$$= \sum_{i=1}^{i=m}\sum_{j=1}^{j=m} H_i.H_j.g_{(x_i,y_j)}.|J| \quad ...(2.52)$$

where (x_i,y_j) are the Gauss points in Cartesian coordinates.

It will now be shown how the Gauss quadrature can be used to evaluate the integrals in Equations (2.53) - (2.55), representing the moment-thrust-curvature relations. The steel section may be represented by three rectangular blocks as shown in Fig. 2.11.

Then the integrals in each rectangle can be replaced with the following equations :

$$N = \sum_{i=1}^{i=m}\sum_{j=1}^{j=m} H_i.H_j.\sigma_{(i,j)}.|J| \quad .....(2.53)$$

$$M_\xi = \sum_{i=1}^{i=m}\sum_{j=1}^{j=m} H_i.H_j.\sigma_{(i,j)}.\eta_{(i,j)}.|J| \quad .....(2.54)$$

$$M_\eta = \sum_{i=1}^{i=m}\sum_{j=1}^{j=m} H_i.H_j.\sigma_{(i,j)}.\xi_{(i,j)}.|J| \quad .....(2.55)$$

Values of the axial force N and the neutral axis inclination α are assumed and the curvature ϕ is varied between specified limits. To obtain the values of M_ξ and M_η in every combination of N, α and ϕ, the iteration of the neutral axis position can be done with the Newton-Raphson method.

Firstly d_n is assumed, with Equation (2.38) the strain in every Gauss point is computed. Secondly with Equation (2.39), the strains due to warping at the Gauss points of the flanges can be obtained. Then, stresses can be computed using those strains obtained previously and considering residual strains. Further, the internal axial force N_1 may be obtained from Equations (2.47) - (2.52). These steps are repeated with a small increment Δd_n to d_n, and the value of the internal axial force obtained is N_2. The correction of d_n can be computed with the following equation :

$$c_{dn} = \Delta d_n .(N - N_1) / (N_2 - N_1) \quad ...(2.56)$$

The iteration is continued with the corrected value of d_n. These steps should be repeated, until the difference in values of N and N_1 may be neglected. The moments M_ξ and M_η may now be determined using Equations (2.54) - (2.55).

Convergence is normally achieved within two or three cycles. However, success of this iterative procedure depends on how close the chosen initial values are to the final values. If the assumed values are very far, the process may fail to converge even if there is a solution.

Once the cross-sectional stresses are obtained using Equations (2.37)-(2.38), the inelastic resistances of the section can be computed easily from Equations (2.53)-(2.55).

Comparison between the result of the computer program and moment-thrust-curvature curves given by Chen [40] for WF8x31 section can be seen in Fig. 2.12. The differences between two curves are small.

2.6. EXTERNAL FORCE EQUATIONS

To calculate the equilibrium configuration of a beam-column subject to an axial load N, lateral loads P_x and P_y and moments about X and Y axes, it is necessary to compute external forces at a general displaced section. Several methods for calculation are available in literature (see, for example, Chen and Atsuta [43]). The external forces at a typical cross-section for an assumed configuration are shown in Fig. 2.3. The right hand screw rule will be adopted for positive moment in the following

external force equations. The forces acting in the Z-X and the Z-Y plane are shown in Fig. 2.3. The applied moments at a distance z from the left end of the beam-column are :

$$M_x = M_{xo} - R_{yo}.z - N.v_c - \sum_{i=1}^{i=nl} P_{yi}.\langle z-z_i \rangle \quad .....(2.57)$$

$$M_y = M_{yo} + R_{xo}.z + N.u_c + \sum_{i=1}^{i=nl} P_{xi}.\langle z-z_i \rangle \quad .....(2.58)$$

$$R_{xo} = (-M_{yo} + M_{yl} - \sum_{i=1}^{i=np} P_{xi}.(L-z_i))/L \quad .....(2.59)$$

$$R_{yo} = (M_{xo} - M_{xl} - \sum_{i=1}^{i=np} P_{yi}.(L-z_i))/L \quad .....(2.60)$$

where : M_{xo} = applied major axis bending moment at O

M_{xl} = applied major axis bending moment at L

M_{yo} = applied minor axis bending moment at O

M_{yl} = applied minor axis bending moment at L

N = applied axial force

P_x = applied point load in the X direction

P_y = applied point load in the Y direction

R_{xo} = minor axis reaction force at O

R_{yo} = major axis reaction force at O

np = number of point loads

nl = number of point loads to the left side of the section

Moments M_x and M_y are affected by the angle of twist of the section θ. For convenience, in the next derivation moments M_x and M_y will be transformed to the axes ξ and η using the following equations :

$$M_\xi = M_x + \theta . M_y \qquad \text{.....(2.61)}$$

$$M_\eta = M_y - \theta . M_x \qquad \text{.....(2.62)}$$

In addition to components of M_ξ and M_η along the ξ and η axes, they also have components along the axis which is perpendicular to the cross-section and is inclined from the Z axis. These components result in a twisting moment, as shown in Fig. 2.13.

$$M_{\zeta_1} = M_x . du/dz + M_y . dv/dz \qquad \text{.....(2.63)}$$

where : $\sin (du/dz) = du/dz$ and

$\sin (dv/dz) = dv/dz$

A second contribution to M_ζ is due to the end shears, as shown in Fig. 2.14.

$$M_{\zeta_2} = -R_{xo} . v + R_{yo} . u \qquad \text{.....(2.64)}$$

A third contribution to M_ζ arises due to components N du/dz and N dv/dz acting through the centroid. Therefore the third contribution of torque about the centre of twist is :

$$M_{\zeta 2} = N \frac{du}{dz} y - N \frac{dv}{dz} x \qquad \text{.....(2.65)}$$

The fourth contribution arises due to the transversal loads as shown in Fig. 2.15 may be expressed :

$$M_{\zeta 4} = \sum_{i=1}^{i=nl} P_{yi}(u-u_i) - \sum_{i=1}^{i=nl} P_{xi}(v-v_i) \qquad \text{.....(2.66)}$$

The fifth contribution arises due to the reaction at the both ends as shown in Fig. 2.16 is :

$$M_{\zeta 5} = -\sum_{i=1}^{i=np} P_{xi}.v \left(\frac{L - z_p}{L}\right) + \sum_{i=1}^{i=np} P_{yi}.u \left(\frac{L - z_p}{L}\right) \qquad \text{..(2.67)}$$

The total twisting moment is the sum of all components which have been mentioned above, thus :

$$M_\zeta = M_{\zeta 1} + M_{\zeta 2} + M_{\zeta 3} + M_{\zeta 4} + M_{\zeta 5} \qquad \text{.....(2.68)}$$

Combining Equations (2.56) - (2.68), the external moments become :

$$M_{\xi} = M_{xo} + -\frac{z}{L}\{-M_{xo} + M_{xl} + \sum_{i=1}^{i=np} P_{yi}.(L-z_i)\} - N.v_c$$

$$- \sum_{i=1}^{i=nl} P_{yi}\langle z-z_i\rangle + \theta\,[\, M_{yo} + -\frac{z}{L}\{-M_{yo} + M_{yl}$$

$$- \sum_{i=1}^{i=np} P_{xi}(L-z_i)\} + N.u_c + \sum_{i=1}^{i=nl} P_{xi}.\langle z-z_i\rangle\,] \quad ....(2.69)$$

$$M_{\eta} = M_{yo} + -\frac{z}{L}\{-M_{yo} + M_{yl} - \sum_{i=1}^{i=nl} P_{xi}\,(L-z)\} + N.u_c$$

$$+ \sum_{i=1}^{i=nl} P_{xi}\,\langle z-z_i\rangle - \theta\,[\, M_{xo} + -\frac{z}{L}\{-M_{xo} + M_{xl}$$

$$+ \sum_{i=1}^{i=np} P_{yi}\,(L-z_i)\} - N.v_c - \sum_{i=1}^{i=nl} P_{yi}\,\langle z-z_i\rangle\,] \quad ....(2.70)$$

$$M_\zeta = [M_{xo} + -\frac{z}{L}-\{-M_{xo} + M_{xl} + \sum_{i=1}^{i=np} P_{yi} \cdot (L-z_i)\}$$

$$- N.v_c - \sum_{i=1}^{i=nl} P_{yi} \langle z-z_i \rangle + N.y_o \;] \; -\frac{du}{dz}-$$

$$+ [\; M_{yo} + -\frac{z}{L}-\{-M_{yo} + M_{yl} - \sum_{i=1}^{i=np} P_{xi} \cdot (L-z_i)\}$$

$$+ N.u_c + \sum_{i=1}^{i=nl} P_{xi} \langle z-z_i \rangle + N.x_o \;] \; -\frac{dv}{dz}-$$

$$+ -\frac{v_c}{L}-\{M_{yo} - M_{yl} + \sum_{i=1}^{i=np} P_{xi} \; (L-z_i)\}$$

$$+ -\frac{u_c}{L}-\{M_{xo} - M_{xl} - \sum_{i=1}^{i=np} P_{yi} \; (L-z_i)\}$$

$$+ \sum_{i=1}^{i=nl} P_{yi} \; (u - u_i) - \sum_{i=1}^{i=nl} P_{xi} \; (v - v_i)$$

$$- -\frac{v}{L}- \sum_{i=1}^{i=np} P_{xi} \; (L-z_p) + -\frac{u}{L}- \sum_{i=1}^{i=np} P_{yi} \; (L-z_p) \qquad \ldots(2.71)$$

The Equations (2.57)-(2.71) do not include the effect of initial imperfections and end restraints. The necessary modifications are discussed below.

The forces in the X-Z plane of a restrained beam-column with imperfections, u_o are shown in Fig. 2.16. Similar imperfections, v_o are present in the Y-Z plane, and total deflections, u and v will be used in the next derivation as follows :

$$u = u_c + u_o \qquad \text{.....(2.72)}$$

$$v = v_c + v_o \qquad \text{.....(2.73)}$$

where u_o and u are initial and total deflections in X axis, and v_o and v are initial and total deflections in Y axis.

Referring to Fig. 2.17 the boundary conditions become :

$$M_{txo} = M_{xo} + M_{rxo} \qquad \text{.....(2.74)}$$

$$M_{txl} = M_{xl} + M_{rxl} \qquad \text{.....(2.75)}$$

$$M_{tyo} = M_{yo} + M_{ryo} \qquad \text{.....(2.76)}$$

$$M_{tyl} = M_{yl} + M_{ryl} \qquad \text{.....(2.77)}$$

where : M_{txo}, M_{tyo} = total major and minor moments at O respectively

M_{txl}, M_{tyl} = total major and minor moments at L respectively

M_{rxo}, M_{ryo} = major and minor restraint moments at O respectively

M_{rxl}, M_{ryl} = major and minor restraint moments at L respectively

When the restraint is in the elastic range, restraint moments may be expressed as the Equations (2.78 - 2.81). To determine the restraint effect in the elastic and inelastic range, Virdi [40] has shown it is convenient to use the moment-end rotation characteristic of the end restraints (Fig. 2.18).

$$M_{rxo} = -K_{xo} \left(\frac{dv}{dz}\right) \quad (z=0) \qquad \text{.....(2.78)}$$

$$M_{rxl} = K_{xl} \left(\frac{dv}{dz}\right) \quad (z=L) \qquad \text{.....(2.79)}$$

$$M_{ryo} = K_{yo} \left(\frac{du}{dz}\right) \quad (z=0) \qquad \text{.....(2.80)}$$

$$M_{ryl} = -K_{yl} \left(\frac{du}{dz}\right) \quad (z=L) \qquad \text{.....(2.81)}$$

where : K_{xo}, K_{xl} = stiffnesses of major axis end restraints at O and L, respectively

K_{yo}, K_{yl} = stiffnesses of minor axis end restraints at O and L, respectively

M_{rxo}, M_{rxl} = major axis restraining moments at O and L, respectively

M_{ryo}, M_{ryl} = minor axis restraining moments at O and L, respectively

Finally, the external bending moments may now be written as :

$$M_{\xi} = M_{xo} + M_{rxo} + -\frac{z}{L}- \{ M_{xl} + M_{rxl} - M_{xo} - M_{rxo}$$

$$+ \sum_{i=1}^{i=np} P_{yi} (L-z_i) \} - N.v_c - \sum_{i=1}^{i=nl} P_{yi} \langle z-z_i \rangle$$

$$+ \theta [M_{yo} + M_{ryo} + -\frac{z}{L}- \{ M_{yl} + M_{ryl} - M_{yo}$$

$$- M_{ryo} + \sum_{i=1}^{i=np} P_{xi} (L-z_i) \} + N.u_c$$

$$+ \sum_{i=1}^{i=nl} P_{xi} \langle z-z_i \rangle] \qquad \text{.....(2.82)}$$

$$M_{\eta} = M_{yo} + M_{ryo} - -\frac{z}{L}- \{ M_{yl} + M_{ryl} - M_{yo} - M_{ryl}$$

$$+ \sum_{i=1}^{i=np} P_{xi} (L-z_i) \} + N.u_c + \sum_{i=1}^{i=nl} P_{xi} \langle z-z_i \rangle$$

$$- \theta [M_{xo} + M_{rxo} + -\frac{z}{L}- \{ M_{xl} + M_{rxl} - M_{xo}$$

$$- M_{rxo} + \sum_{i=1}^{i=np} P_{yi} (L-z_i) \} - N.v_c$$

$$- \sum_{i=1}^{i=nl} P_{yi} \langle z-z_i \rangle] \qquad \text{.....(2.83)}$$

$$M_{\zeta} = [\, M_{xo} + M_{rxo} + \frac{z}{L} \{ M_{xl} + M_{rxl} - M_{xo} - M_{rxo} + \sum_{i=1}^{i=np} P_{yi} (L-z_i) \} - N.v_c - \sum_{i=1}^{i=nl} P_{yi} \langle z-z_i \rangle + N.v_o \,] \frac{du}{dz} + [\, M_{yo} + M_{ryo} + \frac{z}{L} \{ M_{yl} + M_{ryl} - M_{yo} - M_{ryo} - \sum_{i=1}^{i=nl} P_{xi} (L-z_i) \} + N.u_c + \sum_{i=1}^{i=nl} P_{xi} \langle z-z_i \rangle \,] \frac{dv}{dz} + \frac{v_c}{L} \{ M_{yo} + M_{ryo} - M_{yl} - M_{ryl} + \sum_{i=1}^{i=np} P_{xi} (L-z_i) \} + \frac{u_c}{L} \{ M_{xo} + M_{rxo} - M_{xl} - M_{rxl} - \sum_{i=1}^{i=np} P_{yi} (L-z_i) \} + \sum_{i=1}^{i=nl} P_{yi} (u-u_i) - \sum_{i=1}^{i=nl} P_{xi} (v-v_i) - \frac{v}{L} \sum_{i=1}^{i=np} P_{xi} (L-z_i) + \frac{u}{L} \sum_{i=1}^{i=np} P_{yi} (L-z_i) \qquad \ldots\ldots(2.84)$$

Equations 2.82-2.84 can be applied to beam-columns with axial and concentrated transverse loads. Solution to the problem on beam-columns with distributed load can be made with approximation, the load is divided into several divisions and each division is represented by a concentrated load as shown in Fig. 2.18.

3. SOLUTION FOR DEFLECTED SHAPE

3.1. THEORY

The method is based on satisfying equilibrium between internal stress resultants and external forces using equations developed previously. Two basic algorithms are required for calculating the deflected shape of the beam-column. The first one relates to the stress resultants within the section for an assumed strain distribution over the cross-section. Moment-thrust-curvature relations described in Chapter 2 are adopted for this purpose. The second algorithm deals with convergence to the values of the asumed deflections, so that the internal stress resultants balance the external forces.

For the reduction of continuum to a system with a finite number of degrees of freedom, finite difference methods are employed in computing derivatives of functions. Let the beam-column length be divided into n equal segments as shown in Fig. 3.1. End O is identified as nodal point 1 and end L as nodal point (n+1). Further, to simplify the derivation, deflections u_i, v_i and θ_i will be replaced by w_{3i-2}, w_{3i-1} and w_{3i} respectively.

If 'in' and 'ex' are used as subscripts for internal resistances and external forces respectively, then

$$M_{\xi in} - M_{\xi ex} = 0 \qquad \text{.....(3.1)}$$

$$M_{\eta in} - M_{\eta ex} = 0 \qquad \text{.....(3.2)}$$

$$M_{\zeta in} - M_{\zeta ex} = 0 \qquad \text{.....(3.3)}$$

As described in Chapter 2, Equations (3.1) - (3.3) are functions of deflections. When the deflections do not satisfy the equilibrium conditions, there will be some differece between the internal stress resultansts and the external forces. These errors will be written as Z. Thus, there are three equations of Z that can be obtained for every nodal point. In general, the equation of Z may be expressed as :

$$Z_i = Z_i(w_1, w_2, w_3, \ldots w_m) = M_{i_{in}} - M_{i_{ex}} \qquad \ldots\ldots\ldots\ldots\ldots(3.4)$$

where : $m = 3(n+1)$

To get the correct deflection values, the Newton-Raphson method is employed for the iteration. According to this method, the correction value δ_{wi} may be obtained from :

$$\begin{bmatrix} \frac{\partial Z_1}{w_1} & \frac{\partial Z_1}{w_2} & \frac{\partial Z_1}{\partial w_3} & \ldots\ldots & \frac{\partial Z_1}{\partial w_m} \\ \frac{\partial Z_2}{w_1} & \frac{\partial Z_2}{\partial w_2} & \frac{\partial Z_2}{\partial w_3} & \ldots\ldots & \frac{\partial Z_2}{\partial w_m} \\ \frac{\partial Z_3}{\partial w_1} & \frac{\partial Z_3}{\partial w_2} & \frac{\partial Z_3}{\partial w_3} & \ldots\ldots & \frac{\partial Z_3}{w_m} \\ \ldots\ldots & \ldots\ldots & \ldots\ldots & \ldots\ldots & \ldots\ldots \\ \ldots\ldots & \ldots\ldots & \ldots\ldots & \ldots\ldots & \ldots\ldots \\ \frac{\partial Z_m}{\partial w_1} & \frac{\partial Z_m}{\partial w_2} & \frac{\partial Z_m}{\partial w_3} & \ldots\ldots & \frac{\partial Z_m}{\partial w_m} \end{bmatrix} \begin{bmatrix} \delta w_1 \\ \delta w_2 \\ \delta w_3 \\ \ldots \\ \ldots \\ \delta w_m \end{bmatrix} = - \begin{bmatrix} Z_1 \\ Z_2 \\ Z_3 \\ \ldots \\ \ldots \\ Z_m \end{bmatrix} \qquad \ldots\ldots\ldots\ldots(3.5)$$

The next trial value of w_i can be computed with :

$$w_i^{k+1} = w_i^k + \delta w_i \quad \text{.....(3.6)}$$

where k is the number of iteration.

The Jacobian matrix elements in Equation (3.5) are derivatives of Z. Equations (3.1) - (3.4) show that Z is a function of internal stress resultants and external forces. In computing internal stress resultants, strains and stresses within a section are affected by the curvature which is the second derivative of deflections. With the help of finite difference methods, derivatives of functions at a point are approximated by an algebraic expression consisting of the value of the function at that point and several nearby points. In this thesis, only three points are considered in the moment-thrust-curvature computation. This approximation makes a number of matrix element values become zero and the problem becomes simplified.

In computing the elements of Jacobian matrix, the end restraint effects, when present, should be considered. Without considering these, iteration of deflections may oscilate and not converge. Rotation of an end restraint generates moments which can influence the external forces at all nodal points. Neglecting the third order derivative, rotations about ξ axis at both ends of the beam-column can be approximated with finite difference methods as follows :

$$x_o = -\frac{1}{2\Delta z}\left(- 3w_2 + 4w_5 - w_8 \right) \quad .....(3.7)$$

$$x_1 = -\frac{1}{2\Delta z}\left(3w_{m-1} - 4w_{m-4} + w_{m-7} \right) \quad ..(3.8)$$

Taking zero values for deflections at both ends into account, Equations (3.7) - (3.8) yield :

$$\psi_{xo} = -\frac{1}{2\Delta z}\left(3w_5 - w_8 \right) \quad .....(3.9)$$

$$\psi_{x1} = -\frac{1}{2\Delta z}\left(- 4w_{m-4} + w_{m-7} \right) \quad .....(3.10)$$

Similarly

$$\psi_{yo} = -\frac{1}{2\Delta z}\left(4w_4 - w_7 \right) \quad .....(3.11)$$

$$\psi_{y1} = -\frac{1}{2\Delta z}\left(- 4w_{m-5} + w_{m-8} \right) \quad .....(3.12)$$

The restraint moment Equations (2.88) - (2.91) can be reformed :

$$M_{rxo} = - \frac{K_{xo}}{2\Delta z}\left(3w_5 - w_8 \right) \quad .....(3.13)$$

$$M_{rxl} = - \frac{K_{xl}}{2\Delta z} (4w_{m-4} - w_{m-7}) \quad .....(3.14)$$

$$M_{ryo} = \frac{K_{yo}}{2\Delta z} (4w_4 - w_7) \quad .....(3.15)$$

$$M_{ryl} = \frac{K_{yl}}{2\Delta z} (4w_{m-5} - w_{m-8}) \quad .....(3.16)$$

If the moments affected by the end restrains about X and Y axes at nodal point i are M_{rxi} and M_{ryi} respectively, then

$$M_{rxi} = \frac{(n+1-i)}{n} M_{rxo} + \frac{(i-1)}{n} M_{rxl} \quad .....(3.17)$$

$$M_{ryi} = \frac{(n+1-i)}{n} M_{ryo} + \frac{(i-1)}{n} M_{ryl} \quad .....(3.18)$$

From Equations (3.13) - (3.18) derivatives of M_{rxi} and M_{ryi} may be written as follows :

$$\frac{\partial M_{rxi}}{\partial w_5} = - \frac{(n+1-i)}{n} \cdot \frac{4K_{xo}}{2\Delta z} \quad .....(3.19)$$

$$\frac{\partial M_{rxi}}{\partial w_8} = \frac{(n+1-i)}{n} \cdot \frac{K_{xo}}{2\Delta z} \quad .....(3.20)$$

$$\frac{\partial M_{rxi}}{\partial w_{m-4}} = - \frac{(i-1)}{n} \cdot \frac{4K_{xl}}{2\Delta z} \quad .....(3.21)$$

$$\frac{\partial M_{rxi}}{\partial w_{m-7}} = \frac{(i-1)}{n} \cdot \frac{K_{xl}}{2\Delta z} \qquad .....(3.22)$$

$$\frac{\partial M_{ryi}}{\partial w_{4}} = \frac{(n+1-i)}{n} \cdot \frac{K_{yo}}{2\Delta z} \qquad .....(3.23)$$

$$\frac{\partial M_{ryi}}{\partial w_{7}} = -\frac{(n+1-i)}{n} \cdot \frac{K_{yo}}{2\Delta z} \qquad .....(3.24)$$

$$\frac{\partial M_{ryi}}{\partial w_{m-5}} = \frac{(i-1)}{n} \cdot \frac{4K_{yl}}{2\Delta z} \qquad .....(3.25)$$

$$\frac{\partial M_{ryi}}{\partial w_{m-8}} = -\frac{(i-1)}{n} \cdot \frac{K_{yl}}{2\Delta z} \qquad .....(3.26)$$

3.2. COMPUTATIONAL PROCEDURE

Based on the theory described above, a step by step procedure for obtaining failure loads is now outlined.

Step 1 Read in beam length, cross-sectional data, stress-strain characteristics of the beam material, residual-stress and imperfection data, number of used nodal and Gauss points, restraint data, loading conditions and loading increments.

Step 2 Compute geometric properties, section-area, Gauss-point coordinates, Jacobian matrix determinant, torsion constant and shear centre of the section.

Step 3 Compute residual-strain.

Step 4 Assume the imperfection and trial values for beam deflections.

Step 5 Compute rotation of the beam ends and derivative values needed for the next steps.

Step 6 For every nodal point, compute the external-moments due to the working load.

Step 7 For every nodal point, compute the moment-thrust-curvature relations for given curvature and axial-force. Linear interpolation method is adopted to get the neutral-axis position. Strain due to warping is considered. The internal-moments are computed after the neutral-axis position has been obtained.

Step 8 Compute the difference values between the external and internal moments. The differences so obtained are used to determine the correction of deflections in the Step 14. If the iteration is in the first cycle, then the next step will be Step 9. Otherwise, it will be Step 14.

Step 9 Change the value of u at nodal point (i). Then, compute the internal-moments at nodal points (i-1), (i) and (i+1). Compute the values of :

$$\frac{\partial M_{\xi(i-1)}}{\partial u_i}, \frac{\partial M_{\eta(i-1)}}{\partial u_i}, \frac{\partial M_{\zeta(i-1)}}{\partial u_i}, \frac{\partial M_{\xi(i)}}{\partial u_i}, \frac{\partial M_{\eta(i)}}{\partial u_i},$$

$$\frac{\partial M_{\zeta(i)}}{\partial u_i}, \frac{\partial M_{(i+1)}}{\partial u_i}, \frac{\partial M_{\eta(i+1)}}{\partial u_i} \text{ and } \frac{\partial M_{\zeta(i+1)}}{\partial u_i}$$

Step 10 Similarly for change of value of v, compute :

$$\frac{\partial M_{\xi(i-1)}}{\partial v_i}, \frac{\partial M_{\eta(i-1)}}{\partial v_i}, \frac{\partial M_{\zeta(i-1)}}{\partial v_i}, \frac{\partial M_{\xi(i)}}{\partial v_i}, \frac{\partial M_{\eta(i)}}{\partial v_i},$$

$$\frac{\partial M_{\zeta(i)}}{\partial v_i}, \frac{\partial M_{\xi(i+1)}}{\partial v_i}, \frac{\partial M_{\eta(i+1)}}{\partial v_i} \text{ and } \frac{\partial M_{\zeta(i+1)}}{\partial v_i}$$

Step 11 Change the value of θ at node (i). Compute the internal-moments at node (i-1), (i) and (i+1). Then, compute the values of :

$$\frac{\partial M_{\xi(i-1)}}{\partial \theta_i}, \frac{\partial M_{\eta(i-1)}}{\partial \theta_i}, \frac{\partial M_{\zeta(i-1)}}{\partial \theta_i}, \frac{\partial M_{\xi(i)}}{\partial \theta_i}, \frac{\partial M_{\eta(i)}}{\partial \theta_i},$$

$$\frac{\partial M_{\zeta(i)}}{\partial \theta_i}, \frac{\partial M_{\xi(i+1)}}{\partial \theta_i}, \frac{\partial M_{\eta(i+1)}}{\partial \theta_i} \text{ and } \frac{\partial M_{\zeta(i+1)}}{\partial \theta_i}$$

Step 12 Compute the element matrix values as the effect of restraint moments.

Step 13 After the Steps 9-12 have been done at all the nodal points along the beam, the matrix equation (3.5) may now be formed. Steps 9-13 have to be done once only, at the first cycle.

Step 14 Compute the correction values of the beam-deflections with the help of the matrix obtained from Steps 9-12. If all the correction values are less than the specified minimum correction values, then it may be assumed that the stable deflected shape has been obtained and Step 15 may now follow. Otherwise, correction to deflections should be made, and computation may be continued to Step 5. If the correction of deflections have been done several times, and stability cannot be obtained, then the loads should be reduced to the previous level at which convergence had been obtained. Reductions are also made to the loading increments. After the reduction to the loading increment has been done several times as specified, and the convergence still cannot be obtained, then the final load for which convergence has been obtained, may be specified as the collapse load.

Step 15 Increase the loads by the specified increment, and repeat Steps 5-14.

In determining flange shear (Eq. 2.38-2.39) in Step 11, it is found that, in elastic range, Equation (2.4) will give zero value to dM_{η_f}/dz, because the incremental value of θ at nodal point n affects the same to the flange moments, M_{n-1} and M_{n+1}, moments at nodal points (n-1) and (n+1). To make the iteration converge, Equation (2.4) for the first derivative should be modified. With reference to Fig. 3.2, the first derivative Equation (2.4) may be expressed as :

$$M_n = \frac{1}{\Delta z}(M_n - M_{n-1} - c_n) \qquad \ldots.(3.27)$$

where : $c_{n-1} = M_{n-1} - \frac{1}{2}(M_n + M_{n-2})$

$$c_n = M_n - \frac{1}{2}(M_{n+1} + M_{n-1})$$

$$c_{n+1} = M_{n+1} - \frac{1}{2}(M_{n+2} + M_n)$$

are correction terms.

Assuming values of c at two nodal points nearby are equal, c_n may be determined as follows :

$$c_n = -\frac{1}{4}(M_{n-1} - M_n - M_{n+1} + M_{n+2}) \quad ...(3.28)$$

or,

$$c_n = -\frac{1}{4}(M_{n-2} - M_{n-1} - M_n + M_{n+1}) \quad ...(3.29)$$

The particular equations used depend on the location of the point n.

3.3. COMPUTER PROGRAM "BECOL"

The program BECOL has been written for the inelastic stability of restrained pin-ended beam-columns having an axial load, biaxial end moments and some lateral loads in X and Y directions along the length. The beam-column cross-sections are uniform along the length, and may be double or single symmetric ones. The cross-section consists of three parts, the web and the two flanges. Every part may have different stress-strain characteristics. Different Gauss point numbers can be used for the flanges and the web, in the directions X and Y. The applied end moments in the two bending planes may all be different. The restraints at both ends are applied in the form of moment-

rotation characteristics which can be nonlinear. Lateral loads on the beam-column act through the original centroidal axis. Ultimate loads can be obtained by increasing some or all components of the loads.

As described in Chapter 2, the analysis essentially consists of obtaining equilibrium shapes corresponding to increasing values up to the peak of the applied load versus deflection curve. The Newton Raphson method is employed for the iteration in the analysis.

4. EXPERIMENTAL WORK

4.1. INTRODUCTION

A total of eight full scale tests were carried out on eccentrically loaded steel beam-columns. The test programme was originally proposed to explore the steel beam-column behaviour in the inelastic range. It was intended to study the effect of torsion on steel beam-column ultimate load.

4.2. DETAIL OF TEST PROGRAMME

Full scale tests were conducted on pin-ended steel beam-columns of 203mm - 203mm @ 46kg/m Universal Beam section. The tests reported here were divided into two groups of length, namely S and L. All beam-columns in the group S were 4m long, and the others were 6m. These length were chosen to represent the intermediate and the slender beam-columns respectively. Three loading types as shown in Fig. 4.1 were adopted. Loading Type A was a combination of an axial load and a major axis bending moment at both ends of the beam-column. The major axis end moment ratio was 1/3. Loading Type B was a combination of an axial load and a major axis bending moment at each end of the beam-column. The major axis end moment ratio was -1. Loading Type C was a combination of an axial load and biaxial bending moment at

both ends of the beam-column. The major and minor axes end moment ratios were 1/3 and 1 respectively. In all tests, bending moments at both ends were held constant, whereas the axial load was varied from zero up to the collapse load. Details of the cross section properties and the types of loading used are shown in Table 4.1.

4.3. MATERIAL TESTS

The tensile test specimens, as shown in Fig. 4.2, were taken from the cross-section of the rolled beam-column in accordance with BS 18. One was cut from the flange and the other two were cut from the web. During the tensile tests, two strain gauges were scanned through a computerised data logger. A plotter was attached to the computer to print the strain-stress curves. The test results are shown in Fig. 4.3 and Tables 4.2 - 4.4. In the theoretical work reported later, these stress-strain curves have been used for the computations.

4.4. INSTRUMENTATION

Strains were measured at three pre-selected sections in every specimen by means of electrical resistance strain gauges. There were thirty gauges in every section. The gauges were applied back-to-back on the flanges and the web of specimens according to the pattern shown in Fig. 4.4.

These gauges were intended to measure the strain distribution at the section, so that the yield zone could be detected. The length of each gauge was 6mm with an average gauge factor of 2.14 (supplied by the manufacturer).

Before mounting the strain gauge element on the surface of the specimens, the surface was smoothed and cleared of all dirt, so that the gauges could be mounted properly. In order to make the strain gauges work satisfactorily, it was necessary to prevent them from coming into contact with moisture. Absorption of moisture by the gauge matrix could result in an apparent reduction of the gauge factor and in extreme cases passage of current through a damp gauge could result in failure of wire due to corrosion. Ingress of moisture was prevented by coating the gauge with polythylene sheet obtained from CN Adhesives. Better measuring results could be expected by using smaller quantities of CN Adhesive spread as thinly as possible. After mounting and wiring up, a protective covering was placed over the gauges and the strain gauge circuit was tested.

During the beam-column testing period, strain gauges were scanned through a computerised data logger, SPECTRA-ms Measurement System. A SPECTRALAB software was used to scan, process, store and print the data collected.

Deflection of specimens under loading was measured using dial gauges. These gauges were supported on a rig isolated from the loading rig. Deflections were measured at five sections. These were located at quarter length, midlength, three-quarters length and one section close to each of the ends. Normally, there were three gauges in every section, one gauge was required for horizontal direction and the other two for vertical direction. With the two gauges in the vertical direction, it was intended to measure the twisting angle as well. The gauges had an accuracy of 0.01mm and could travel 25mm. Measurement of lateral displacement was also done at both ends of the beam-column, because, as a beam-column specimen was loaded the load cell and bearing rotated about axes parallel to the X and Y axes. These rotations resulted in displacements of the beam-column ends. Owing to friction at the moving surfaces, there was a tendency for dial gauges to stick, particularly if the spring return was relied upon to make the gauge follow the movement of the test specimen. To prevent this the gauges were tapped lightly before taking a reading.

To record rotational displacement at midlength of the beam-column, a mirror was set up at the web. The mirror reflected the readings from a stationary scale placed at an appropriate distance to give reasonable magnification of movements viewed through a telescope after each increment of load. The arrangement is shown in Fig. 4.5.

4.5. LOADING RIG

A rig to test beam-columns of length from 4m to 9m was available in the departmental laboratories. It was designed to test columns in the horizontal position, to enable easy monitoring of various gauges, and to keep the entire column length under observation throughout the duration of the test. A general arrangement of the rig together with some equipment used during the tests, is shown in Fig. 4.6-4.8.

The rig consists mainly of a substantial steel reaction block, designed and constructed to support a maximum horizontal load of 5000kN at a height of 1m. This force was transferred to the strong reinforced concrete floor. Detail of the reaction block at the ends are shown in Fig. 4.9.

In the first test, it was found that one of the reaction blocks lifted up under load. To prevent the rig from deflecting exessively, two sets of Macalloy bars were then placed in the rig. The rig already had provision for these bars but due to somewhat low ultimate load expected, it was initially considered unnecessary to install these bars. Thus the horizontal reaction was obtained partly from these Macalloy bars and partly from the strong concrete floor.

The horizontal testing position of the beam-columns provided convenient with regard to instrumentation, recording and overall observation. To test the beam-column horizontally, the dead weight of the specimen obviously generated additional bending moment, but this effect was assumed to be small and could be neglected.

The pin ended condition of the test was achieved by applying the load through a Glacier bridge bearing of rotational, non-translational type at the jack end. At the load cell end, freedom of rotation was provided by a tilting plate with a concave surface, and the load cell itself had a matching close fitting convex head, coated with PTFE.

The axial loading was applied by a double-acting hydraulic cylinder jack with a capacity of 5000kN maximum. This axial load was measured by a digital voltmeter connected to the load cell, and also by a meter in the pump circuit which activated the jack. The end moments were applied through moment-arms and a separate small hydraulic jack with capacity 300kN. The force generated by this small jack was measured by a meter in the pump circuit only.

To indicate the extent of yield zones, the first specimen was white-painted and the second one was white-washed. It was found that the white-wash could give better indication of the yield zone than the paint used. Accordingly the rest of the specimens were white-washed.

4.6. LOAD PATH FOLLOWED DURING THE TESTS

At the beginning of each test, full end moments were applied first, followed by a small axial load. The axial load was incremented by small amounts, up to failure. When the applied axial load reached about 80% of the predicted collapse load value, the loading increment was then reduced to 25kN. This amount was dictated by the accuracy of the scale used.

4.7. TEST PROCEDURE

For each specimen, a preliminary test was conducted to ensure the proper functioning of the instruments. This was applied to every specimen before the actual test. In the preliminary test, full bending moments at both ends and only axial loads up to a quarter of the predicted collapse load were applied. During this period, all the instruments were checked, and reset when necessary.

All initial gauge readings were recorded before the start of the actual test. The full bending moment at both ends were then applied. Another set of readings were recorded at this stage, which included all strain gauge readings, the major and minor axis dial gauge readings and the mirror reading for twist at the midlength. The bending moment at both ends were held constant by monitoring the meter of the pump circuit. Axial loads were then applied in

small increments. After each increment a complete set of readings was also recorded. During the test, travel capacity of the dial gauges was checked. Resetting of dial gauges was effected before they could not travel further.

In the inelastic range it was necessary to wait until the specimen settled down before taking strain and displacement readings. A specimen was considered to be in equilibrium when no appreciable change occured in the reading of the measurement monitor. Settling down required about ten minutes for most beam-columns.

During the last increment of load, the rate of displacement increased rapidly indicating that the ultimate load of the beam-column had been exceeded.

4.8. TEST RESULTS AND COMMENTS

The experimental research programme undertaken was divided into two main groups according to slenderness ratios :

Group S : Short beam-columns with slenderness ratio $L/r_v = 78.$

Group L : Long beam-columns with slenderness ratio $L/r_v = 117.$

In the first test, for Specimen S1, the rig was not provided with Macalloy bars. Thus, the horizontal reactions were supplied by the strong floor only. Due to the bending moment resulting from the 1m lever arm, one of the reaction block was lifted about 15mm. Obviously this movement affected the specimen deflections, and corrections were made by taking the beam-column end deflections into account. Later, to prevent the rig from deflecting exessively, starting from the second test, Macalloy bars were placed in the rig. Thus, the horizontal reaction was supplied partly by the strong floor and partly by those Macalloy bars.

It was interesting to note that the mode of failure of the beam-columns in both groups, S and L, were the same. Except for Specimens S4 and L4, all beam-columns failed out of the plain of the applied bending moment. At failure, in all cases, physical collapse occured with large minor axis deflection and twist. Further, local buckling occured at the compression flange, close to the ends where the maximum major axis moment was applied. Judging by the presence of yield pattern on the whitewashed surfaces, this local buckling was inelastic in nature.

All the experimental results are presented graphically in Fig. 4.12-4.27. The major and minor axis deflections, twisting angle and strain values are plotted for selected nodal points only. Discussion of the results are presented in Chapter 5, when comparing with theory, and Chapter 6.

4.8.1. Specimens S1 and L1

Specimen S1 and L1 were tested with loading type A. Major axis bending moments at both ends were 4500kN-cm and 1500kN-cm. These moments were generated by applying a small jack at the moment-arms. The small jack also contributed 60kN axial load to the beam-column. A variable axial load was generated by the double acting cylinder jack. Due to the initial deflections and the nature of lateral-torsional instability, this load generated minor axis bending moments to the beam-column.

The paint of Specimen S1 started flaking at the compression flange close to the large applied moment when the total axial load reached 1010kN. The same happened with Specimen L1 with the whitewash when the total axial load reached 960kN. The failure of the specimens was caused by a combination of lateral bending and twisting. Specimen S1 collapsed when the total axial load reached 1185kN, Whereas Specimen L1 collapsed when the total axial load reached 1010kN.

4.8.2. Specimens S2 and L2

Loading type B was adopted to test Specimen S2 and Specimen L2. The applied major axis bending moments for these tests were 3000kN-cm and -3000kN-cm. To generate these moments, two small jacks were applied at the moment

arms. These jacks contributed 120kN axial load to the specimen.

The white-wash started flaking when the axial load reached 1370kN for Specimen S2, and to 1120kN for Specimen L2, at the compression flanges close to the ends, and at the web laterally along the beam-column. The failure occured when the total axial load reached 1570kN for Specimen S2, and 1270kN for Specimen L2.

4.8.3. Specimens S3 and L3

In common with Specimens S1 and L1, Specimens S3 and L3 were tested with loading type A. In these tests, compared with the former, smaller bending moments were applied. The moments were 1500kN-cm and 500kN-cm, and the small jacks contributed 20kN axial load to the beam-column. Again, additional minor axis bending moments were taken into account for the lack of straightness.

Flaking of the white-wash occured first at the compression flange close to the ends, when the applied axial load reached 1020kN for Specimen S3, and 1070kN for Specimen L3. Finally, the collapse occured when the axial load reached 1520kN for Specimen S3, and 1120kN for Specimen L3.

4.8.4. Specimen S4

The loading type C was first adopted to test Specimen S4. The constant forces to generate major and minor axes bending moments at both ends were 40kN and 5kN respectively. Thus the applied major bending moments at the two ends were 3000kN-cm and 1000kN-cm, whereas the minor axis bending moments at the two ends were 300 kN-cm each. The forces which were applied at the moment arms contributed a total of 45kN axial force to the beam-column.

When the axial load reached 1445kN, the white-wash started flaking at the compression flange close to both ends. Later, the beam-column collapsed when the applied axial load reached 1495kN. Unexpectedly, the specimen bent about the minor axis, and in the opposite direction of the applied moment. On dismantling, it was found that the bolt holes of the beam-ends were not in the correct position. For this reason, the axial load acted with eccentricity 3mm and generated minor axis bending moment in the opposite direction to the applied moment. Since the bending moment generated by the eccentric loading was larger than the applied moment, the deflected shape was dictated by this moment.

4.8.5. Specimen L4

For this test loading type C was adopted. The minor axis bending moments equal at two ends, were 1200kN-cm. The major axis bending moments were 3000kN-cm and 1000kN-cm. The jacks applied to generate end-moments contributed 60kN axial load to the specimen.

Flaking of the whitewash occured firstly at the compression flange close to the end with the large applied moment when the total axial load reached 760kN. Later, collapse was reached at 860kN total axial load.

4.8.6. Conclusions from the Test Results

The experiments showed that all specimen failures occured with large minor axis deflection and twist. The slopes of minor axis deflection curves near failure were less than those of the major axis. The growth of the twisting deformations was excessive and the slopes of the curves were nearly zero at the peak. These failures were characteristic lateral torsional buckling failures. Even when minor axis bending moments were not applied in Loading Cases 1 and 2, the same type of failure occured (Specimens S1, S2, S3, L1, L2 and L3). From Fig.4.12-4.19 the dominant effects which caused failures could be determined. For Specimens S4, L1 and L2, the dominant effect was minor axis deflection. The failure of Specimens S1, S3, L3 and L4 was

caused by minor axis deflection and twist. Both effects were equal. Finally, twist was the dominant effect which caused the failure of Specimen S2.

5. VALIDATION OF THE PROPOSED METHOD

5.1. INTRODUCTION

The main purpose of the analytical method described in Chapter 2 and 3 was to simulate actual tests, so that exploratory calculations could be done with a computer to generate data needed for design. Before some relevant design data were presented which could be used with confidence, it was necessary to validate the proposed analytical method. Since the theoretical analysis was based on a simulated and idealized material, it was also necessary to validate the theory with actual experimentation. The experiments conducted for this purpose have been described in Chapter 4. Theoretical correlation with the results will be considered in this Chapter.

5.2. COMPARISON OF THE RESULTS WITH PREVIOUS WORKS

To verify the biaxial bending equations in the elastic range, the proposed method was used to solve the problems on biaxially loaded elastic columns which had been presented by Thurlimann [14], Dabrowski [15] and Culver [12]. The examples chosen for comparison were Problem 1 and Problem 2 of the above publications. The cross sectional properties and the loading conditions of the examples were as follows :

$b = 8.$ in $e_x = 5.$ in

$d = 13.675$ in $e_y = 5.$ in

$t_f = 0.528$ in $E = 30{,}000$ Ksi

$t_w = 0.333$ in . $L/r_y = 60$ and 140

For the comparison, the results are also presented relative to the current solutions and summarised in Tables 5.1-5.2.

From Tables 5.1-5.2 the average values of the horizontal and the vertical directions were computed. The average value obtained from Thurlimann's paper [14] was 0.997 with a standard deviation 0.016, whereas the average value determined from Dabrowski's paper [15] was 0.947 with a standard deviation 0.201. In this case, the deflection v at 10 kips axial loading of Problem 2, obtained by Dabrowski seemed to have an exeptional deviation. When this result was excluded, the average value became 0.992, and the standard deviation became 0.009. Further, the average value obtained from Culver's [12] was 0.992 with a standard deviation 0.008.

Two values of twisting angle at the midlength, obtained with the proposed method, were quite different in comparing with those of the previous work. It was obtained when the applied load was low. This inaccuracy could be related with the different allowable error used in the computer program. Since the inaccuracy only occured at low

loading, and the proposed method was specially developed to determine the ultimate load, the results obtained with 10 kips axial load were excluded for comparison. Thus, the average value for the angle of twist obtained from Thurlimann's was 1.013 with a standard deviation 0.034. From Dabrowski's, the average value was 1.043 with a standard deviation 0.032. Computation from Culver's gave the average value 1.033 with a standard deviation 0.039.

It has been shown that the current results are in close agreement with those of Culver, Thurlimann and Dabrowski. Slight differences are attributable to the differences in numerical approach.

Birnstiel [29] has conducted experiments to observe the behaviour of isolated steel H-columns loaded eccentrically with respect to both principal axes of the end cross sections. The results were then examined and compared by Harstead, Birnstiel and Leu [28], Sharma and Gaylord [35], Syal and Sharma [57], and Chen and Atsuta [58]. The agreement between those results appeard to be satisfactory. For this reason, it is advantageous to examine the proposed method with these works. The details of the section properties, the yield stresses and the loading conditions are summarised in Tables 5.3 - 5.4. The material is assumed to behave in an elastic-perfectly plastic manner. Comparison of the results is presented in

Table 5.5 which shows the nominal values of the ultimate loads, and in Table 5.6, which shows the relative values to the current results. The average ratio of ultimate loads obtained from Birnstiel [29] was 1.004 with a standard deviation 0.034. The corresponding correlation with Harstead [28] was 1.015 with a standard deviation 0.034. Comparison with Sharma and Gaylord [35] gave the average value 0.960 with a standard deviation 0.051. Further comparison, with Syal and Sharma [57] showed the average ultimate load ratio as 1.006 with a standard deviation 0.038. Finally, Chen and Atsuta's results[58] yielded the average value 0.983 with a standard deviation 0.100.

Further comparison of the current theoretical results was made with those of Virdi's and Sen's [59]. The method developed by Virdi [39,40] ignored torsional effects altogether, as it was developed primarily for torsionally stiff sections. The method developed by Sen [41] on the other hand included the effects of twisting and warping. Eight cases were analyzed, with three different lengths. The three length of 90in, 123in and 153in corresponded to weak axis slenderness ratio of 43, 59 and 74 respectively representing stocky, medium, and slender columns. Six of the columns analyzed were pin-ended while two of the longer columns had minor axis flexure restraint. One column (L150W) had a flexural end restraint stiffness 12,000 tonf-in/rad, and the other (L150H), of 20,000 tonf-

in/rad. The details of the columns analyzed are shown in Tables 5.7-5.8. The section properties were :

$b = 8.117$ in $\quad t_f = 0.683$ in

$d = 8.500$ in $\quad t_w = 0.405$ in

Comparison of the results is given in Table 5.9. In the case without considering torsional effects, in comparison with Virdi's, the average value of the ultimate load is 0.988 with a standard deviation 0.031. If the results of the restrained beam-column are excluded, the average value becomes 1.004 with a standard deviation 0.014. Thus, agreement of the numerical results of Virdi and the proposed method is satisfactory. On the other hand, Sen's results are quite different with those of the proposed method. In this case, the average value obtained is 0.920 with a standard deviation 0.071. There might be some different consideration in the analysis.

The validity of the proposed method for applications with lateral loadings was checked with Ho's [46] formula which almost exactly fitted the theoretical results given by Chen [42]. The problem chosen was Case (6), beam-columns of W 8x31 were analyzed under uniformly distributed load and the action of a single major axis end moment (Fig.5.1). Residual stresses was considered with $\sigma_{rc}=0.3\sigma_y$ and following the AISC pattern (Fig.2.1).

The material was assumed to have elastic-perfectly plastic stress-strain curve. Solutions were obtained for a beam-column with major axis slenderness ratio of 60, and loading factors q were chosen as 0 and 2.5. The section properties, yield stress and elastic modulus were :

$b = 203.2$ mm $\qquad t_f = 11.1$ mm

$d = 203.2$ mm $\qquad t_w = 7.3$ mm

$E = 207{,}000$ MPa $\qquad \sigma_y = 248.4$ MPa

Comparison of the results is presented in Table 5.10. The average ultimate load ratio of the current results was 0.972 with a standard deviation 0.037.

It is thus clear that the present computer program for the determination of failure loads in biaxial bending gives close agreement with existing biaxial computer programs discussed in this sections with exeption of Sen's. It remains to be shown that the prediction of ultimate loads for the case of biaxial bending by the present computer program is valid. This is achieved by comparing, in the next section, the theoretical results with the experimental results reported in Chapter 4.

5.3. COMPARISON OF THE THEORETICAL AND EXPERIMENTAL RESULTS

There are several uncertainties involved in actual experiments. Some of these are :

(a) Variation of imperfections along the beam-column length.

(b) Simulating theoretical support conditions and loading.

(c) Variation in stress-strain relations in different parts of the beam-column.

It was realized that there were too many possible combinations of those effects. Therefore, to avoid the exhaustive investigation of all the various parameters involved, the main effort was directed towards using the computer program to obtain corelation between experiment and theory, focussing on the effect of of variation of imperfections only. There are two types of imperfections commonly occuring in beam-columns, namely the residual stresses locked in the steel sections and the lack of straightness. The effects of these imperfections were studied in various combinations. A residual stress pattern of AISC type (Fig.2.1) was adopted with $\sigma_{rc} = 0.3\ \sigma_y$. Since the initial deflections were not measured in the experiment, the deflected shape was assumed to be a sine wave and the magnitude of the mid-length deflection was

taken as L/1000, where L was the length of the beam-column. This is now a standard practice.

Computer results were obtained for the following combinations of beam-column imperfections, and are presented in Table 5.11.

Case A : Results without any imperfections

Case B : Results with residual stresses only.

Case C : Results with an initial mid-length deflection of L/1000.

Case D : Results with combination of Case B and Case C imperfections.

Results for Case A show good agreement with the test results. The average value of P_{test}/P_{xy} for this case was 1.075 with a standard deviation of 0.107. The maximum error obtained was 31.5% for Specimen S4, but this was an exeptional deviation. If the results for Specimen S4 were taken from the Case C, where initial deflection was considered on the same side as the eccentricity, the moment generated by the eccentricity was resisted by that of the initial deflection. Then the ultimate load obtained theoretically increased, P_{test}/P_{xy} was reduced to 1.053 with a standard deviation of 0.057, and the maximum error became 12%.

According to the results described above, imperfections did not seem to affect very much to beam-columns strength. But it will be shown later, in the exploratory calcultaions, in Chapter 6, where the imperfection effects to collapse load are studied, that imperfection effects can reduce a large portion of beam-column strength. Since there are no beams perfectly straight in practice, and design must give solution on the safe side, imperfections must be considered in calculations.

It is interesting to compare the experimental load-deflection curve of the eight beam-columns with the theoretical calculated values. In Fig. 4.12 - 4.19 the deflection in horizontal and vertical directions and the angle of twist have been plotted. The theoretical results shown in the graphs were chosen from Cases A and C. As described previously, in Case A the specimens were considered to be perfectly straight. Therefore, when the Loading Type 1 or 2 was applied, theoretically no twist nor deflection in the X axis. Whereas practically, in the experiment the specimens were not perfectly straight, then twist and deflection were found accordingly. In Case C the specimens were considered to have an initial deflection of L/1000 at midlength, which was a standard practice. A standard is supposed to give solutions on the safe side. The initial deflections used are likely to be a bit bigger than the actual ones. Therefore, the ultimate loads

obtained theoretically were lower than those obtained experimentally. The specimens were obviously imperfectly straight, but the initial deflections were not as large as L/1000. Therefore, load-deflection relations obtained experimentally should be in the range between those obtained theoretically, with Cases A and C. These are shown in Fig.4.12-4.19, thus corelation between the experimental and theoretical result could be achived.

Strains recorded through the computer data logger were compared with those obtained theoretically using the method on Case A, where imperfections were not considered. Fig.4.20-4.27 show, in general good agreement between experiment and theory could be achieved, except for Specimen S2, which was the first to be tested using whitewash as yielding indicator. There was no experience in mixing the material with water, so that the whitewash was very thin and the water infiltrated to the strain-gauges. This caused the strain-gauges did not work properly.

6. APPLICATIONS AND DISCUSSION

6.1. INTRODUCTION

It may be stated that a computer program is now available which can be adopted for the stability analysis of beam-columns taking account the effects of torsion and the lateral deflection of the beam-column. Also included in the analysis are the effect of residual stresses and out-of-straightness. The method is not, however suitable for use as a direct design tool, since the procedure demands substantial computer time for each beam-column to be designed. The procedure can be used for verifying existing design method, or for developing new ones through parametric study. The data generated may be used to prepare dimensionless tables or charts for various shape of beam-column cross-sections and slenderness ratios.

In this chapter, the procedure is adopted to study the failure loads of bare steel beam-columns subjected to axial compression and transverse loads with varying values for the parameters such as slenderness ratio and lateral loading.

The solutions of several problems are examined with BS 5400:Part3 [60]. The effects of residual stresses and torsion to failure load are also assessed. Finally, discussion and conclusions drawn from the experimental and theoretical results are outlined.

6.2. APPLICATIONS

Beam-columns subjected to axial compression and transverse load are now investigated. From consideration of cross sectional properties only, the profile WF 8x31 section represents closely the most commonly used wide-flange section in America. Furthermore, curves corresponding to the WF 8x31 section represent a good approximation for any other wide-flange section and are conservative for the sections in the ratio of their shape factor 1.10 [43]. Therefore, the cross sectional properties of UC 203x203x46 which are similar to the WF 8x31 section are adopted for the investigation.

A multilinear stress-strain curve, as mentioned in Chapter 2, can give accurate results. Unfortunately, the curve is usualy very specific and does not represent a good approximation for other materials. For this reason a bilinear stress-strain curve which represents the elastic-perfectly plastic behaviour is employed in generating design data. In addition, an elastic-perfectly plastic assumption will give results on the safe side. Following BS 5400 : Part 3-6.6, the elastic modulus used in the analysis is 205,000 MPa, whereas the yield stress chosen is 355 MPa.

The effect of initial lack of straightness is always to reduce the beam-column strength. In this study the initial deflection is assumed to be a sinusoidal curve.

The initial mid-length deflection is determined following the Perry-Robertson formula, with $\eta = 0.003L/r$ as was used in BS153 [61], the predecessor to BS5400:Part3. Thus, the magnitude may be obtained from :

$$u_o = 0.003 \left(\frac{r^2}{h}\right) \left(\frac{L}{r}\right) \qquad \ldots\ldots\ldots(6.1)$$

where : u_o = initial deflection at midlength of the beam-column

r = radius of gyration

h = distance from centroid of the section to the extreme fibre on the concave side

L = length of the beam-column

The efffect of residual stresses on failure load, when major axist moments do not exist, is always to reduce the calculated value. But, when major axis moments are applied, the effect becomes inconsistent, failure loads are increased when the applied axial loads are low, while they are reduced when the applied axial loads are high. This will be shown later with the results obtained. Since the data generated are intended to be used in design, then the failure loads are computed with and without considering residual stresses. The lower results may be adopted for design requirements.

6.2.1. Loading Cases

In the examples with Loading Case 1, the beam-columns are investigated under axial compression load only (Fig. 6.1). Due to the initial deflection, the axial load also generates minor axis bending moment with the maximum magnitude at midlength of the beam-columns.

The Loading Case 2 deals with axial and concentrated transverse loads. The concentrated load is located at the midlength of the beam-columns. As for Loading Case 1, minor axis bending moment is generated by the axial load due to the initial deflection, together with major axis bending moment which is generated by the transverse load.

More examples are given with Loading Case 3, where a uniformly distributed load is applied. It is followed by Loading Case 4, where a linearly distributed load with the maximum magnitude at the midlength is applied. Finally, further examples are given with Loading Case 5. Again a combination between a linearly distributed load and an axial one is applied, but the maximum magnitude of the distributed load is located at one of the beam-column ends.

6.2.2. Comparison of the Results

The results obtained from the examples are compared with BS 5400. Further, comparison is also made between the results obtained with and without considering torsional effect. To avoid an exhaustive study, comparison of the results is made for beam-columns with slenderness ratios of 60 and 100 only. These slenderness ratios are expected to represent the intermediate and the slender beam-columns which are commonly used in practice.

According to BS 5400 : Part 3-10.6.1, a member subjected to axial compression should be such that the axial load does not exceed the resistance P_D which can be obtained with the following equations :

$$P_D = \frac{A_e \, \sigma_c}{\gamma_m \, \gamma_{f3}} \qquad \text{.....(6.2)}$$

$$\sigma_c = 0.5\,\sigma_y \left[\{1+(1+\eta)\,\frac{5700}{\lambda^2}\} - \sqrt{\{1+(1+\eta)\,\frac{5700}{\lambda^2}\}^2 - \frac{2280}{\lambda^2}} \right] \qquad \text{..(6.3)}$$

$$\lambda = \frac{L_e}{r}\sqrt{\frac{\sigma_y}{355}} \qquad \text{.....(6.4)}$$

For the section applied (UC203x203x46),

$$\eta = 0 \quad \text{when} \quad \lambda < 15$$

and $$\eta = 0.0045(\lambda - 15) \quad \text{when} \quad \lambda > 15$$

Additionally, A_e is the effective area of the section, γ_m and γ_{f3} for the section adopted may be taken as 1.2 and 1.1 respectively. Since the value of r/y of the section is 0.5, then the value of α in the Equation 6.3 may be taken as 0.0045.

According to BS 5400 : Part 3-10.6.2, a member subjected to coexistent compression and bending should be such that all cross sections within the middle third of the length of the member satisfy the following criterion :

$$\frac{P_{max}}{P_D} + \frac{M_{x\,max}}{M_{Dxc}} + \frac{M_{y\,max}}{M_{Dyc}} \leqslant 1.0 \qquad \ldots.(6.5)$$

where : P_{max}, $M_{x\,max}$, $M_{y\,max}$ are the maximum axial load, bending moment about the X-X and Y-Y axes, respectively.

P_D is as defined in Equations 6.2-6.4

M_{Dxc}, M_{Dyc} are the corresponding resistance of the member, with respect to the extreme copression fibres determined in accordance with 9.9.1 of the standard.

In the Loading Cases 2-5, the minor axis bending moments exist due to the initial deflections only. Since the initial deflection has been considered in determining P_D, the value of $M_{y\,max}$ for Equation 6.5 is taken as nil. Accordingly, comparison of the results to BS 5400 can be made with :

$$\frac{P_{max}}{P_D} + \frac{M_{x\,max}}{M_{Dxc}} \leq 1.0 \qquad \text{.....(6.6)}$$

The results are presented in Tables 6.1-6.25 and Fig. 6.2-6.10. It can be seen, comparison of the results of Loading Case 1 with BS 5400 shows a good agreement. The average ultimate load without considering residual stresses is 1.064 with a standard deviation 0.020. If the residual stresses are considered, the ultimate loads are reduced and the average value becomes 1.040 with a standard deviation 0.012.

Application of the method in solving the problems with Loading Cases 2-5 shows the effect of residual stresses is not consistent. The failure loads are increased when the applied axial loads are high, while they are reduced when the applied loads are high. Further, the effect of residual stresses on slender beam-columns is less than that on stocky beam-columns.

The effect of torsion on failure loads is always to reduce the calculated value. The magnitude of the effect is influenced by the slenderness ratio and the applied axial load. The more slender the beam-columns, the greater is the reduction in failure loads. Further, when the applied axial load is high, the reduction in calculated ultimate loads is correspondingly high.

6.3. DISCUSSION

Comparison of the experimental and theoretical results shows that a good agreement can be achieved when Case A, where imperfections are not considered, is applied. Since there are no perfectly straight beam-column in practice, it can be stated that the specimens are almost straight. Therefore the applied axial loads have generated small minor axis bending moment. The occurance of this moment was confirmed by the fact that all specimens with Loading Type 1 or 2 were bent about the minor axis at failure. Realizing that the failure of beam-columns is likely to be influenced by the lack of straightness, a further study was undertaken later. The method was employed to investigate the effect of initial deflection to ultimate loads. The failure loads of Specimens S1 and L3 were determined at maximum initial bow of L/1000, L/5000, L/10000 and L/20000. Comparison of the results are presented in Table 6.26, which shows that different value of computed loads obtained with and without initial deflections is considerable. Further investigation was undertaken to compare the results of Loading Case 1, obtained using initial deflections in accordance with BS5400 and BS153. Table 6.27 shows the maximum bows used and the results with residual stress consideration. It was found that the different initial bow between BS153 and BS5400 caused different results of less than 5%. It is interesting that a

maximum initial bow of as small as L/20,000 can reduce 16.2% of the ultimate load of a beam column with slenderness ratio 117. Thus, initial lack of straightness is a very important factor to be considered in formulating design methods.

The effect of residual stress on failure load has been studied in the application of the method in Section 6.2. Application with Loading Case 1, where axial load was applied, an no transverse loads existed, showed that the effect of residual stress was always to reduce the beam-column strength. This fact is shown in Table 6.1. The magnitude of reduction is around 2.5%.

When a combination of axial load and moment was applied, in Loading Cases 2-5, the effect of residual stress on failure loads was not consistent. It is shown in Tables 6.2-6.17 that the moment resistance is increased when the applied axial load is low, while it is reduced when the applied axial load is high. The increment to the moment resistance when a high axial load is applied, is not very large, but a reduction of as much as 15% can be achieved when the axial load is high.

Another investigation which has been carried in the application of the method is the effect of including torsion in calculating the failure load. Loading Cases 2-5 were applied to beam-columns with slenderness ratios of 60 and 100. The failure loads were determined using the

method with and without considering torsional effect. Comparison of the results is presented in Tables 6.18-6.25. The effect is always to reduce the ultimate load and was influenced by the slenderness ratio and the magnitude of the axial load. A large amount of reduction will be obtained if the slenderness ratio or the applied axial load is high. Reduction of as much as 35.7% can be obtained, even on beam-columns with slenderness ratio 60. Thus, torsional effect should be taken into account in formulating design aids for beam-columns.

It is interesting to compare the results obtained from Loading Case 1 with BS 5400:Part3-10.6.1. It was shown in Fig.6.2, that close agreement could be achieved when residual stresses were considered. It can be seen from the graph, the possible point with $P/P_y=1$ was at $L/r=0$. Thus, BS 5400 seemed to give higher strength at slenderness ratios between 0 and 30. Since very stocky beam-columns are rare in practice, and there are safety factors to be adopted in design, the differences can be tolerated. Further, when the slenderness ratio was greater than 30, the standard gave solutions on the safe side without large margins. Thus, BS 5400 appears to be very progressive in this case.

More comparisons of results with BS 5400 were made on problems with Loading Cases 2-5, where a combination of an axial load and a tranverse one was adopted. The problems are dealt with in BS 5400:Part3:10.6.1-10.6.2. Comparison

of the results was made at slenderness ratios 60 and 100, and is summarised in Tables 6.10-6.17. Application of BS 5400 on Loading Cases 2-5 at slenderness ratio 60, gave values around 10% lower than the present results. The results are on the safe side and the margin is not excessive. However, the application at slenderness ratio 100, gave the results as shown in Tables 6.14-6.17 around 21% lower than those obtained with the present method. Thus, when applying BS 5400 to beam-columns with Loading Cases 2-5 at high slenderness ratio, conservative results are obtained.

Investigation has also been taken on the effect of differences in loading cases. Comparison of the results of all loading cases was presented with Tables 6.2-6.9. It can be seen that the most severe loading was the uniformly distributed load (Case 3). Therefore a uniformly distributed load may be recommended to be adopted in developing approximation design methods.

7. CONCLUSIONS

1. This thesis describes an analytical method for calculating the ultimate loads of steel beam-columns, including the effects of torsion and warping, initial deflections, and residual stresses. A number of loading paths are allowed for. A computer program is now available which can be adopted for stability analysis of beam-columns. The method can be used for verifying existing design methods, or for developing new ones through parametric study.

2. Eight beam-columns have been tested under varying combinations of axial loading and unequal end mements. The beam-columns had two levels of slenderness ratio.

3. Comparison of the results for several loading cases has shown that the most severe loading is the uniformly distributed load. Therefore, a uniformly distributed load may be adopted in developing approximate design methods.

4. Comparisons were made between the experimental and theoretical ultimate loads as well as deflections and strains. The average value of P_{test}/P_{xy} was 1.053 with a standard deviation 0.057, and a maximum error 12%. These figures indicate very good correlation between theory and experiments.

5. The effect of torsion on calculated failure loads is always to reduce the calculated value. The magnitude of the effect is influenced by the slenderness ratio and the applied axial load. The more slender the beam-column, the greater is the reduction in failure load. When the applied axial load is high, the reduction in calculated ultimate loads is correspondingly high. Reduction of as much as 35% can be obtained, even on a beam-column with slenderness ratio 60.

6. The effect of residual stress on failure load when major axis bending moment does not exist (Loading Case 1), is always to reduce the beam-column strength. The magnitude of reduction is around 2-3%.

7. The effect of residual stress on failure load when major axis bending moments are applied is not consistent. The failure loads are increased when the applied axial loads are low, while they are reduced when the applied axial loads are high.

8. The difference in the ultimate loads obtained with and without initial deflections is considerable. A maximum initial bow of as small as L/20,000 can reduce the ultimate load of a beam-column, under axial and transverse loadings, with slenderness ratio 117, by as much as 16%.

9. Comparisons were also made between theoretical results and results predicted by BS5400:Part3. It is found that BS5400 predicts failure loads fairly accurately when applied to beam-columns under axial loading (Loading Case 1). However, when transverse loading is present in the case of slender beam-columns, conservative results are obtained, by as much as 25%.

10. There was no appreciable difference in the computed failure loads obtained on the basis of different measures of initial imperfections, one based on BS153 and the other on BS5400:Part3.

REFERENCES

[1] - VON KARMAN, T. Untersuchungen uber Knickfestigkeit. Mitteilungen uber Forschungsarbeiten auf dem Gebiete des Ingenieurwesens, No. 81, Berlin, 1910.

[2] - WESTERGAARD, H.M. and OSGOOD, W.E. Strength of Steel Columns. Transactions, ASME, Vol. 49, 50, AMP-50-9, p.65, 1928

[3] - JEZEK, K. Naherungsberechnung der Tragkraft Exzentrisch Gedruckter Stalstabe. Der Stahlbau, Vol. 8, p.89, 1935.

[4] - WAGNER, H. Torsion and Buckling of Open Sections. 25th Anniversary Publication, Technische Hochschule, Danzig, 1904-19029, pp. 329-343, 1936; translated as Technical Memorandum No. 807, U.S. National Advisory Commitee for Aeronautics.

[5] - GOODIER, J.N. Buckling of Compressed Bars by Torsion and Flexure. Cornell University Engineering Experiment Station Bulletin, No. 27, Ithaca, N.Y., December, 1941.

[6] - GOODIER, J.N. Flexural-Torsional Buckling of Bars of Open Section Under Bending, Eccentric Thrust or Torsional Loads. Cornell University Engineering Experiment Station Bulletin, No. 28, Ithaca, N.Y., January, 1942a.

[7] - GOODIER, J.N. Torsional and Flexural Buckling of Bars of Thin Walled Open Section Under Compressive and Bending Loads. Journal of Applied Mechanics, Vol. 9, No. 3, pp. A-103-A-107, September, 1942b.

[8] - BLEICH, F. and BLEICH, H. Buckling Strength of Metal Structures. McGraw-Hill Book Co. Inc., New York, 1952.

[9] - TIMOSHENKO, S.P. and GERE, J.M. Theory of Elastic Stability. 2nd edn., McGraw-Hill Book Co. Inc., New York, 1961.

[10] - NEAL, B.G. The Lateral Instability of Yielded Mild Steel Beams of Rectangular Cross-Section. Phil. Trans. of Royal Society, Series A, Vol. 242, January, 1950.

[11] - WITTRICK, W.H. Lateral Instability of Rectangular Beams of Strain Hardening Material Under Uniform Bending. Aeronautical Science, Vol. 19, No. 12, p. 835, December, 1952.

[12] - CULVER, C.G. Exact Solution of Biaxial Bending Equations. Journal of the Structural Division, ASCE, Vol. 92, No. ST2, Proc. Paper 4772, pp. 63-83, April, 1966a.

[13] - CULVER, C.G. Initial Imperfections in Biaxial Bending Equations. Journal of The Structural Division, ASCE, Vol. 92, No. ST3, Proc. Paper 4846, pp. 119-135, June, 1966b.

[14] - THURLIMANN, B. Deformation of and Stresses in Initially Twisted and Eccentriccally Loaded Columns of Thin-Walled Open Cross-Section. Report No. 3 to the Column Research Council and the Rhode Island Department of Public Works, Graduate Division of Applied Mathematics, Report Nos., E797-3, E696-3, Brown University, Providence, Rhode Island, June, 1953.

[15] - DABROWSKI, R. Dunnwandige Staabe Unter Zweiachsig Aussermittigem Druck. Der Stalbau, Wilhelm Enst & Sohn, Berlin - Wilmersdorf, Germany, December, 1961.

[16] - Prawel, S.P. and Lee, G.C. Biaxial Flexure of Columns by Analog Computers. Journal of the Engineering Mechanics Division, ASCE, Vol. 90, No. EM1, Proc. Paper 3805, pp. 83-111, February, 1964.

[17] - BIJLAARD, P.P., FISHER, G.P. and WINTER, G. Strength of Columns Elastically Restrained and Eccentrically Loaded. Proceeding, ASCE, Vol. 79, Separate No. 292, October 1953.

[18] - BIJLAARD, P.P. Buckling of Columns with Equal and Unequal End Eccentricities and Equal and Unequal End Restraints. Proceeding of the Second U.S. Natl. Congress of Applied Mechanics, 1954.

[19] - BAKER, J.F., HORNE, M.R. and HEYMAN, J. The Steel Skeleton. Vol. II, Cambridge University Press, 1956.

[20] - HORNE, M.R. The Elastic-Plastic Theory of Compression Member. Journal of the Mechanics and Physics of Solids, Vol. 4, p. 104, 1956.

[21] - HORNE, M.R. Safe Loads on I-Section Column in Structures Designed by Plastic Theory. Proceedings, Institution of Civil Engineers, Vol. 29, September, 1964.

[22] - HORNE, M.R. The Plastic Design of Columns. British Constructional Steelwork Association, London, Publication No. 23, 1964.

[23] - GALAMBOS, T.V. Inelastic Lateral Torsional Buckling of Eccentrically Loaded Wide-Flange Columns". Ph.D. Dissertation, Lehigh University, 1959.

[24] - OJALVO, M. Restrained Columns. Proceeding, ASCE, Vol. 85, No. EM5, October, 1960.

[25] - FUKUMOTO, Y. and GALAMBOS, T.V. Inelastic Lateral Torsional Buckling of Beam-Columns. Journal of the Structural Division, ASCE, Vol. 92, No. ST2, p.41, April, 1966.

[26] - JOHNSTON, B.G. Buckling Behaviour Above the Tangent Modulus Loads. Journal of the Engineering Mechanics Division, ASCE, Vol. 87, No. EM6, Proc. Paper 3019, pp. 79-99, December, 1961.

[27] - BIRNSTIEL, C. and MICHALOS, J. Ultimate Strength of H-Columns Under Biaxial Bending. Journal of the Structural Division, ASCE, Vol. 89, No. ST2, Proc. Paper 3505, pp. 161-197, April, 1963.

[28] - HARSTEAD, G.A., BIRNSTIEL, C. and Leu, K.C. Inelastic H-Columns Under Biaxial Bending. Journal of the Structural Division, ASCE, Vol. 94, No. ST10, Proc. Paper 6173, pp. 2371-2398, October, 1968.

[29] - BIRNSTIEL, C. Experiments on H-Columns under Biaxial Bending. Journal of Structural Division, ASCE, Vol. 94, No. ST10, Proc. Paper 6186, Oct., 1968, pp. 2429-2449.

[30] - HAUCK, G.F. and LEE, S.L. Stability of Elasto-Plastic Wide Flange Columns. Proceeding, ASCE, Vol. 89, No. ST6, December, 1963.

[31] - MILNER, H.R. The Elastic Plastic Stability of Stanchions Bent About Two Axes. Dissertation presented to the College at University of London, in partial fulfillment of the requirements for the degree of Doctor of Philosophy, December, 1965.

[32] - VINNAKOTA, S. and AOSHIMA, Y. Inelastic Behaviour of Rotationally Restrained Columns Under Biaxial Bending. The Structural Engineer, Vol. 52, No. 7, pp. 245-255, London, England, July, 1974.

[33] - VINNAKOTA, S. and AOSHIMA, Y. Spatial Behaviour of Rotationally and Directionally Restrained Beam-Columns. International Association for Bridge and Structural Engineering, Publications, Vol. 34-II, pp. 169-194, Zurich, 1974.

[34] - VINNAKOTA, S. and AYSTO, P. Inelastic Spatial Stability of Restrained Beam-Columns. Journal of the Structural Division, ASCE, Vol. 100, No. ST11, Proc. Paper 10919, pp. 2235-2254, November, 1974.

[35] - SHARMA, S.S. and GAYLORD, E. Strength of Steel Columns with Biaxially Eccentric Load. Journal of the Structural Division, ASCE, Vol. 95, No. ST12, Proc. Paper 6960, pp. 2797-2812, December, 1969.

[36] - LIM, L.C. and LU, L.W. The Strength and Behaviour of Laterally Unsupported Columns. Fritz Engineering Laboratory Report, No. 329.5, June, 1970.

[37] - SANTATHADAPORN, S. and CHEN, W.F. Analysis of Biaxially Loaded Steel H-Columns. Journal of the Structural Division, ASCE, Vol1. 99, No. ST3, p. 491, March, 1973.

[38] - SANTATHADAPORN, S. and CHEN, W.F. Tangent Stiffness Method for Biaxial Bending. Journal of the Structural Division, ASCE, Vol. 98, No. ST1, January, 1972.

[39] - VIRDI, K.S. Inelastic Column Behaviour - Its Application to Composite Column in Biaxial Bending and Stiffened Plates in Compression. Ph.D. Thesis, University of London, October, 1973.

[40] - VIRDI, K.S. and DOWLING, P.J. The Ultimate Strength of Biaxially Restrained Columns. Proceeding, Instn. Civ. Engrs, pp. 41-58, Part 2, 61, Mar., 1976.

[41] - SEN, T.K. Inelastic H-Column Performance at High Axial Loads. Ph.D. Thesis, University of London, 1976.

[42] - CHEN, W.F. and ATSUTA, T. Theory of Beam-Columns. Vol. 1, McGraw Hill Inc., New York, 1976.

[43] - CHEN, W.F. and ATSUTA, T. Theory of Beam-Columns. Vol. 2, McGRaw Hill Inc., New York, 1976.

[44] - Lui, M.L. and CHEN, W.F. Strength of H-Columns with Small End Restraints. The Structural Engineer, Vol. 61B, No. 1, pp. 17-26, March, 1983.

[45] - LUI, E.M. and CHEN, W.F. End Restraint and Column Design Using LRFD, Engineering Journal, AISC, First Quarter, 20, No. 1, 1983.

[46] - HO, D. Interaction Between Elastic Buckling and Plastic Collapse - A Study of The Failure of Beam-Columns. The Structural Engineer, Vol. 61B, No. 4, pp 79-87, December, 1983.

[47] - VIRDI,K.S. A New Technique for Moment-thrust-curvature Calculations for Columns in Biaxial Bending, Sixt Australian Conference on Mechanics and Strength of Materials. Canterburry, New Zealand, pp. 307-313, 1976

[48] - VIRDI,K.S. Design of Circular and Rectangular Hollow Section columns. Journal of Constructional Steel Research, September, pp. 35-45, 1981.

[49] - VIRDI,K.S. and DOWLING,P.J. Composite Column in Biaxial Loading, Axially Compressed Sructures. Edited by NARAYANAN, R. , Applied Science Publishers Ltd, Essex, 1983.

[50] - BROCKENBROUGH,R.L. and JOHNSTON,B.G. USS Steel Design Manual. United States Steel Corporation, 1983.

[51] - COLLATZ,L. Functional Analysis and Numerical Mathematics. Academic Press, New York, 1966.

[52] - VINNAKOTA,S. Finite Difference Method for Plastic Beam-Columns. In: Theory of Beam-Columns, vol. 2, edited by CHEN,W.F. and ATSUTA,T. , McGraw Hill, New York, 1977.

[53] - TRAHAIR,N.S. The Behaviour and Design of Steel Structures. Chapman and Hall, London, 1977.

[54] - GESUND,H. Stress and Moment Distributions in Three Dimensional Frames Composed of Non Prismatic Members Made of Nonlinear Material. In: Space Structures, pp. 145-153, Blackwell, Oxford and Edinburgh, 1967.

[55] - KOPAL,Z. Numerical Analysis. Chapman and Hall, London, 1961.

[56] - ZIENKIWICZ, O.C. The Finite Element Method in Engineering Science, McGraw Hill, London, 1971.

[57] - SYAL, I.C., and SHARMA, S.S. Biaxially Loaded Beam-Column Analysis. Journal of the Structural Division, ASCE, Vol. 97, No. ST9, Proc. Paper 8384, Sept., 1971, pp. 2245-2259.

[58] - CHEN, W.F., and ATSUTA, T. Ultimate Strength of Biaxially Loaded Steel H-Columns. Journal of the Structural Division, ASCE, Vol. 99, No. ST3, March, 1973, pp. 469-489.

[59] - VIRDI, K.S., and SEN, T.K., Torsion and Computed Ultimate Loads of H-Columns. Journal of the Structural Division, ASCE, Vol. 107, No. ST2, February, 1981, pp. 413-426.

[60] - BRITISH STANDARDS INSTITUTION, BS5400:Part3, Specification for Steel, Concrete and Composite Bridges, London, BSI, 1982.

[61] - BRITISH STADARDS INSTITUTION, BS153:Part 3B and 4, Specification for Steel Girder Bridges, London, 1972.

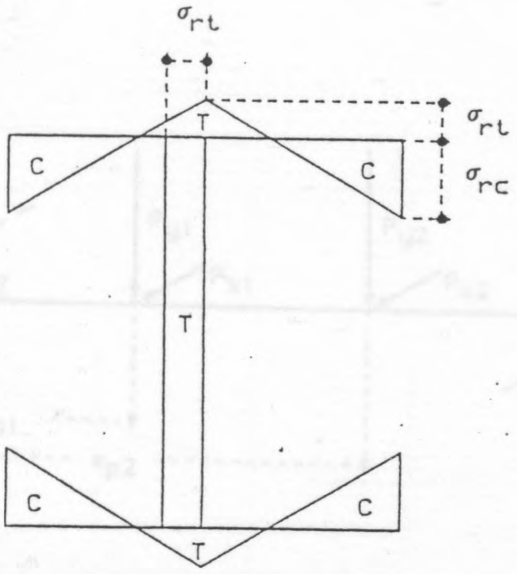

FIG. 2.1. LINEAR RESIDUAL STRESS DISTRIBUTION
(AISC PATTERN)

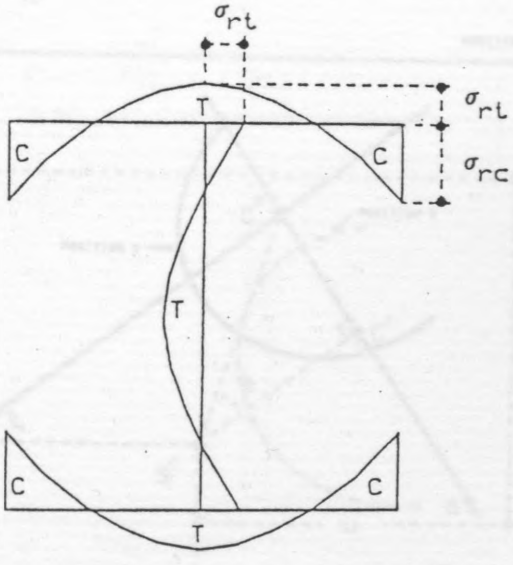

FIG. 2.2. PARABOLIC RESIDUAL STRESS DISTRIBUTION
(CAMBRIDGE PATTERN)

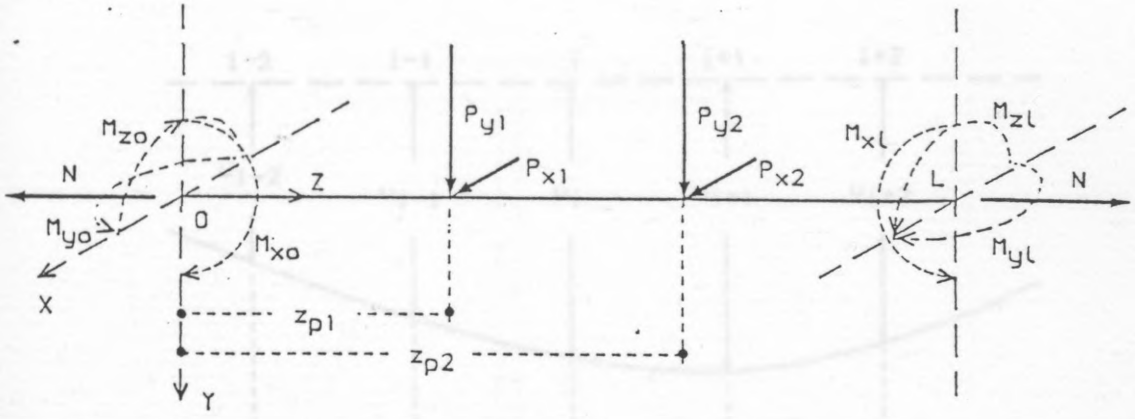

FIG. 2.3 LOADING SIGN CONVENTION USED IN THE ANALYSIS

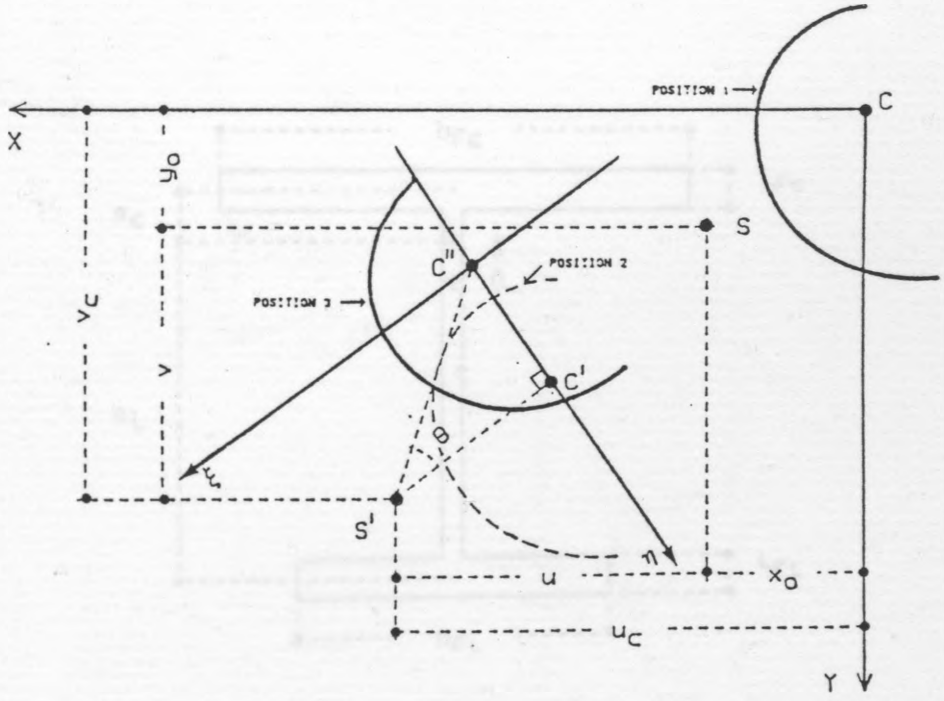

FIG. 2.4. DISPLACEMENT OF GENERAL CROSS SECTION

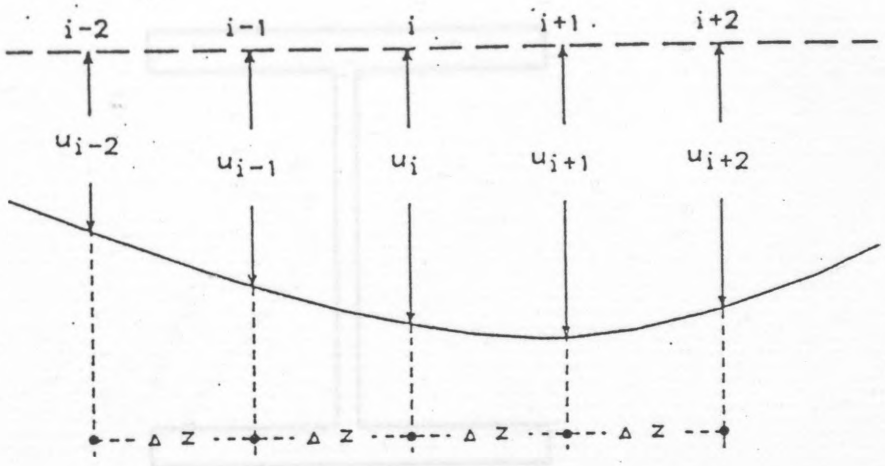

FIG. 2.5. PIVOTAL AND GRID POINTS

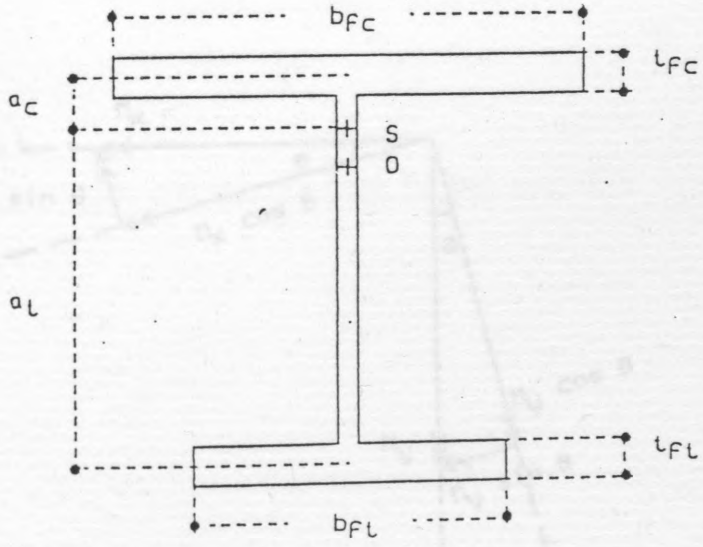

FIG. 2.6. TWIST CENTRE OF MONOSYMMETRIC SECTION

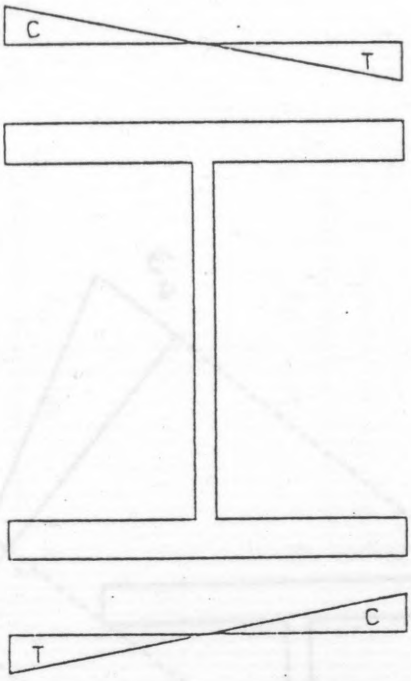

FIG. 2.7. FLANGE STRAIN DISTRIBUTION DUE TO WARPING

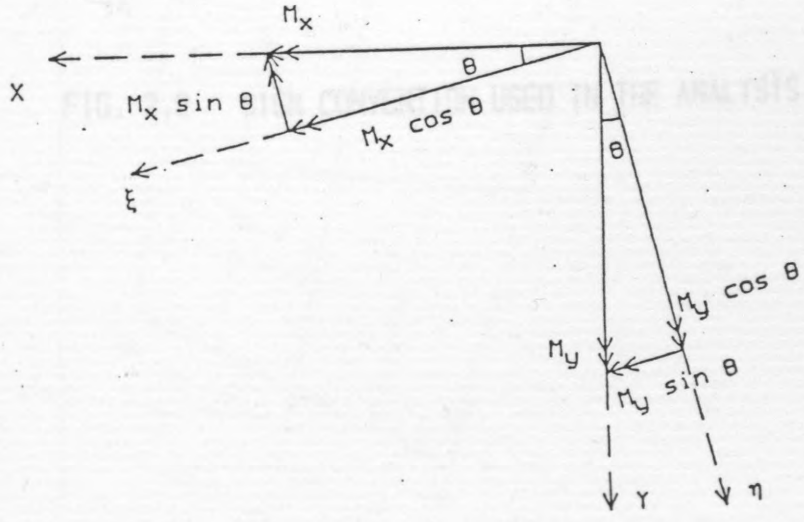

FIG. 2.8. COMPONENTS OF M_x AND M_y

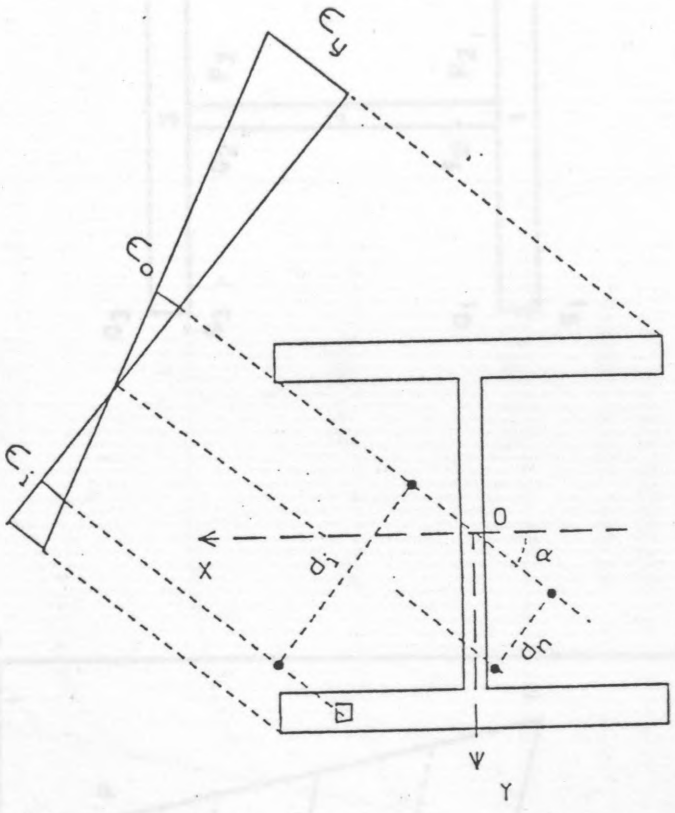

FIG. 2.9 SIGN CONVENTION USED IN THE ANALYSIS

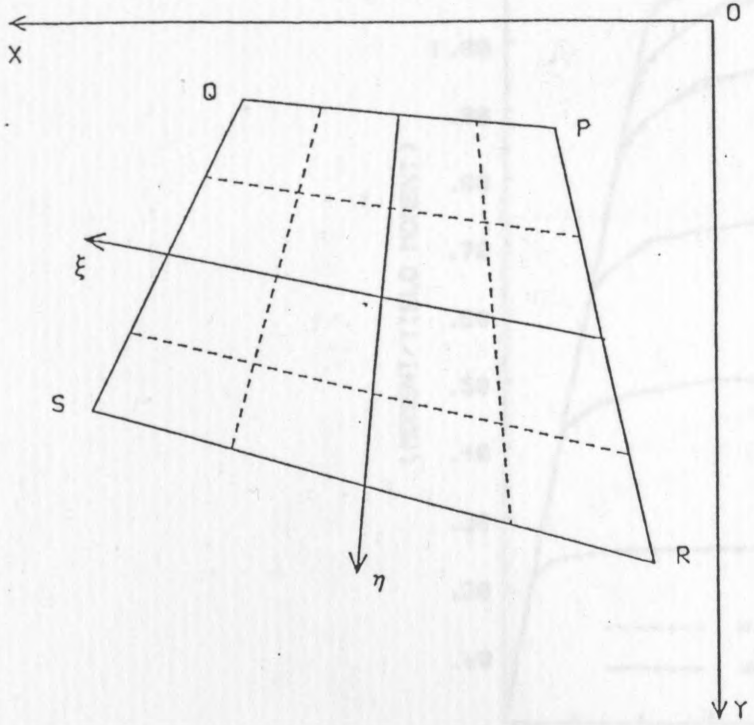

FIG. 2.10. NATURAL AND CARTESIAN COORDINATES SYSTEMS

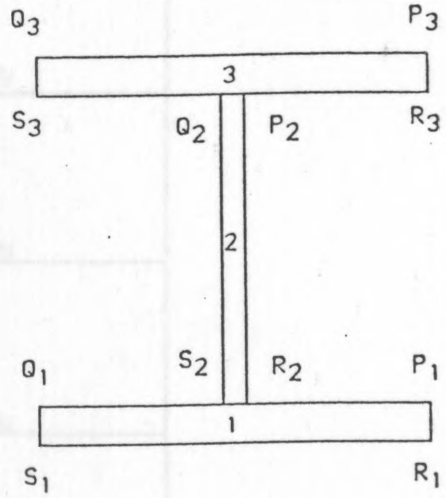

FIG. 2.11. SUBDIVISION OF CROSS SECTION

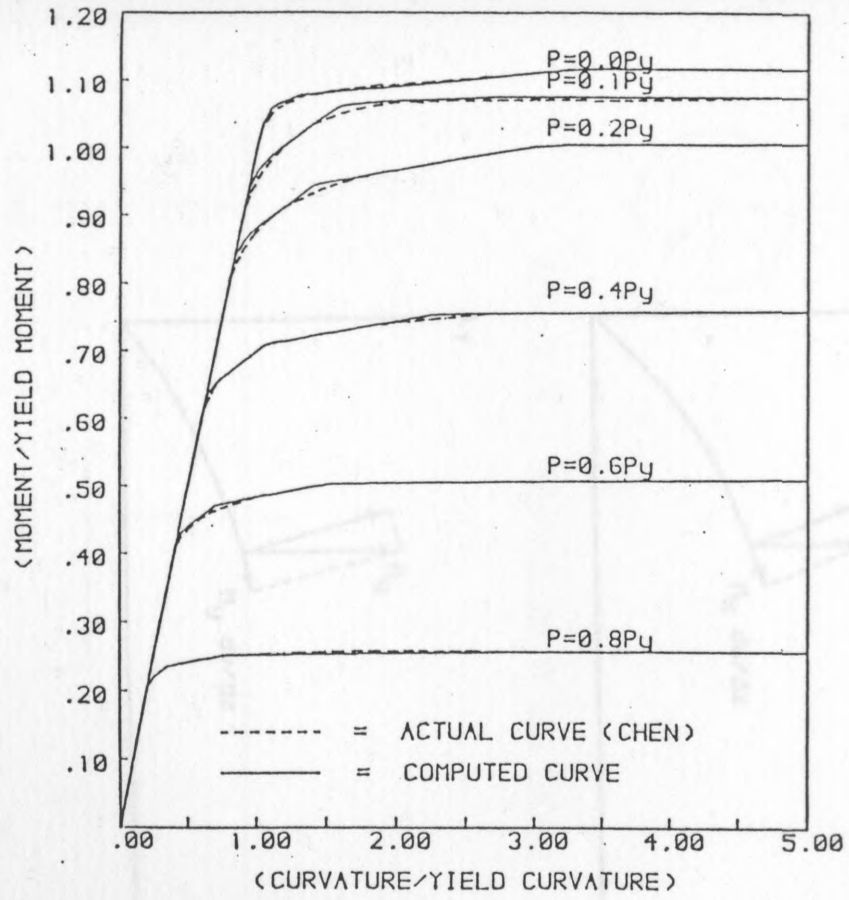

FIG. 2.12. MOMENT-THRUST-CURVATURE RELATIONSHIP

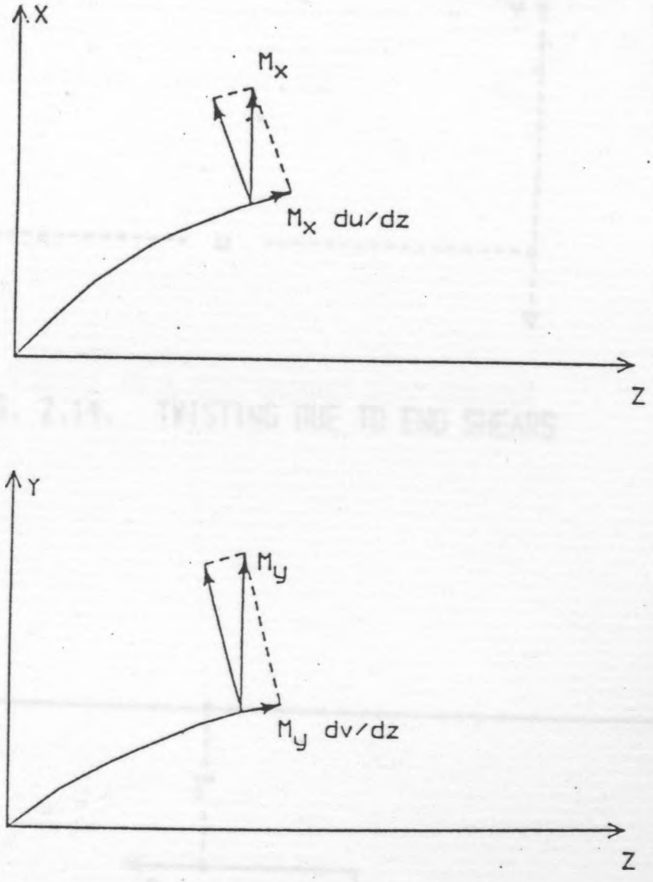

FIG. 2.13. TWISTING DUE TO COMPONENTS OF M_x AND M_y

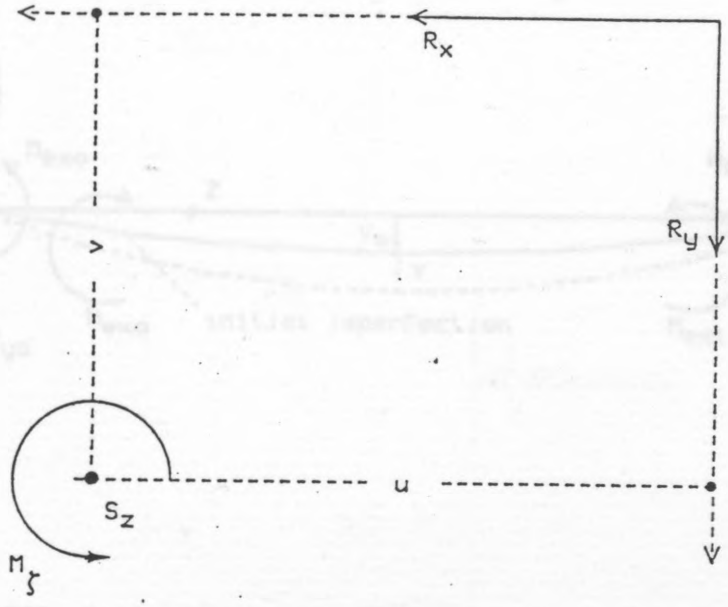

FIG. 2.14. TWISTING DUE TO END SHEARS

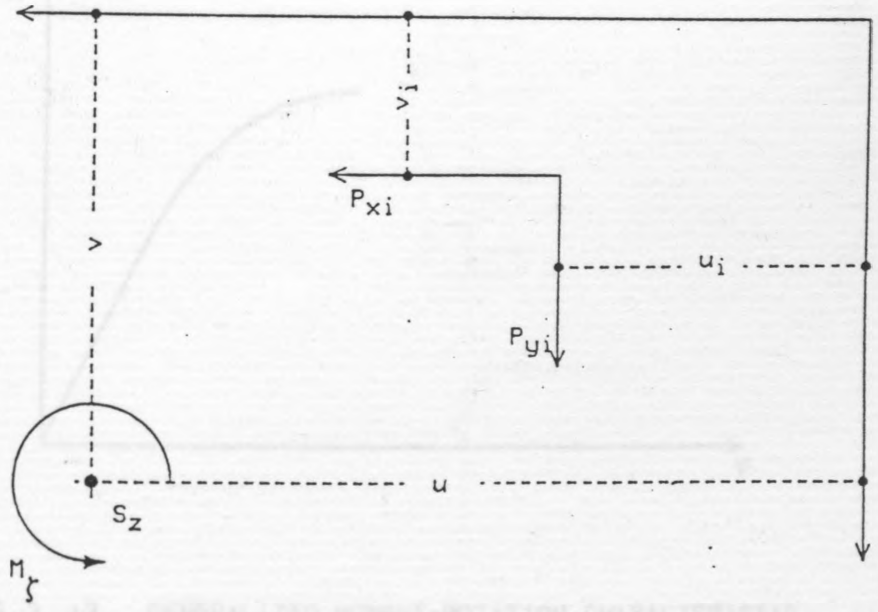

FIG. 2.15. TWISTING DUE TO LATERAL LOAD

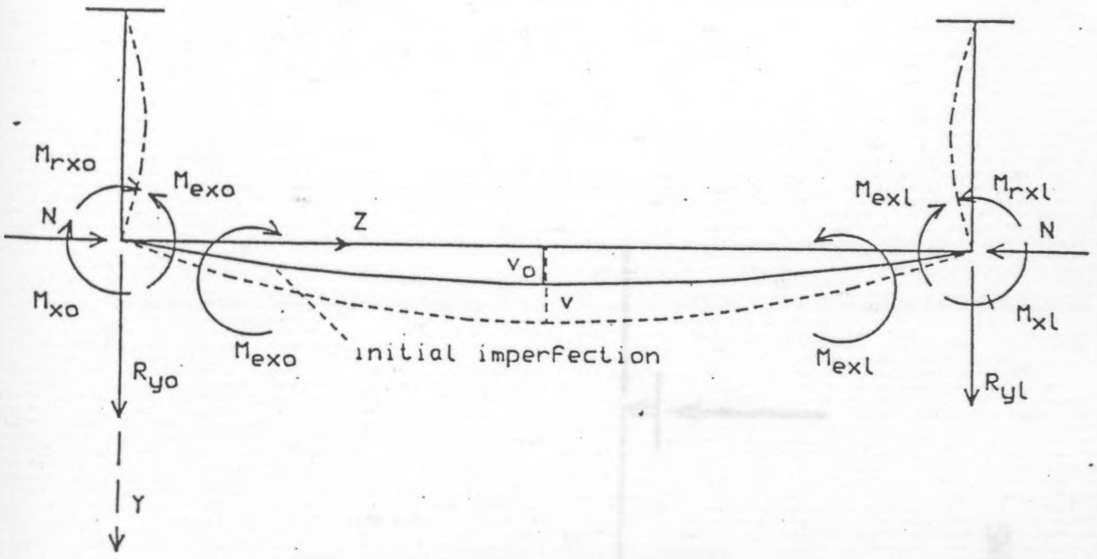

FIG. 2.16. FORCES IN A RESTRAINED BEAM-COLUMN

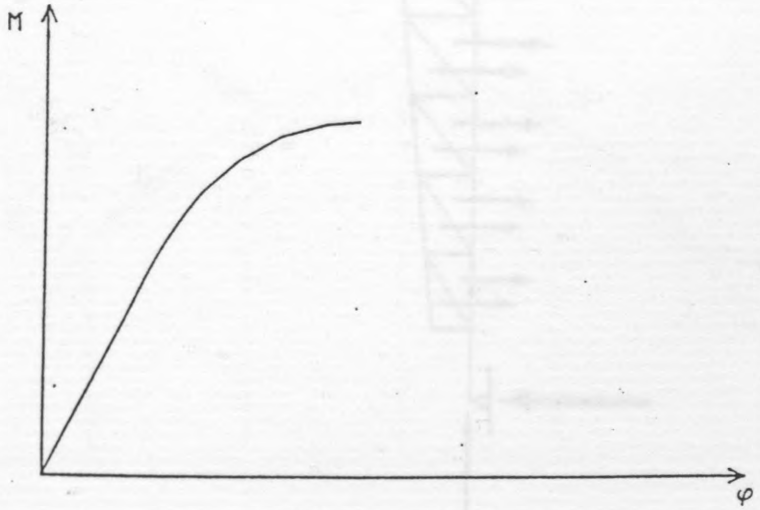

FIG. 2 .17. GENERALIZED MOMENT-ROTATION CHARACTERISTIC OF THE END RESTRAINT ON BEAM-COLUMN

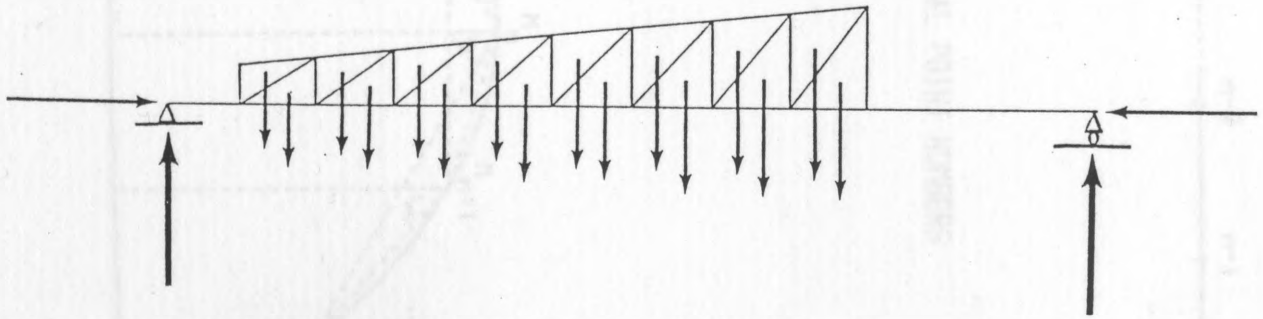

FIG. 2.18. LINEARLY DISTRIBUTED LOAD DIVISIONS

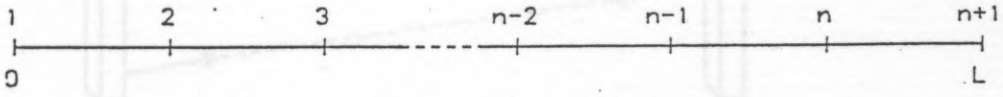

FIG. 3.1. NODAL POINT NUMBERS

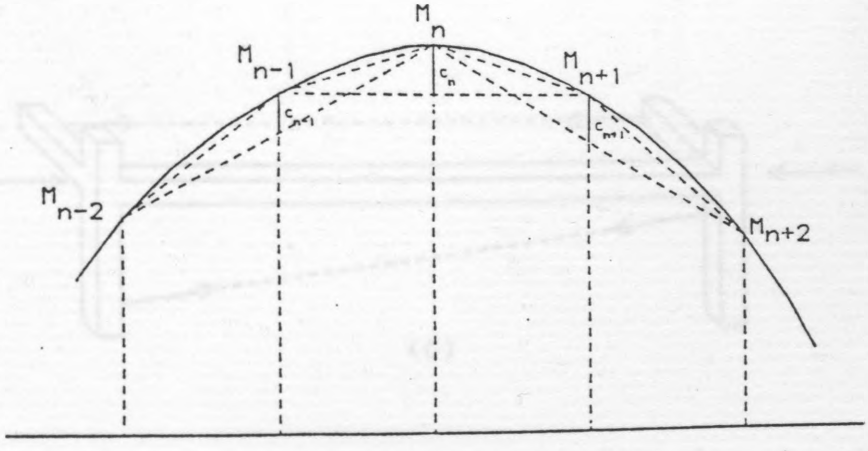

FIG. 3.2. GENERAL FLANGE BENDING MOMENT CURVE.

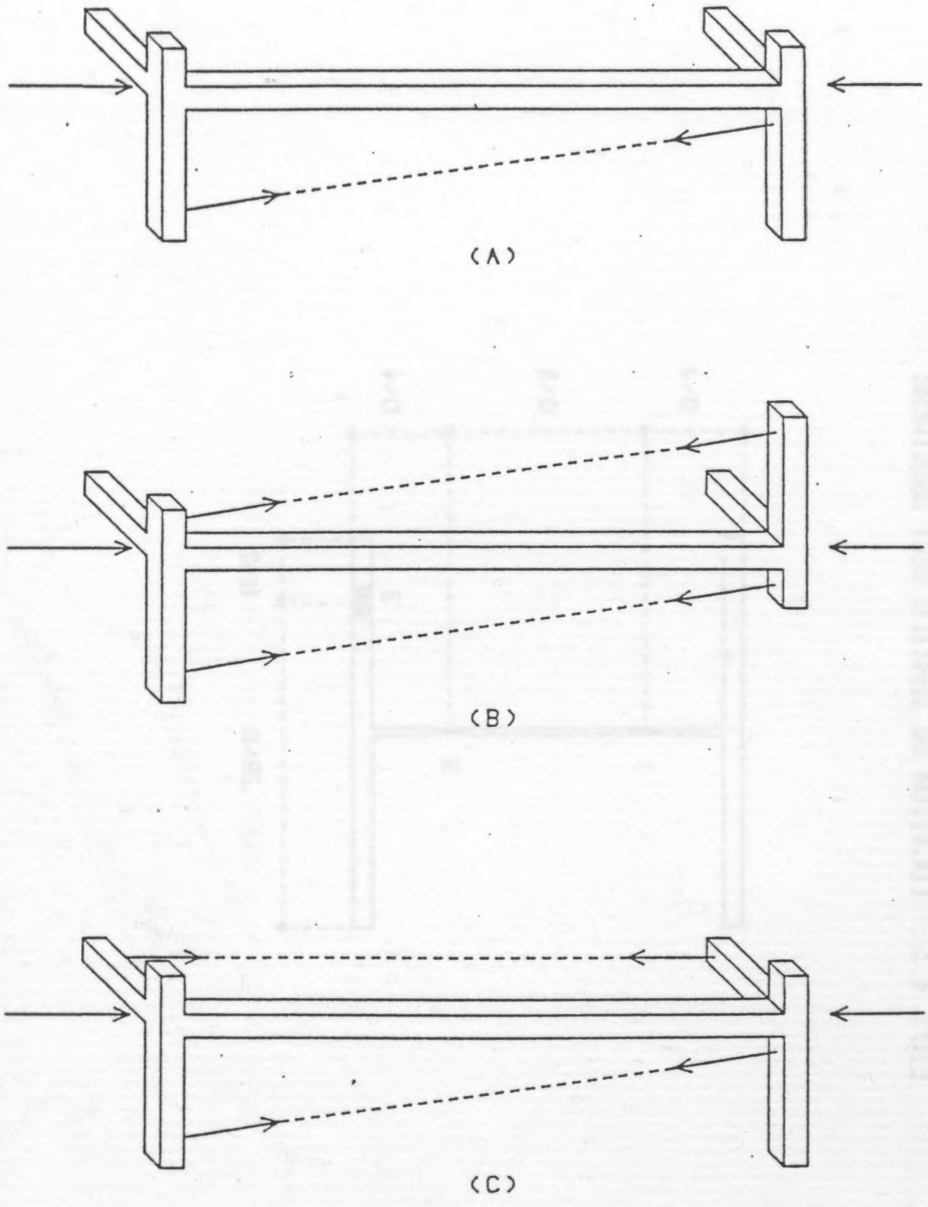

FIG. 4.1. LOADING TYPES

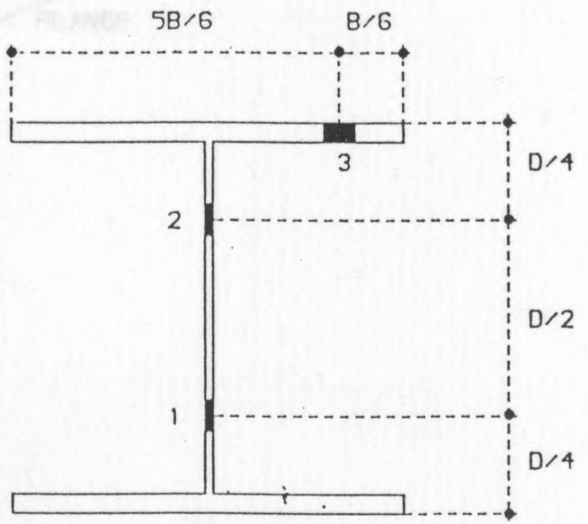

FIG. 4.2 LOCATION OF TENSILE TEST SPECIMENS

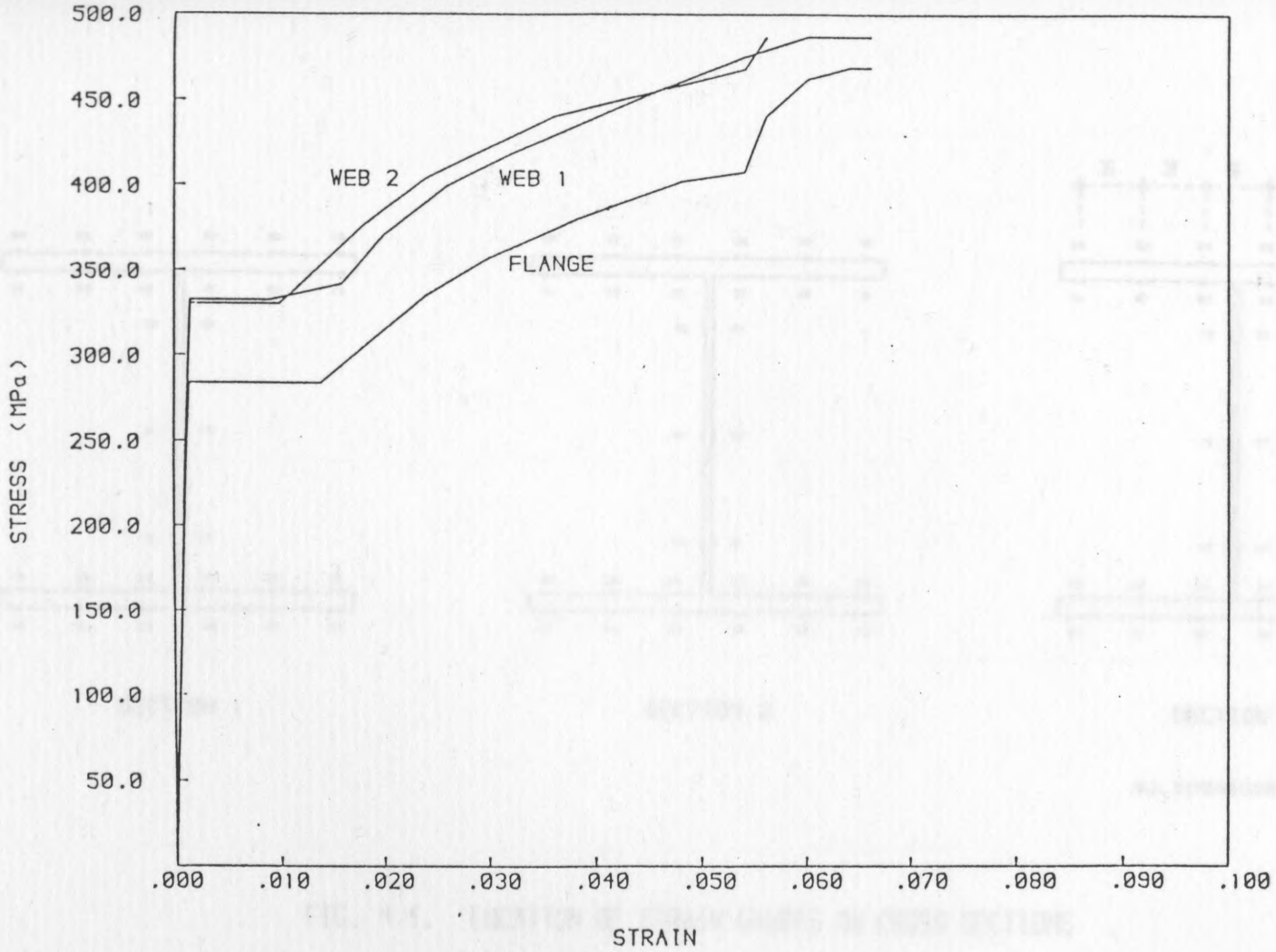

FIG. 4.3. EXPERIMENTAL STRESS-STRAIN CURVES

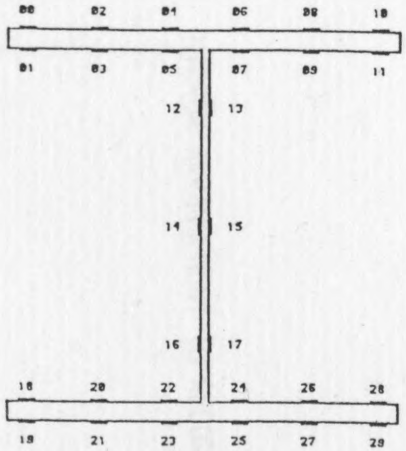

SECTION 1

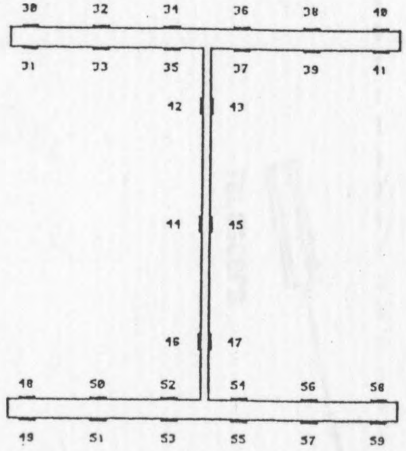

SECTION 2

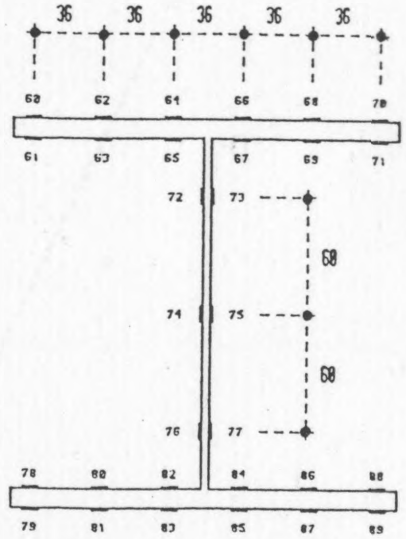

SECTION 3

ALL DIMENSIONS IN MM

FIG. 4.4. LOCATION OF STRAIN GAUGES ON CROSS SECTIONS

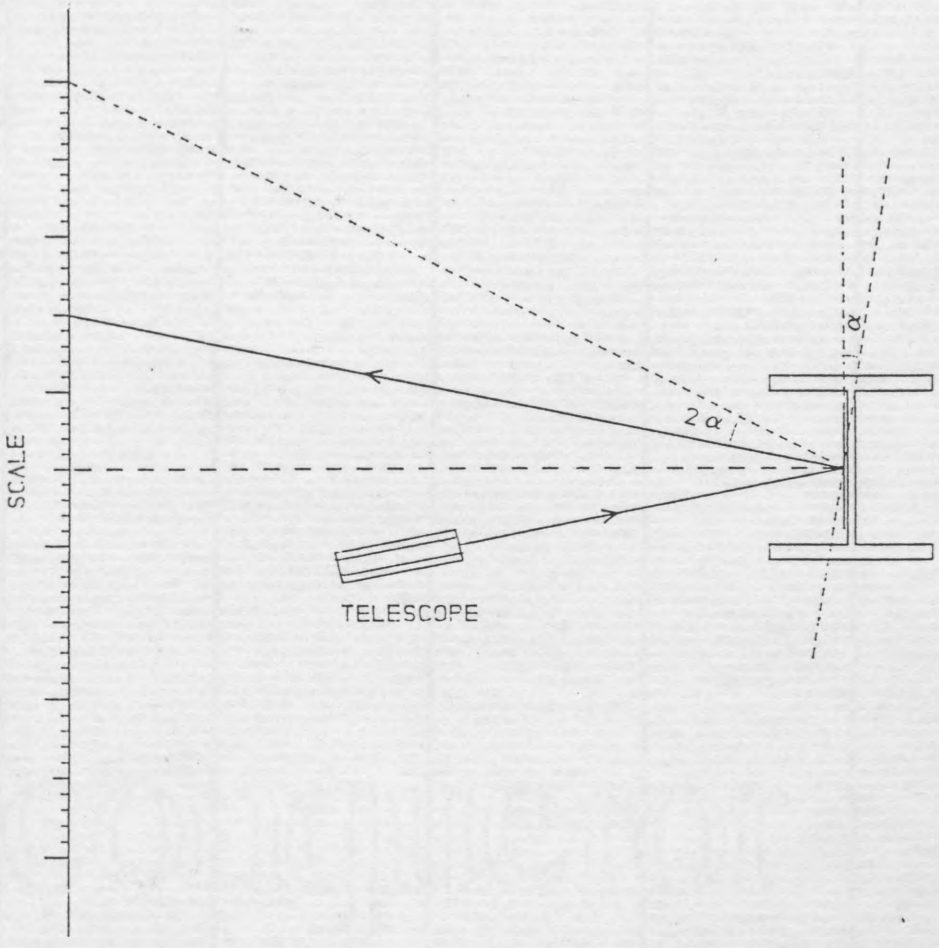

FIG. 4.5 MIRROR ARRANGEMENT TO RECORD ANGLE OF TWIST

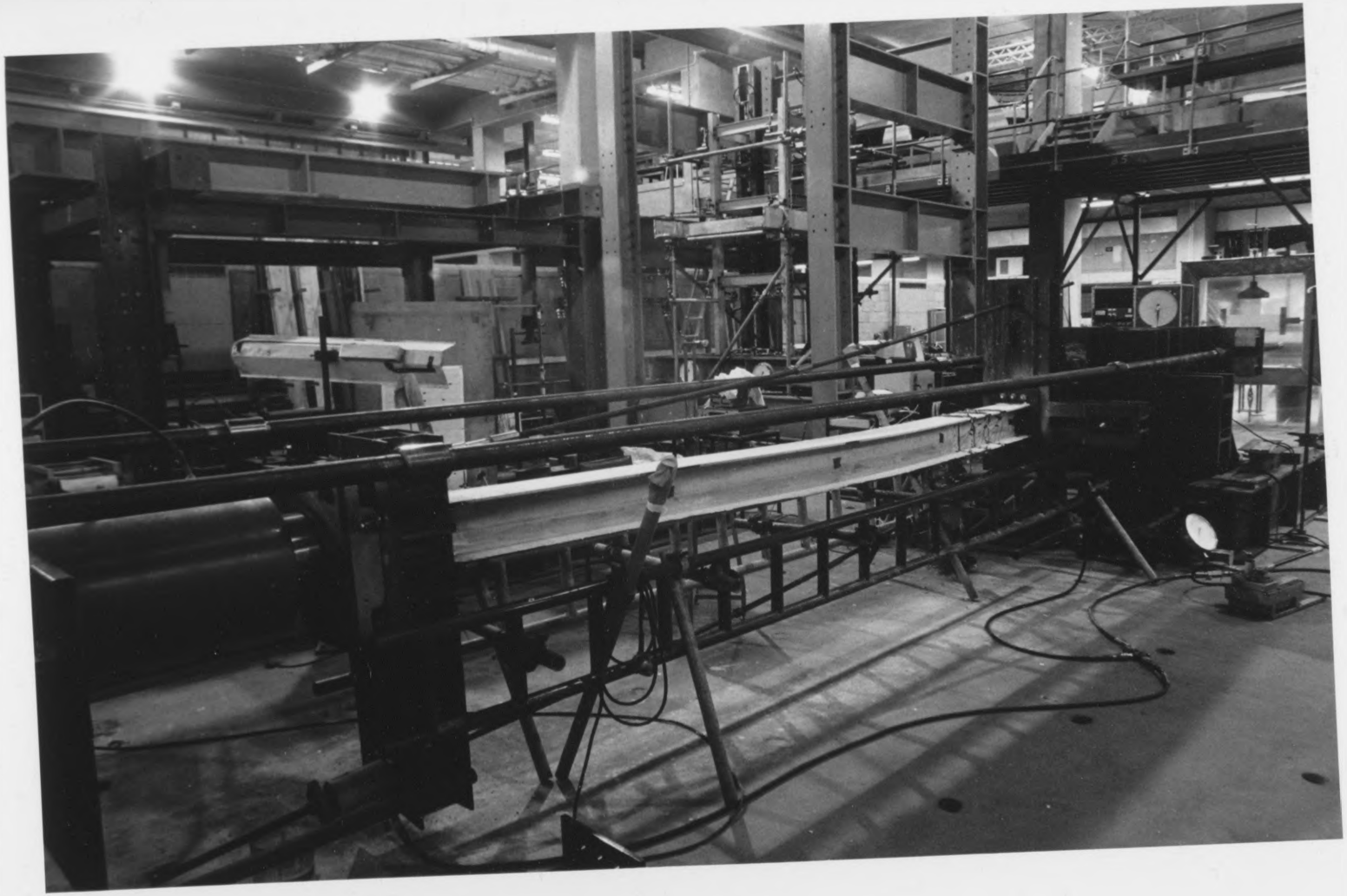

FIG. 4.6. GENERAL VIEW OF THE RIG

FIG. 4.7. GENERAL VIEW OF THE RIG

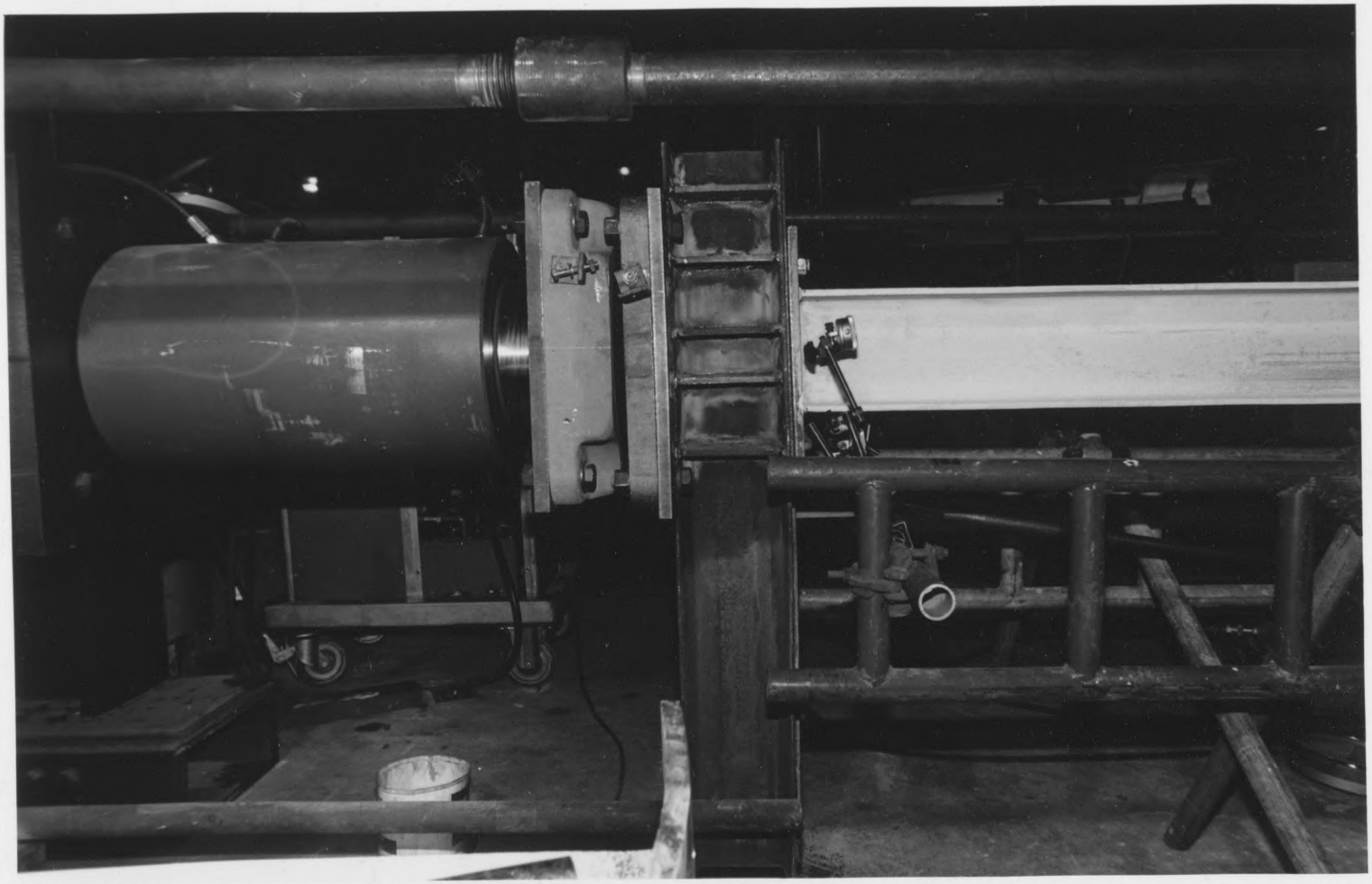

FIG. 4.8. DETAILS OF THE REACTION BLOCK WITH THE CYLINDER JACK

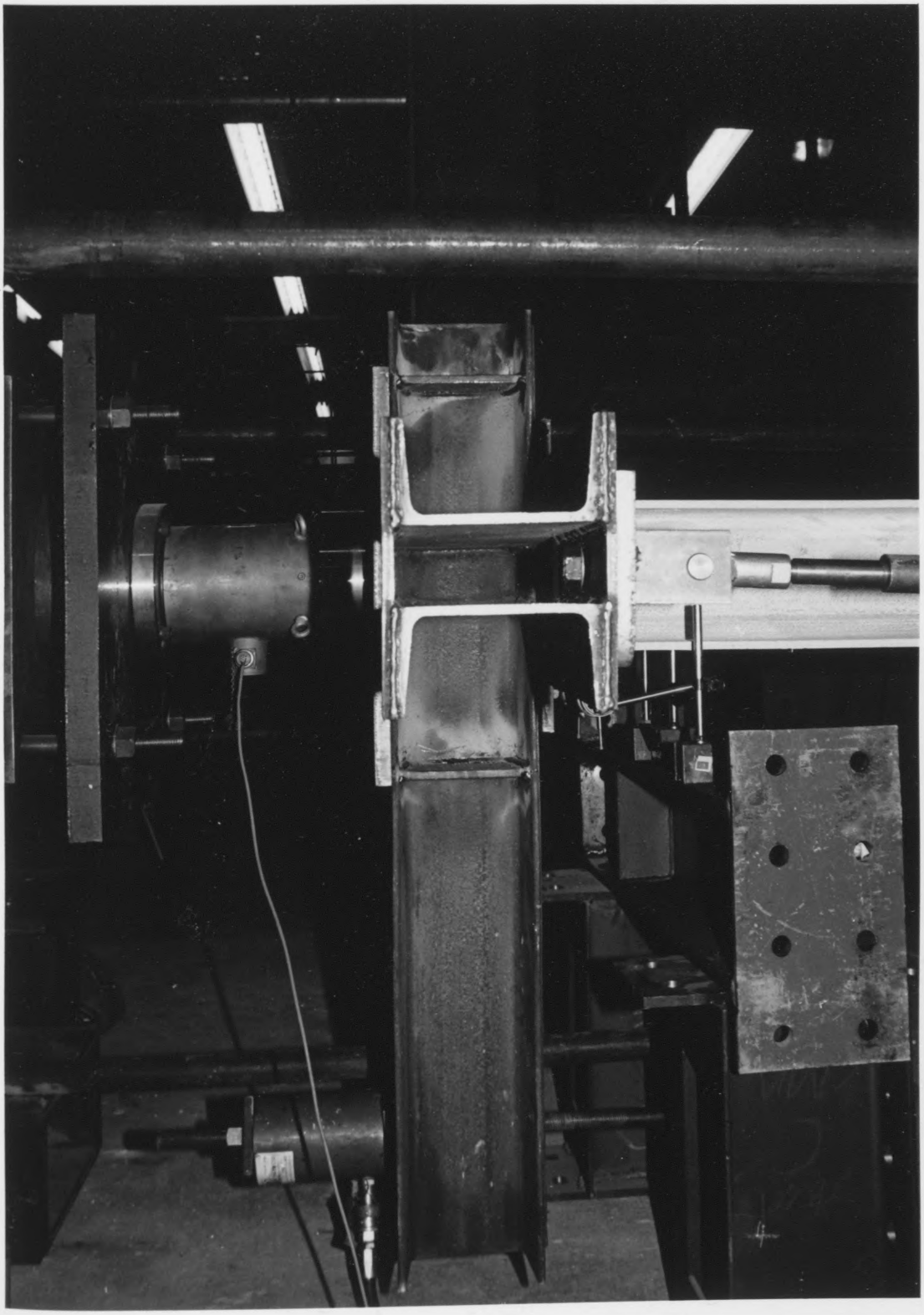

FIG. 4.9. DETAILS OF THE REACTION BLOCK WITH THE LOAD CELL

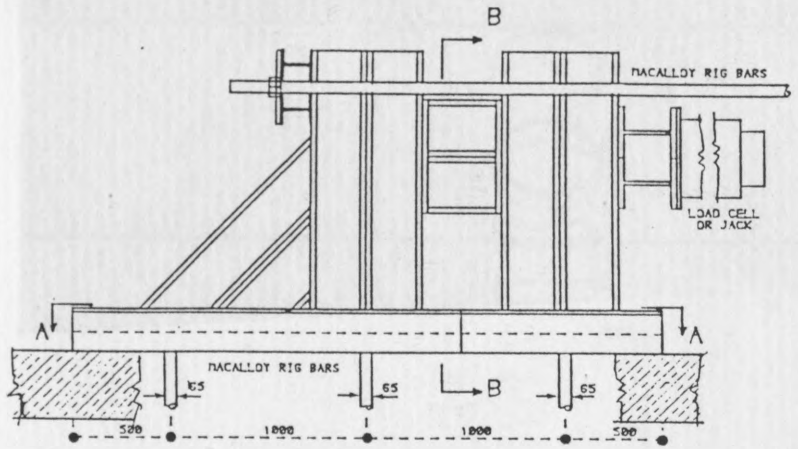

ELEVATION

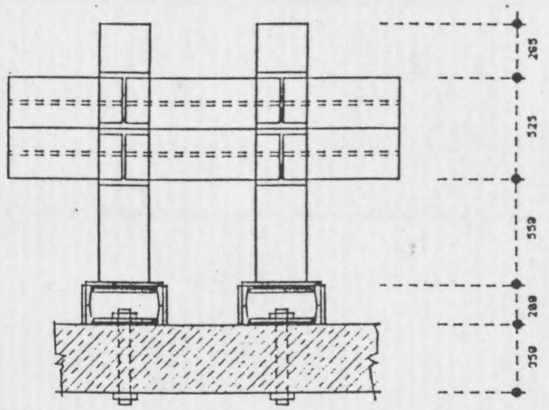

B - B

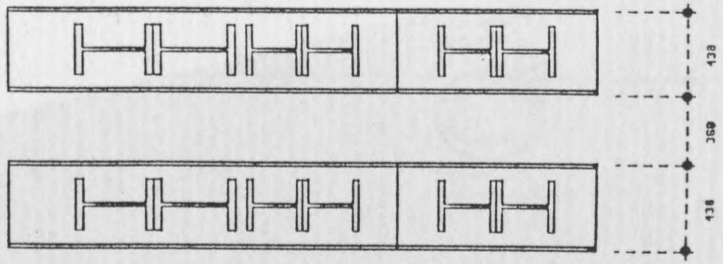

A - A

SCALE 1 : 40

DIMENSIONS IN MM

FIG. 4.10. DETAILS OF THE REACTION BLOCK AT THE ENDS

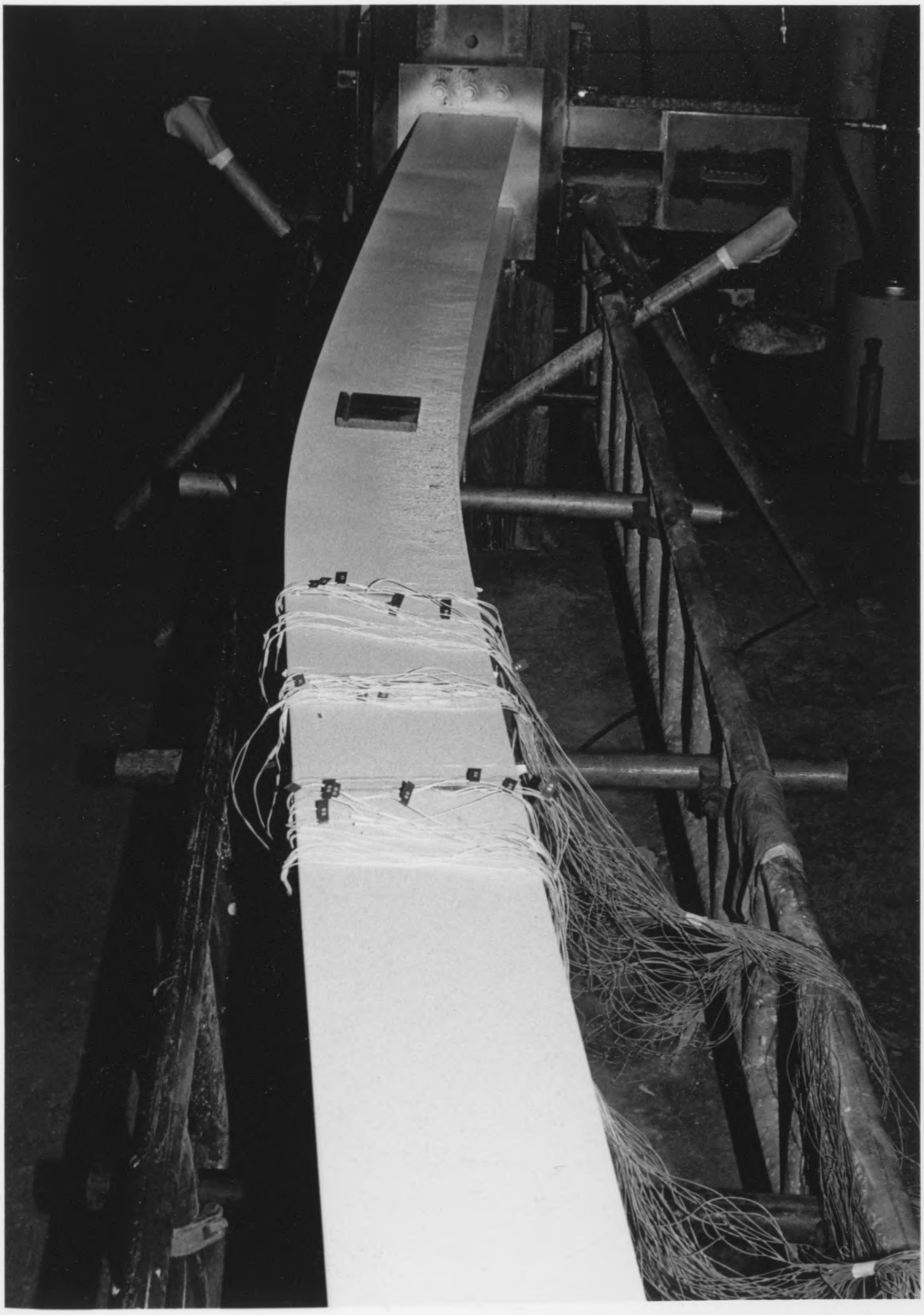

FIG. 4.11. TYPICAL DEFLECTED SHAPE AT FAILURE

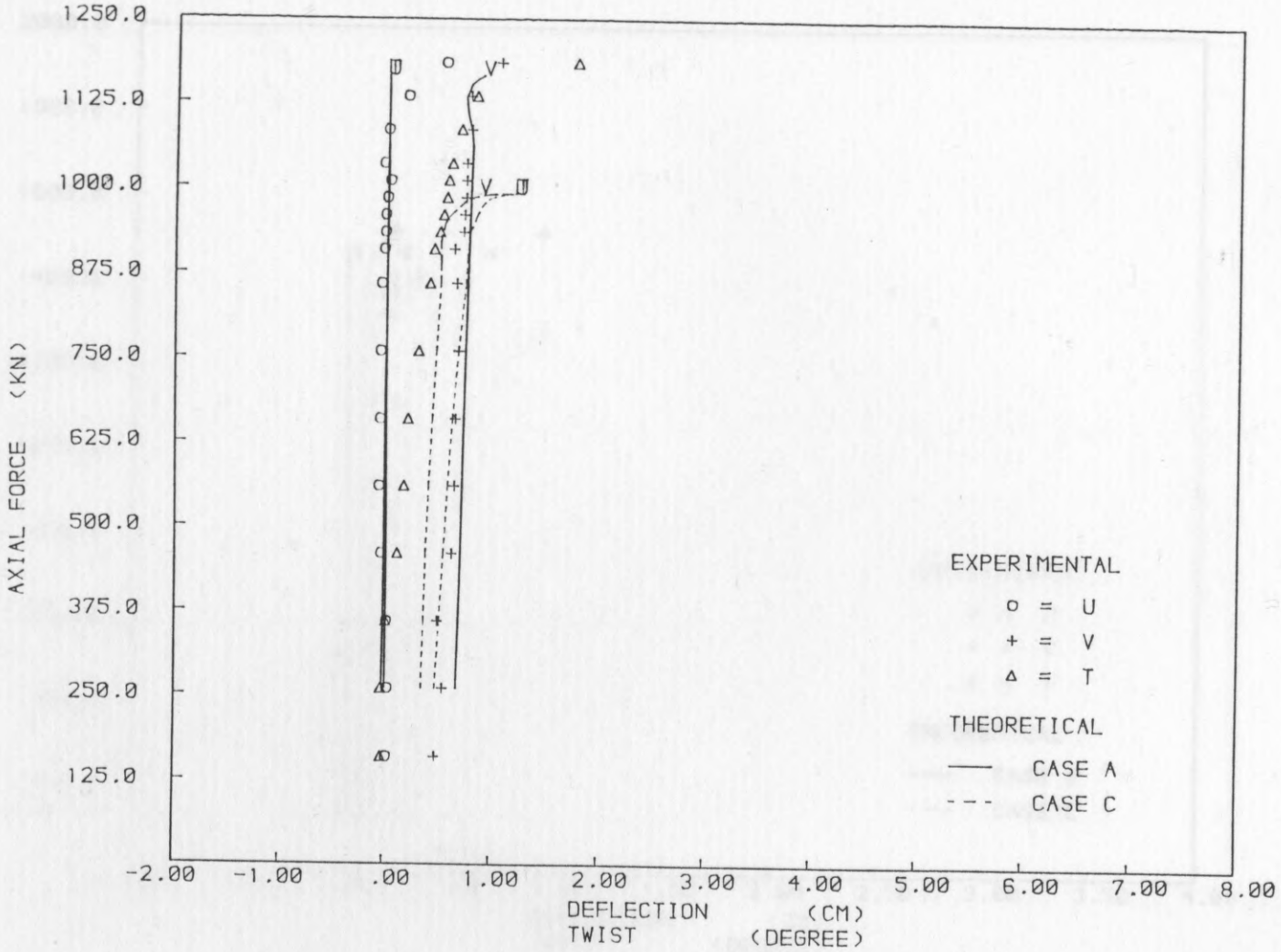

FIG.4.12. LOAD-DEFLECTION CURVE - S1

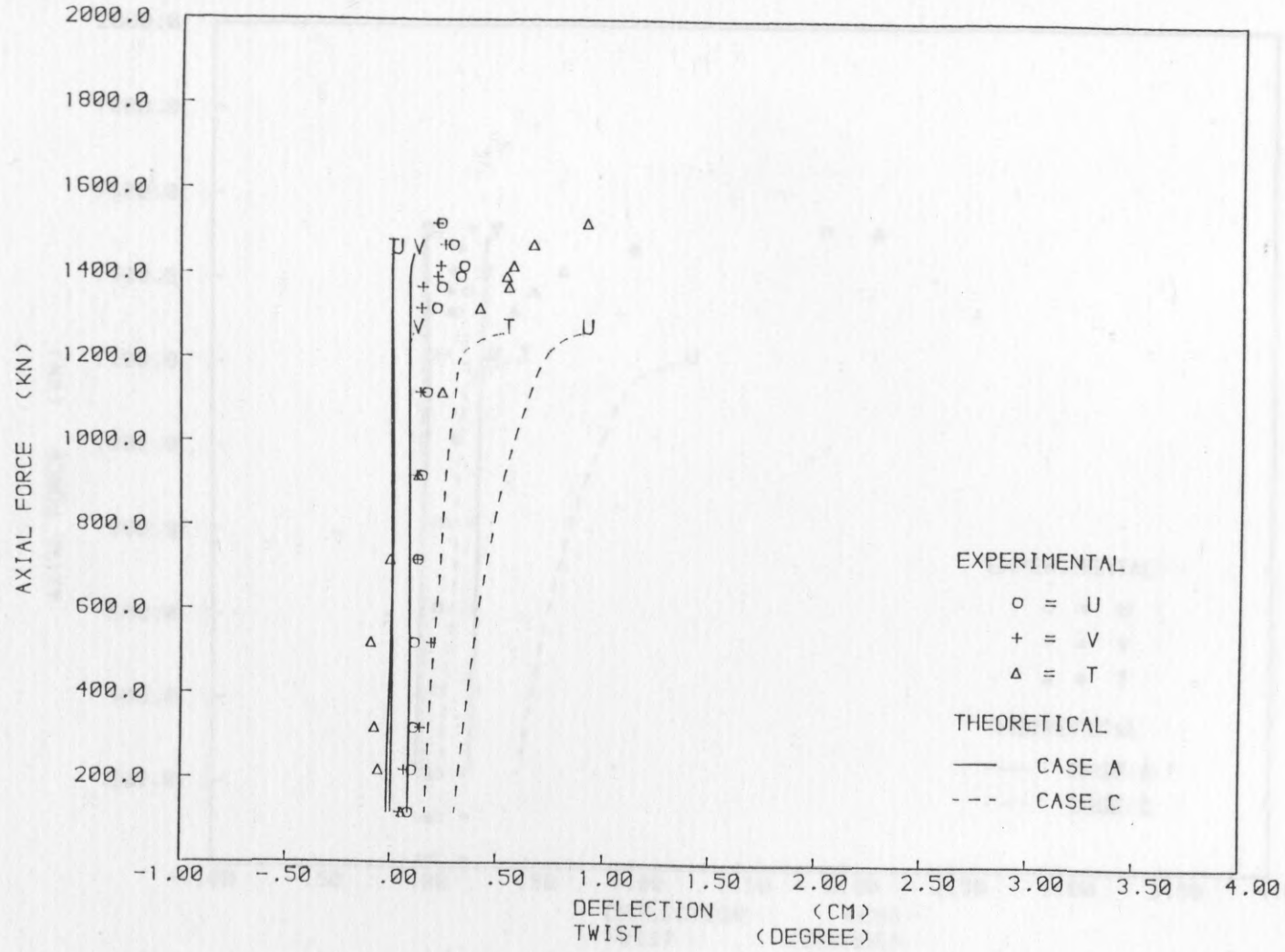

FIG.4.13. LOAD-DEFLECTION CURVE - S2

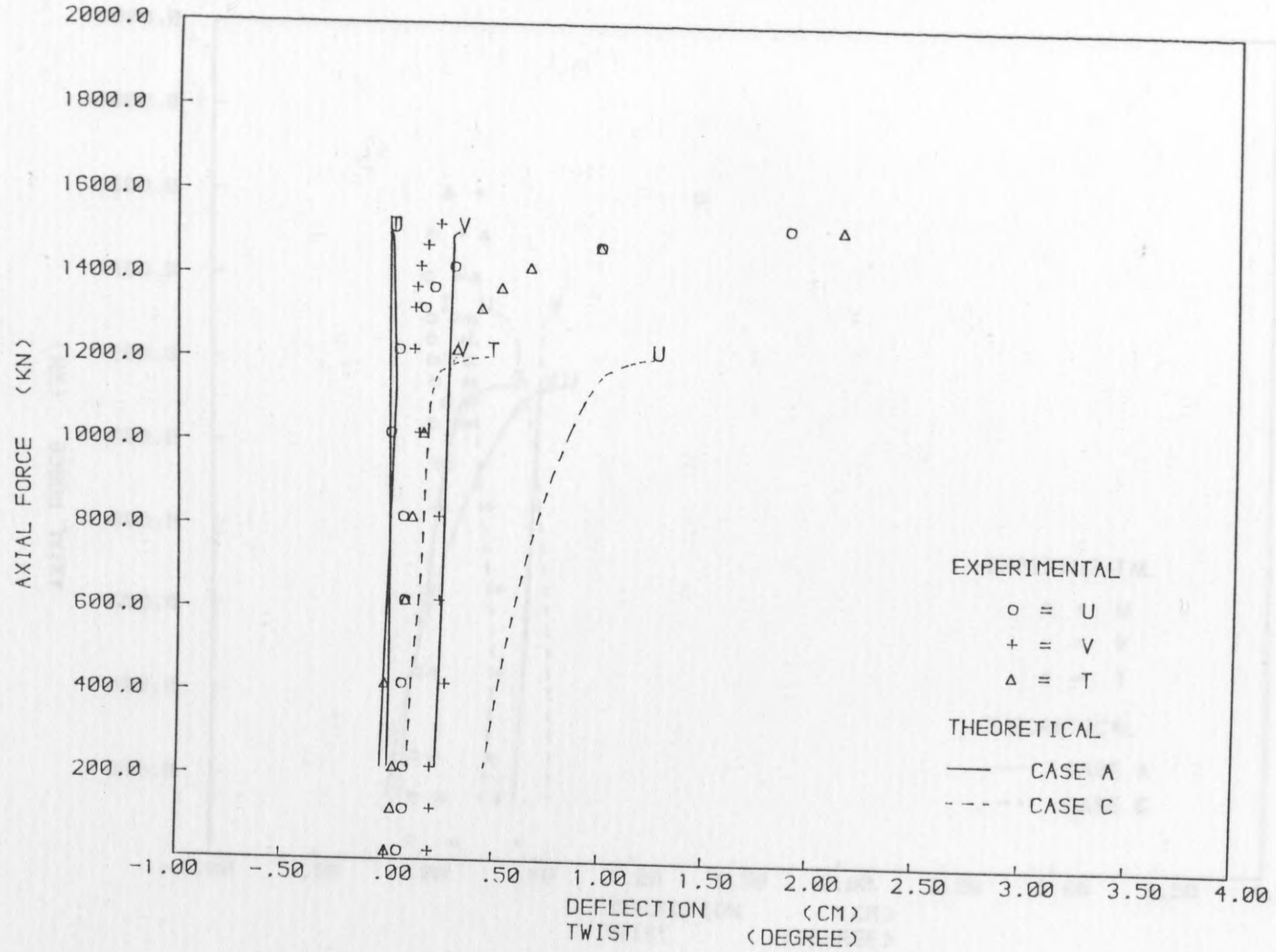

FIG.4.14. LOAD-DEFLECTION CURVE - S3

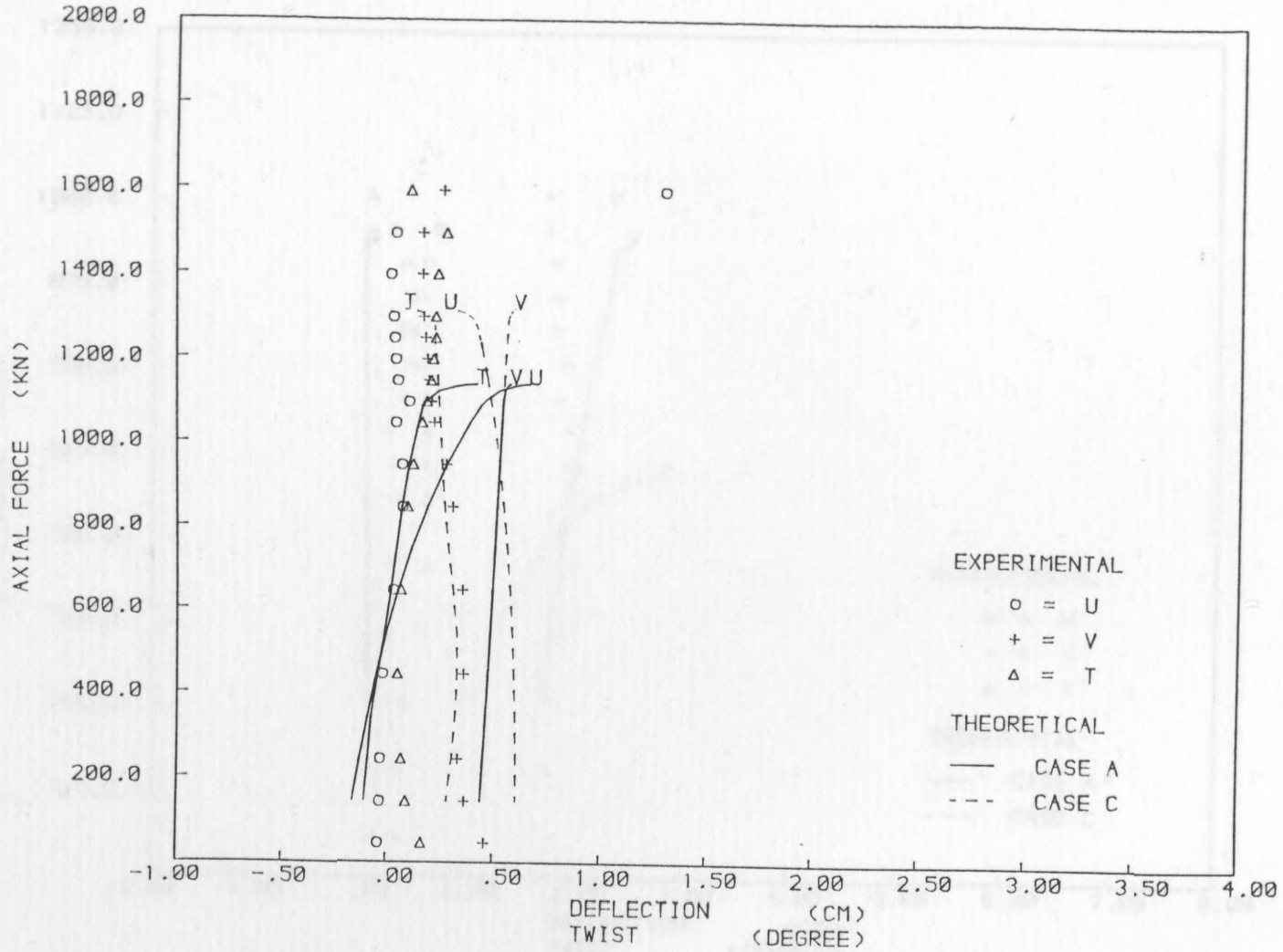

FIG.4.15. LOAD-DEFLECTION CURVE - S4

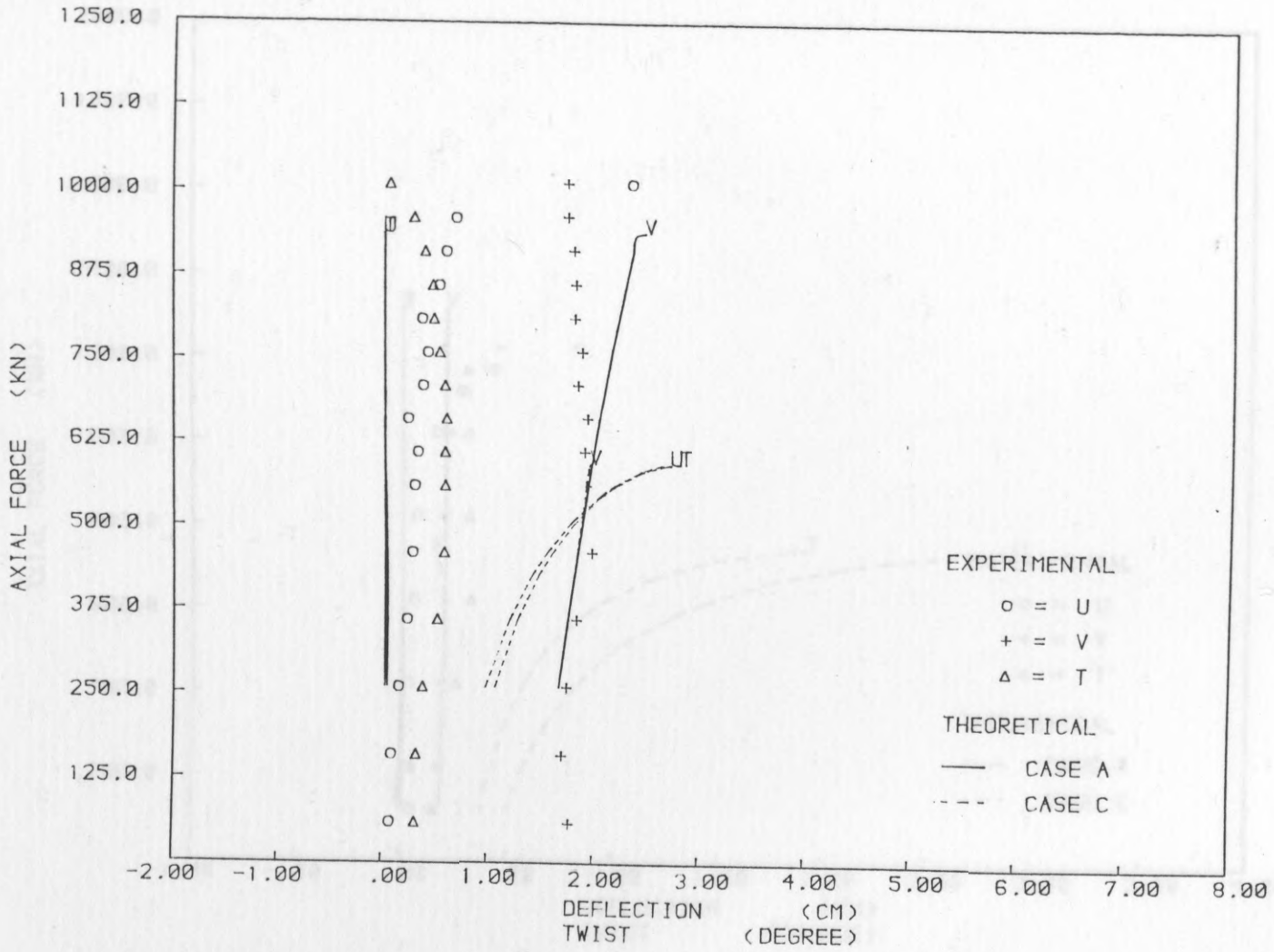

FIG.4.16. LOAD-DEFLECTION CURVE - L1

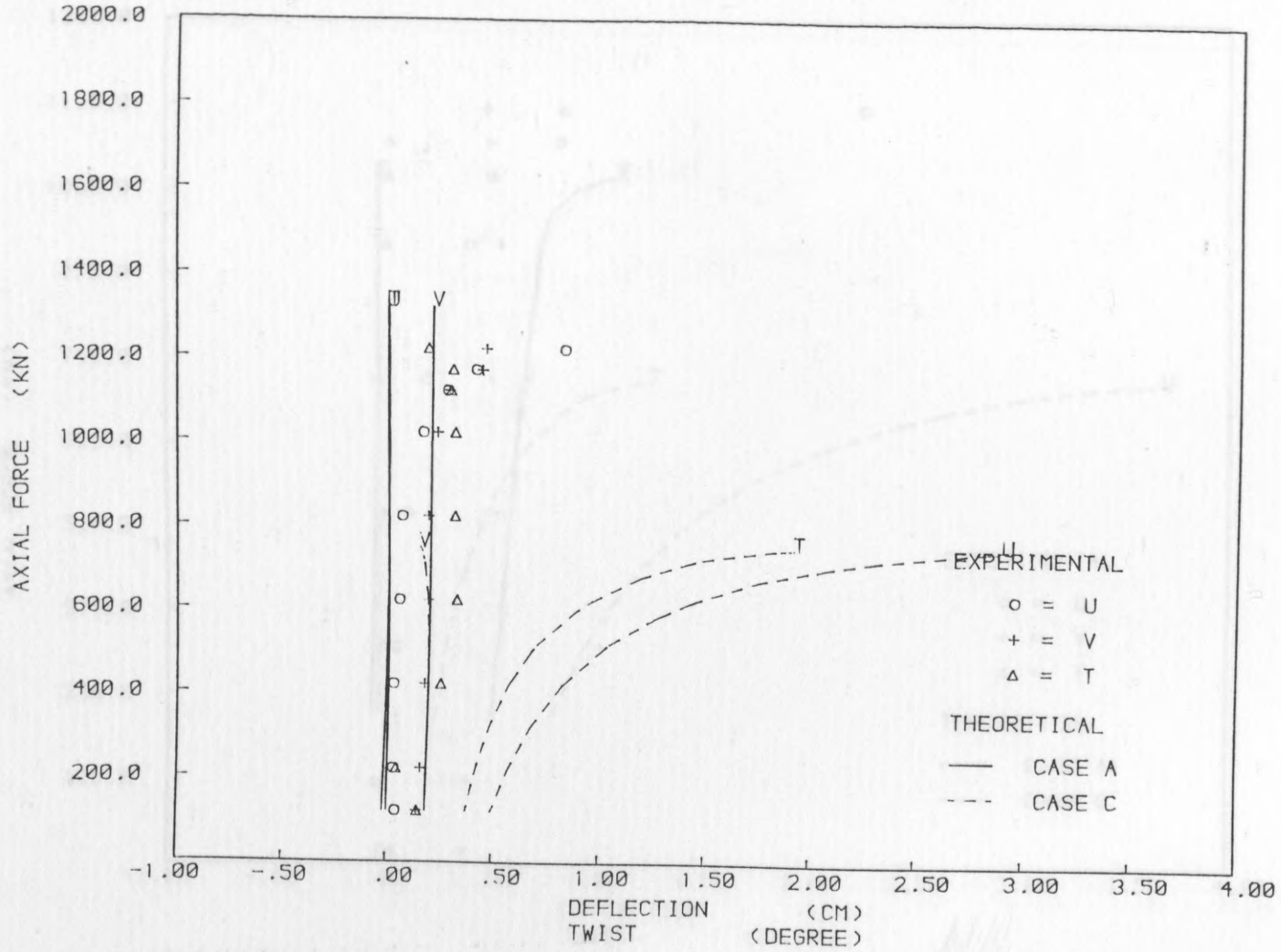

FIG.4.17. LOAD-DEFLECTION CURVE - L2

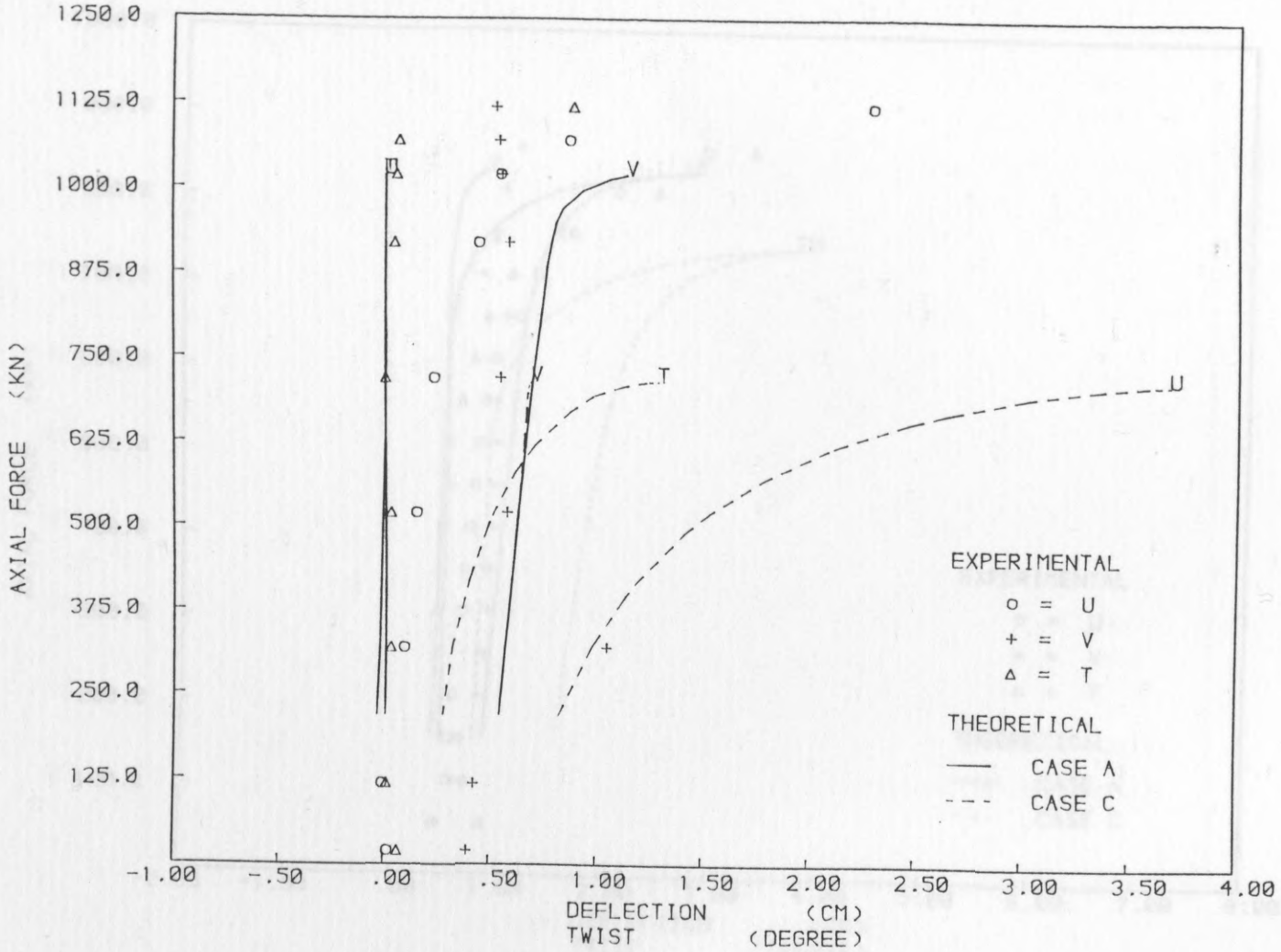

FIG.4.18. LOAD-DEFLECTION CURVE - L3

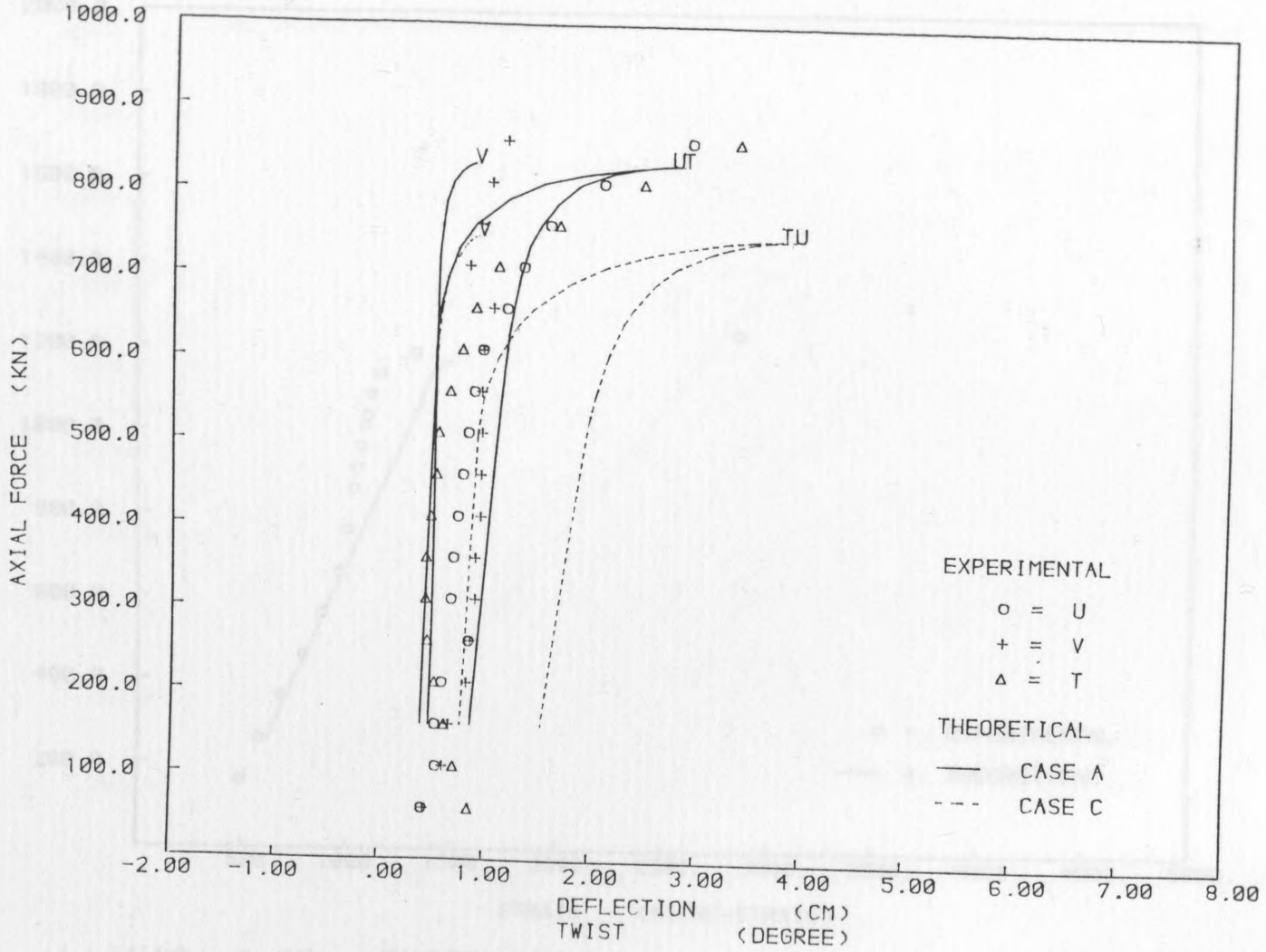

FIG.4.19. LOAD-DEFLECTION CURVE - L4

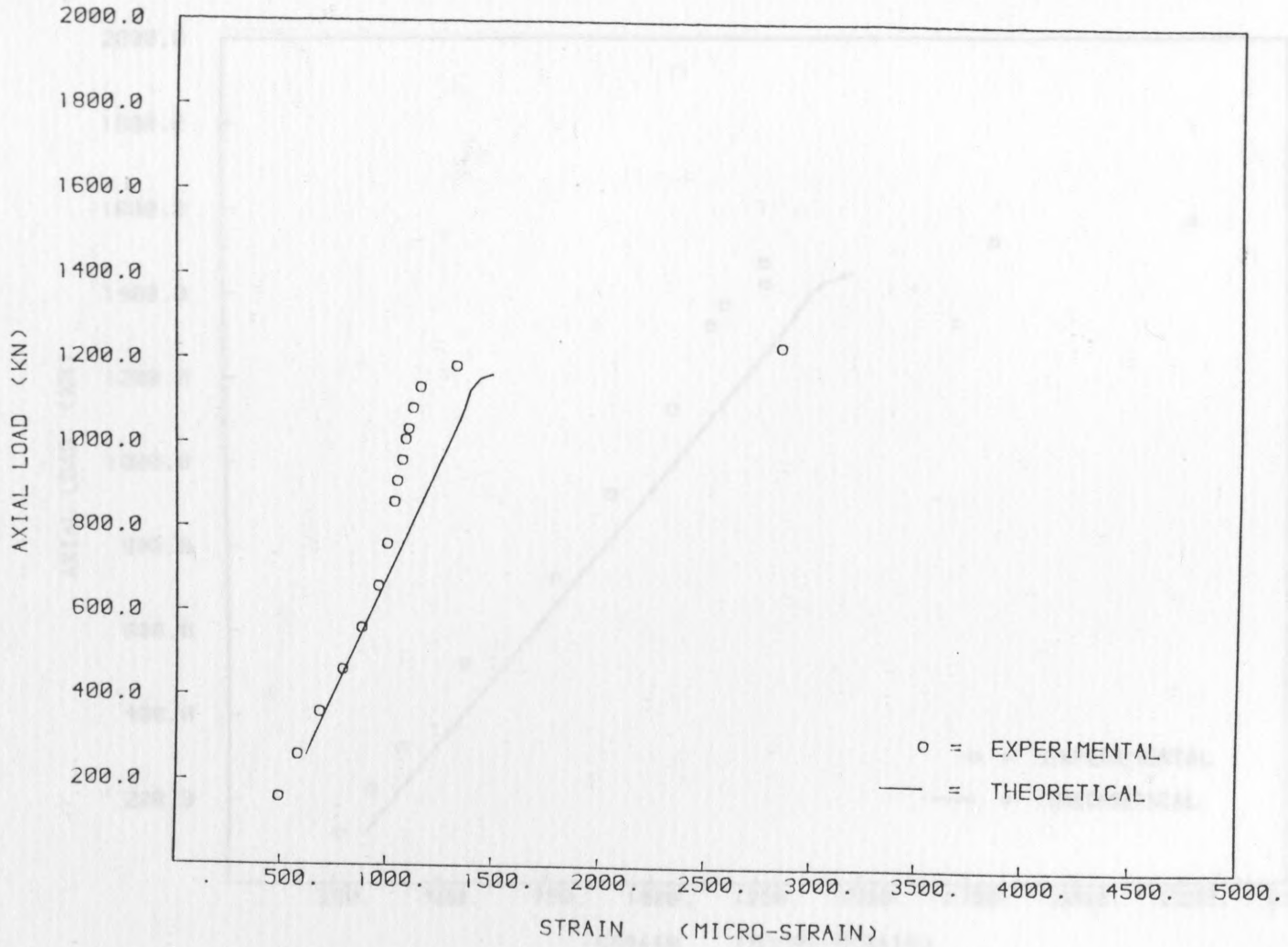

FIG. 4.20. EXPERIMENTAL LOAD-STRAIN RELATIONS - S1

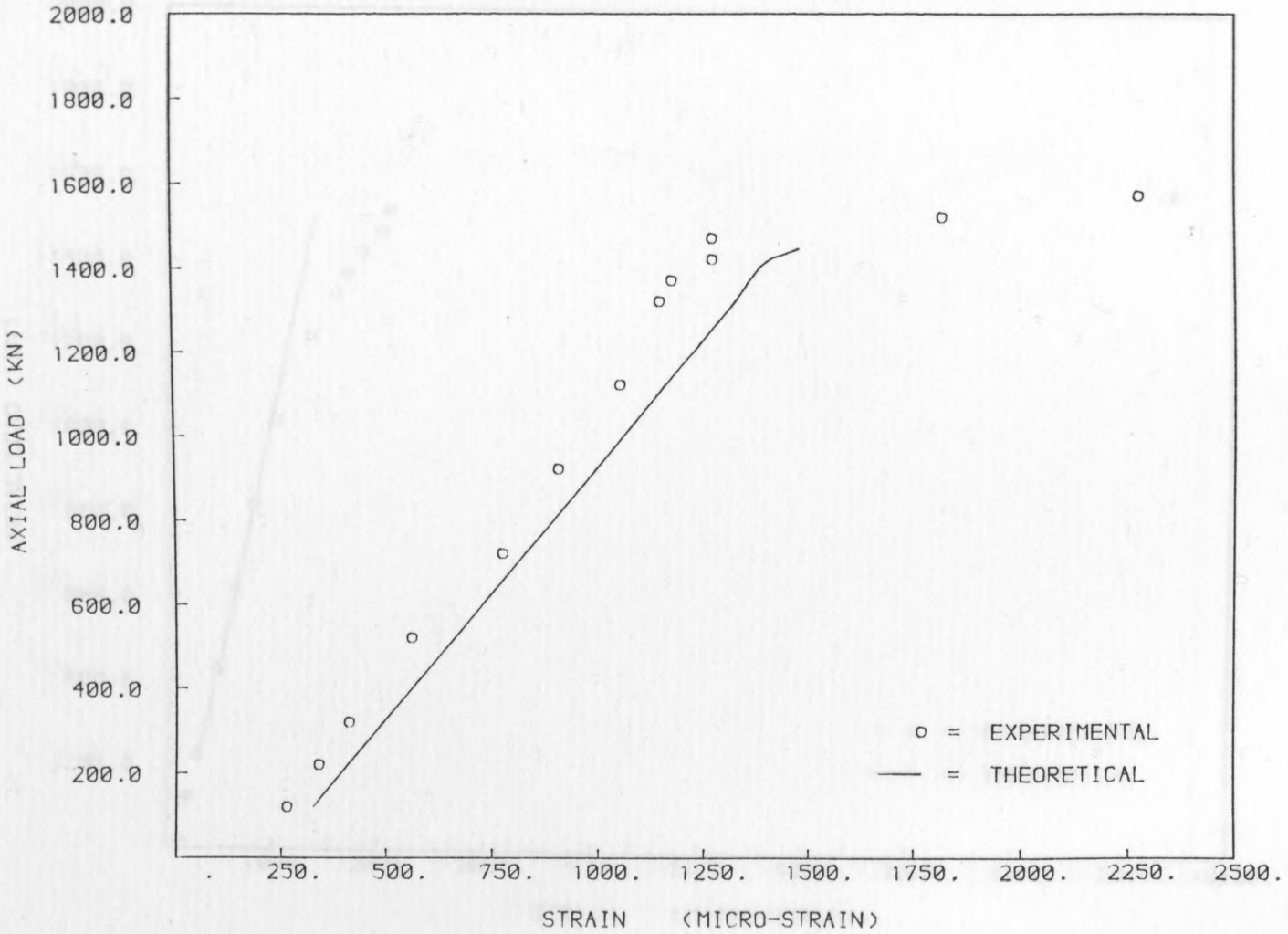

FIG. 4.21. EXPERIMENTAL LOAD-STRAIN RELATIONS - S2

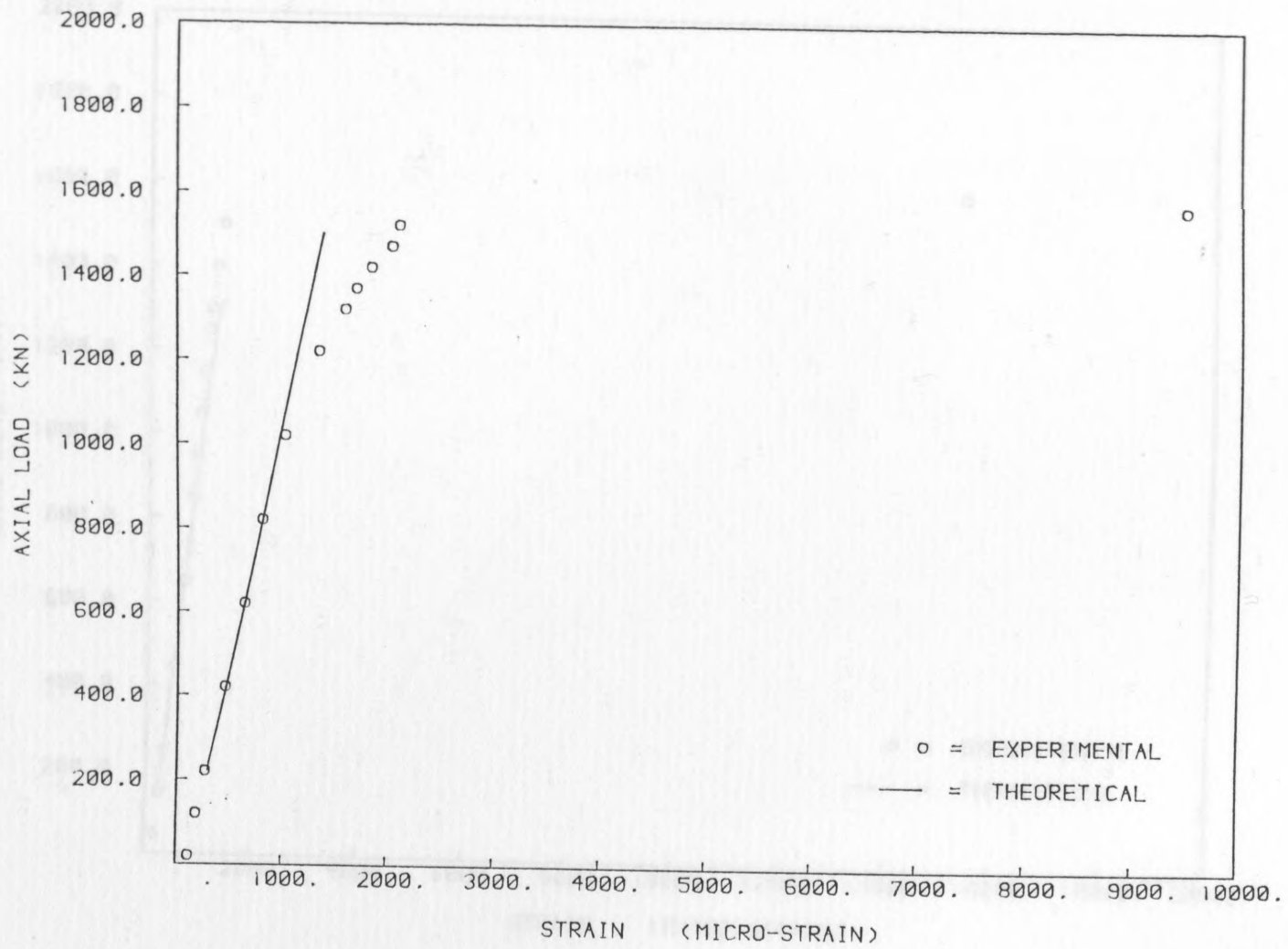

FIG. 4.22. EXPERIMENTAL LOAD-STRAIN RELATIONS - S3

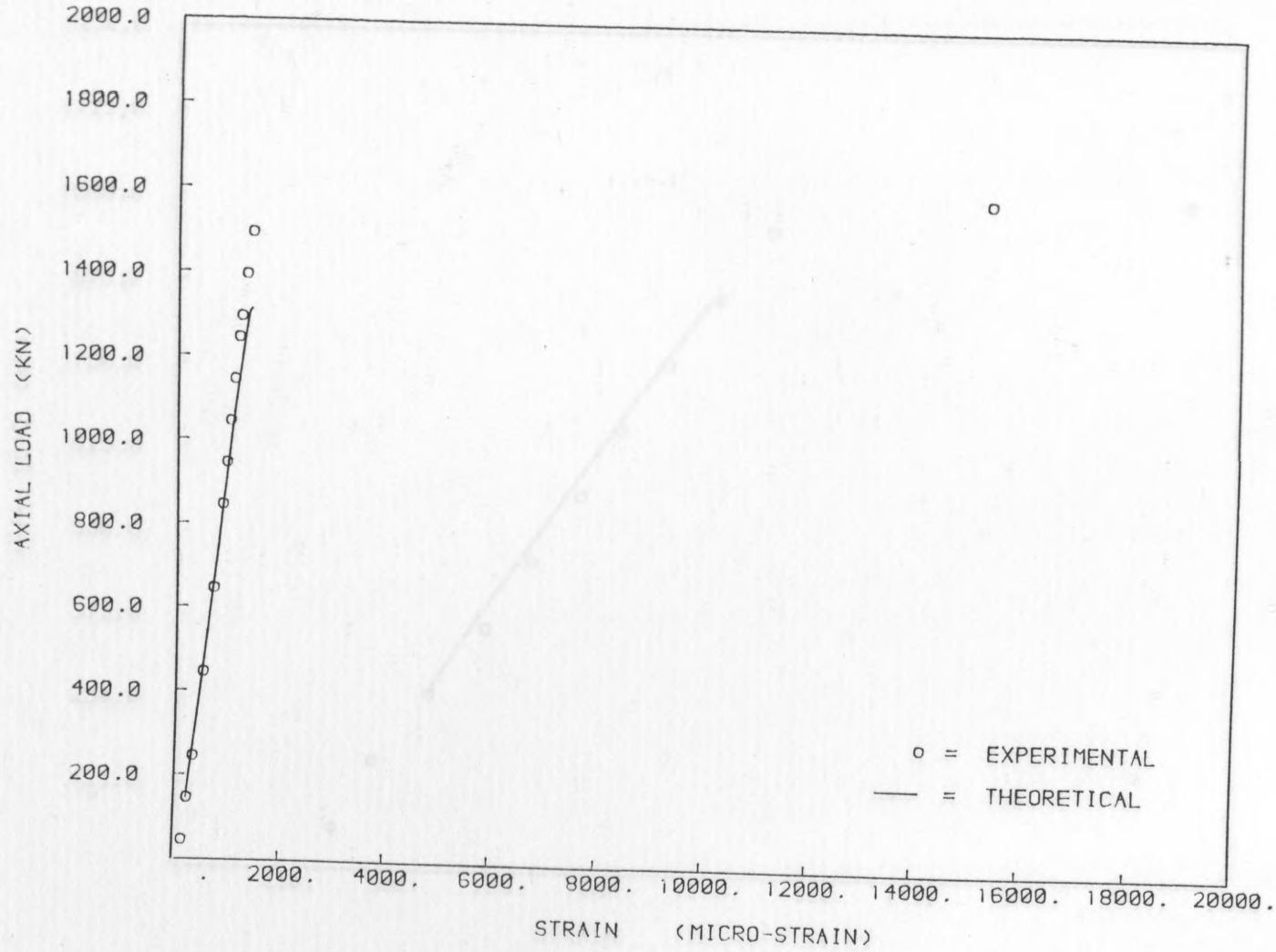

FIG. 4.23. EXPERIMENTAL LOAD-STRAIN RELATIONS - S4

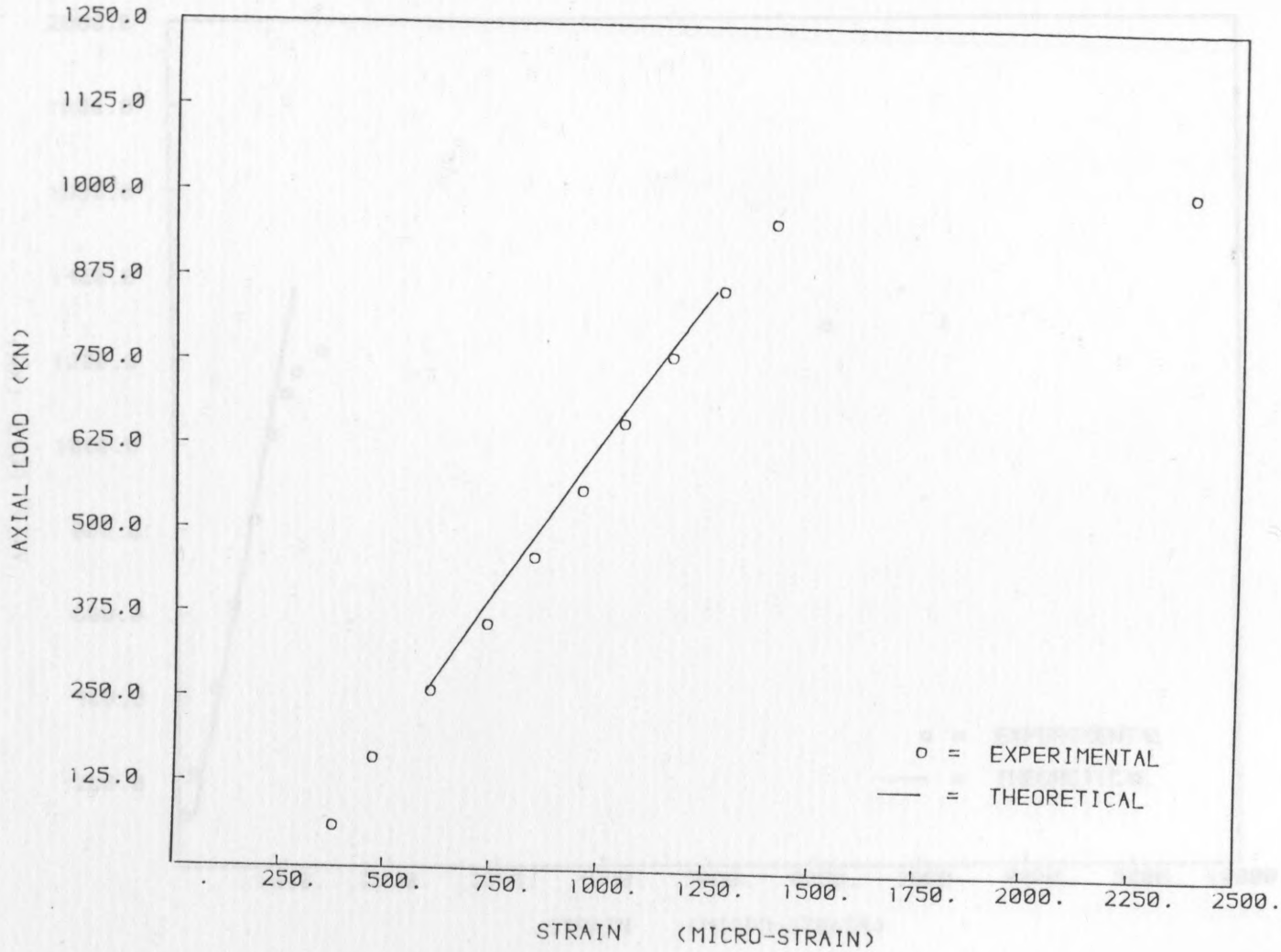

FIG. 4.24. EXPERIMENTAL LOAD-STRAIN RELATIONS - L1

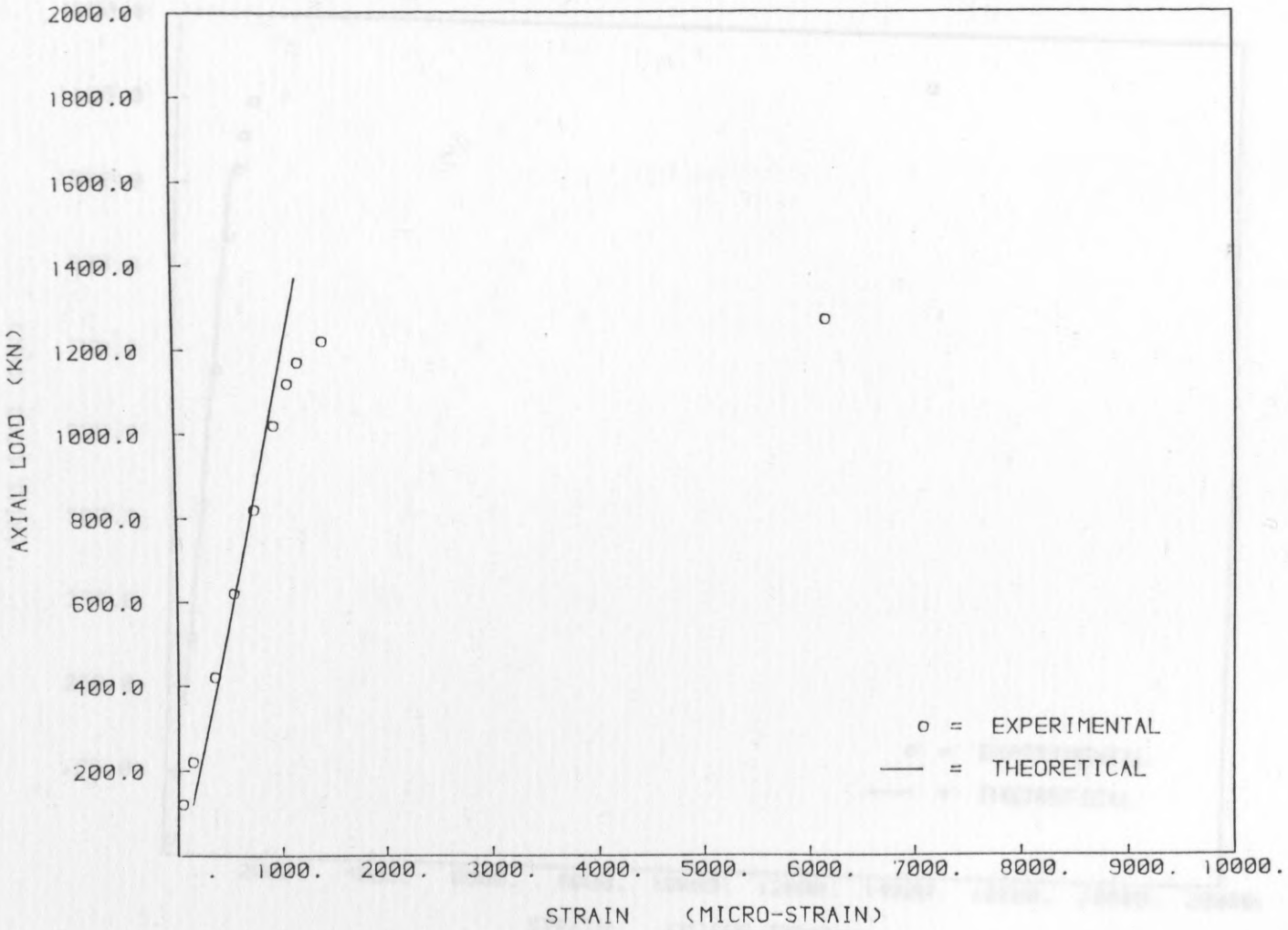

FIG. 4.25. EXPERIMENTAL LOAD-STRAIN RELATIONS - L2

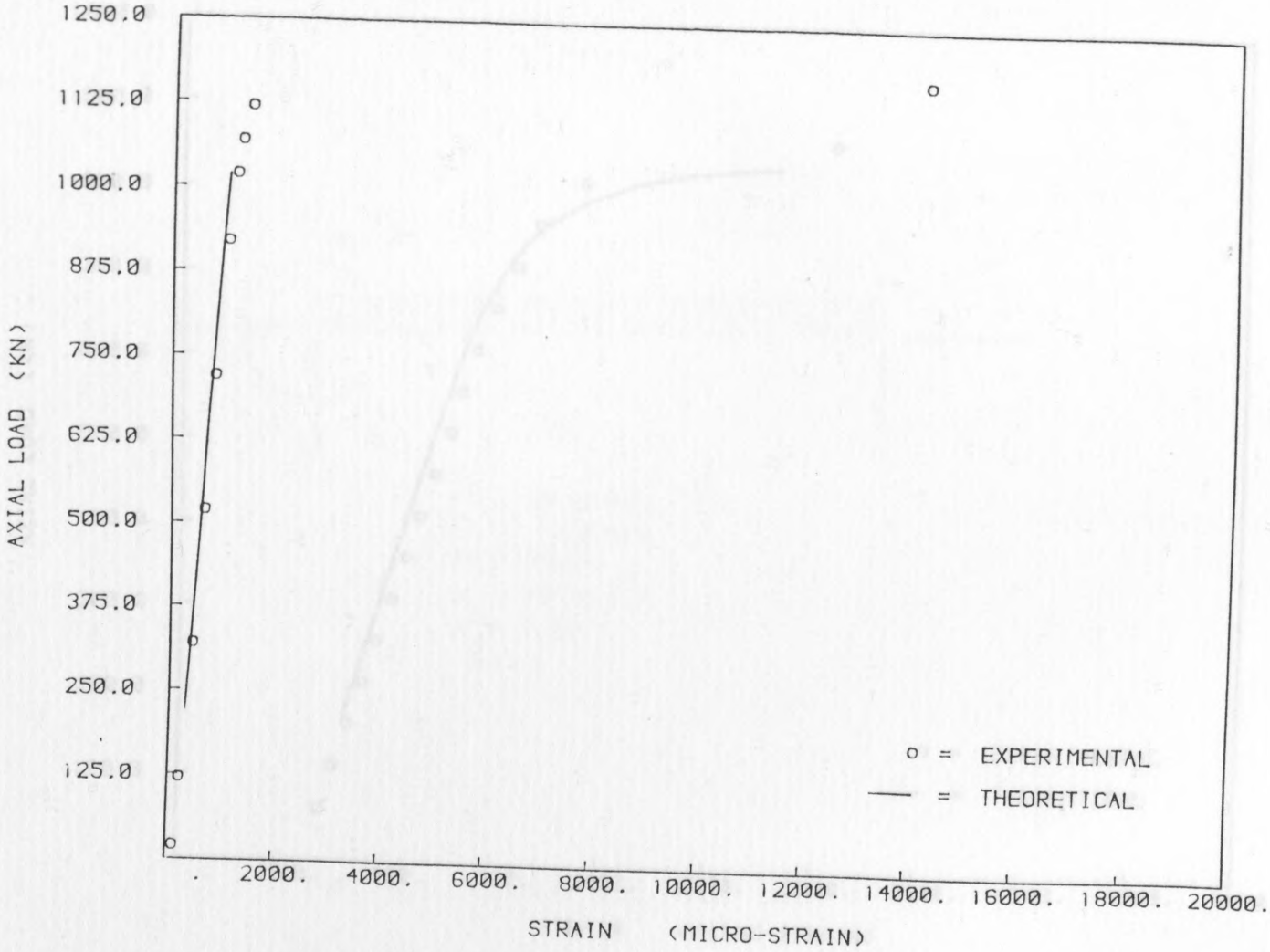

FIG. 4.26. EXPERIMENTAL LOAD-STRAIN RELATIONS - L3

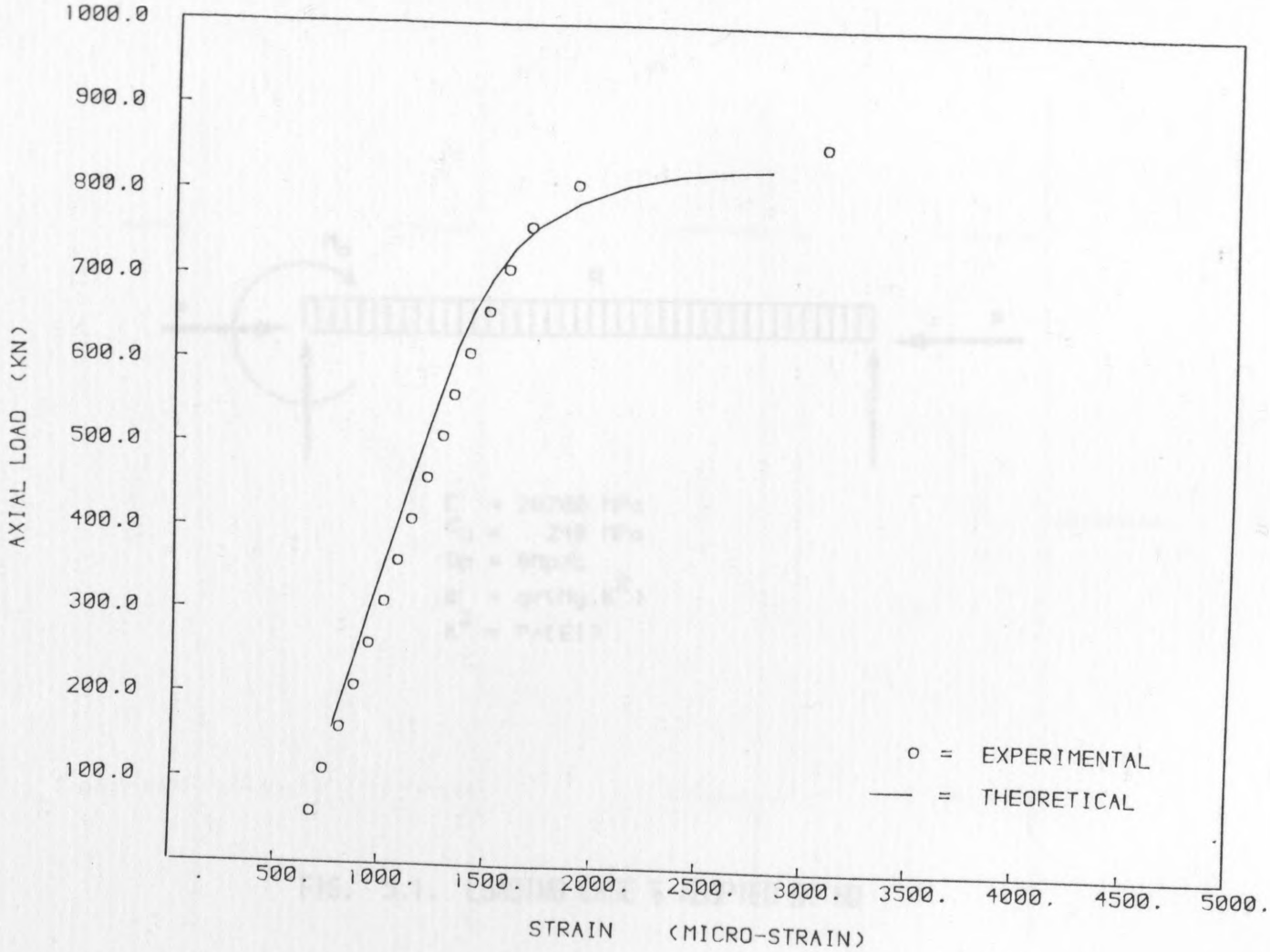

FIG. 4.27. EXPERIMENTAL LOAD-STRAIN RELATIONS - L4

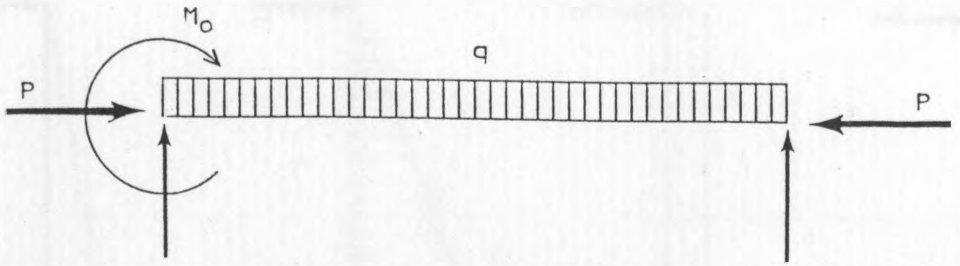

$E = 20700$ MPa
$\sigma_y = 248$ MPa
$Qp = 8Mp/L$
$a = q/(My.K^2)$
$K^2 = P/(EI)$

FIG. 5.1. LOADING CASE 6 ADOPTED BY HO

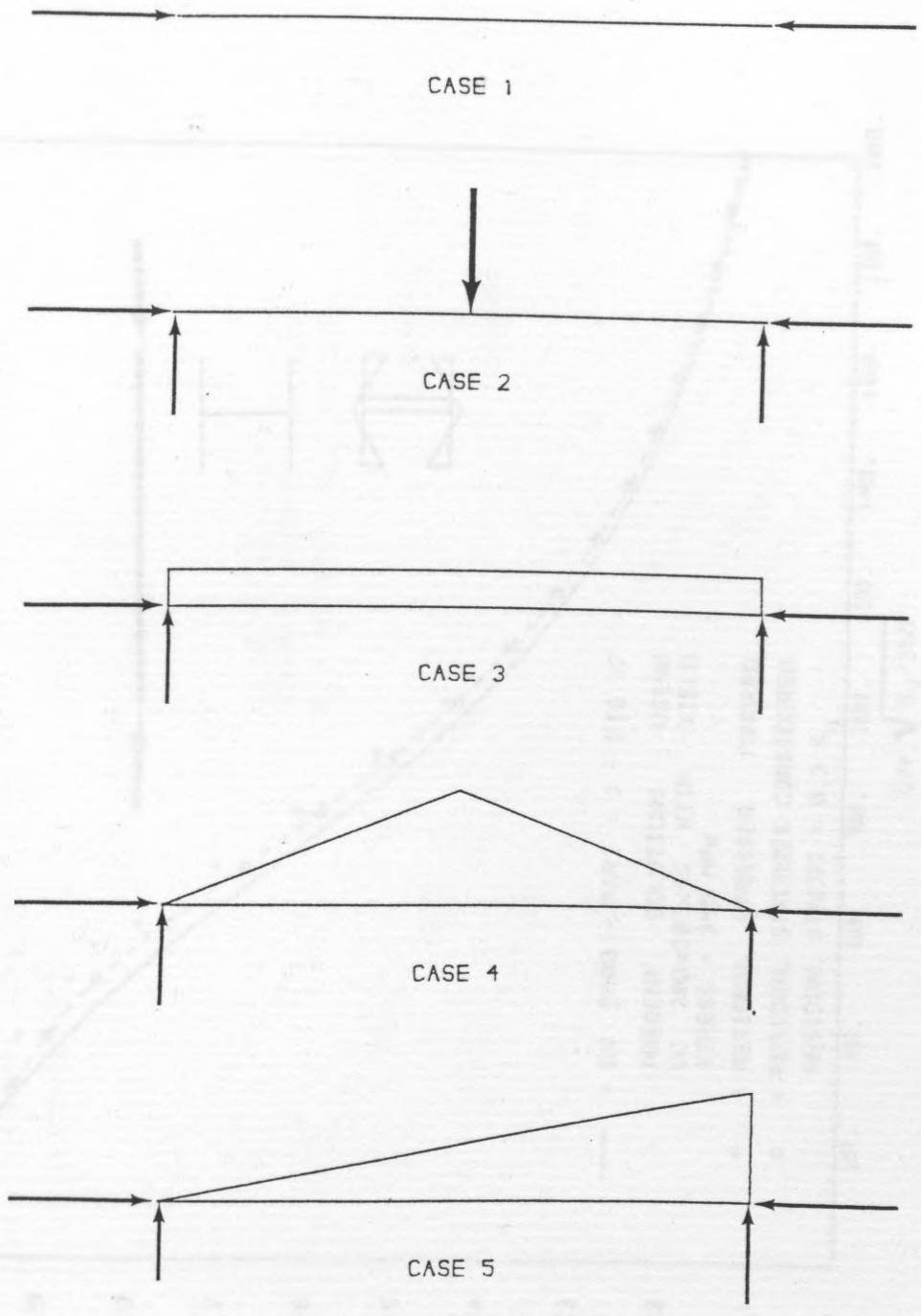

FIG. 6.1. LOADING CASES

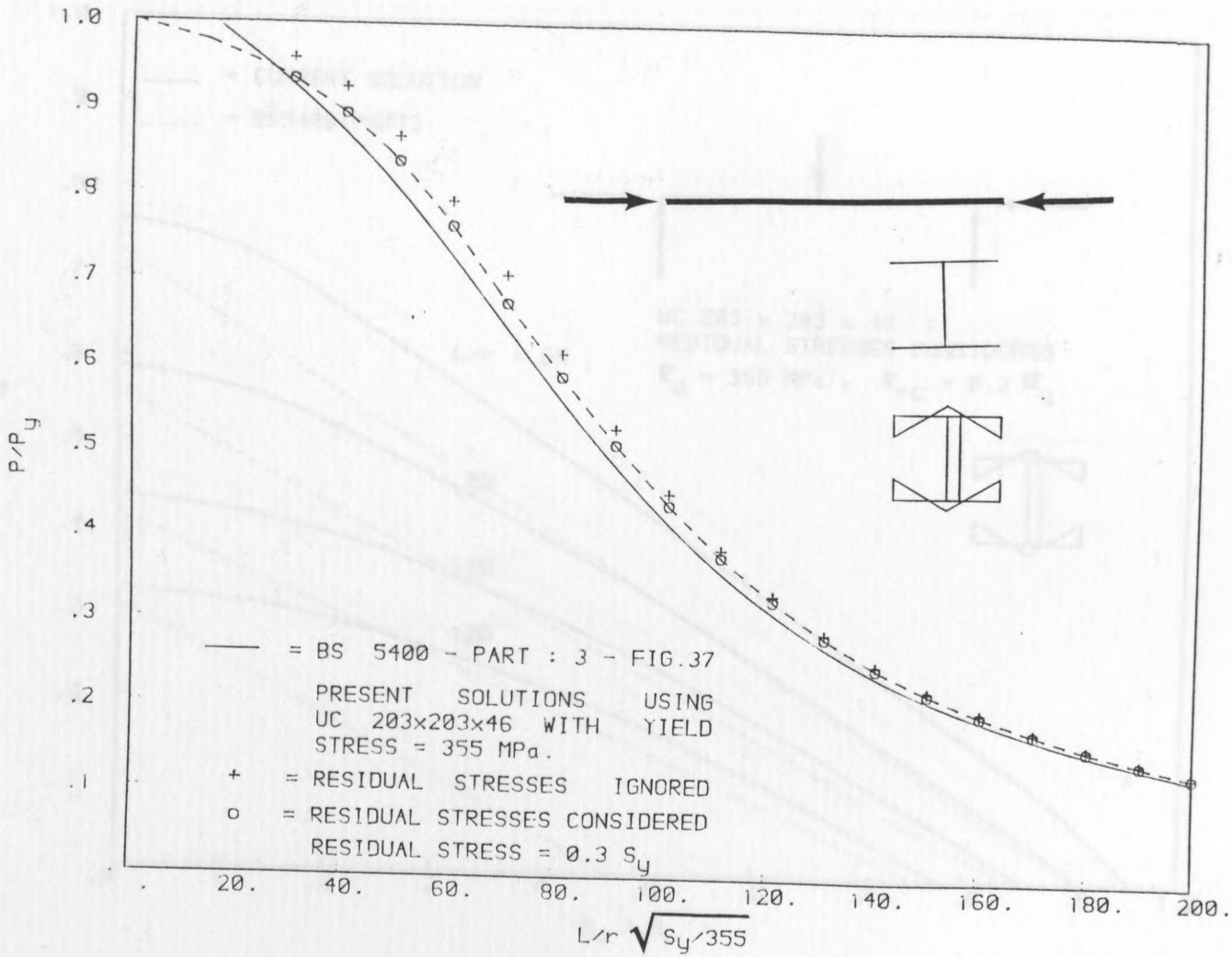

FIG. 6.2. RESULTS OF CASE 1

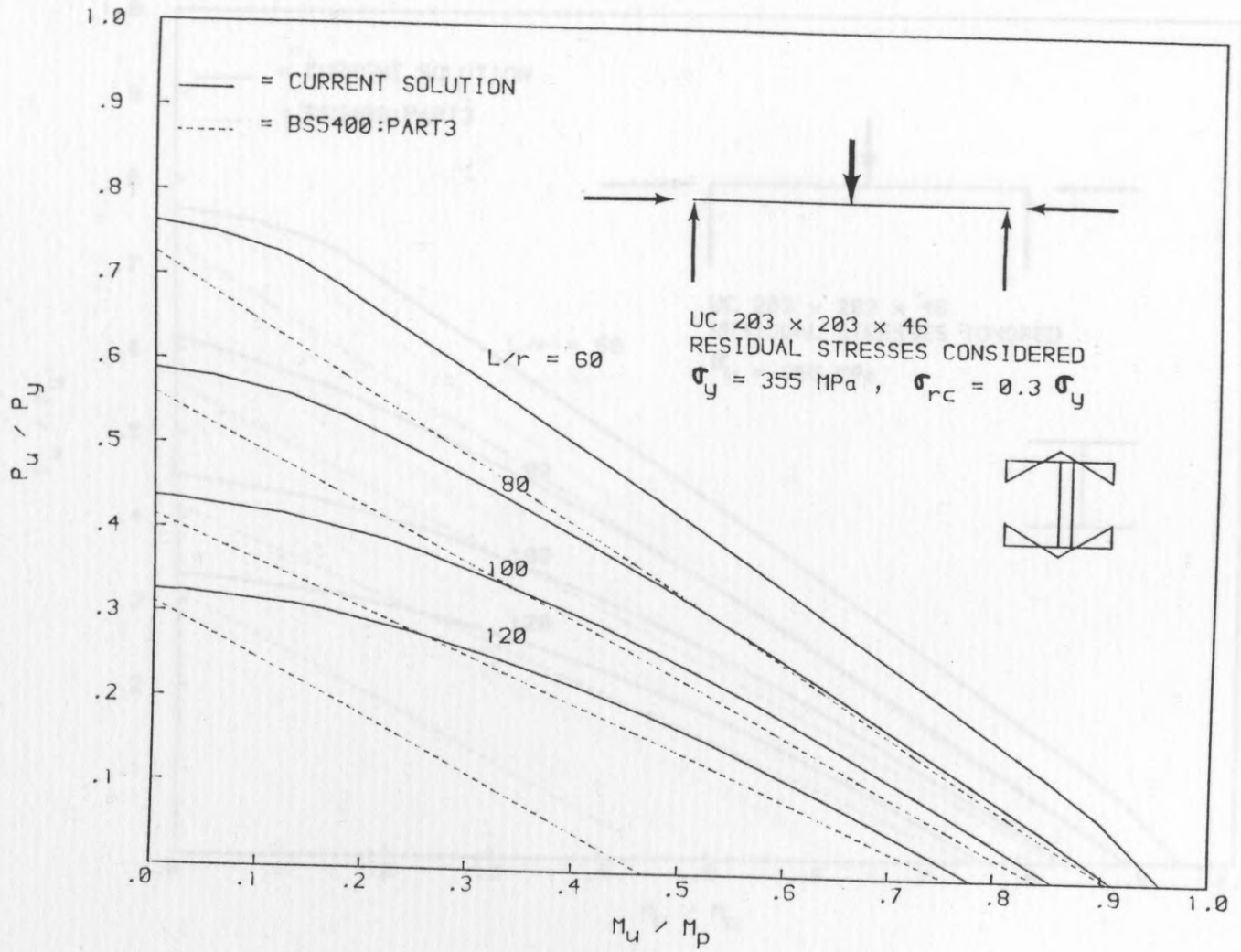

FIG. 6.3. INTERACTION CURVE OF CASE 2

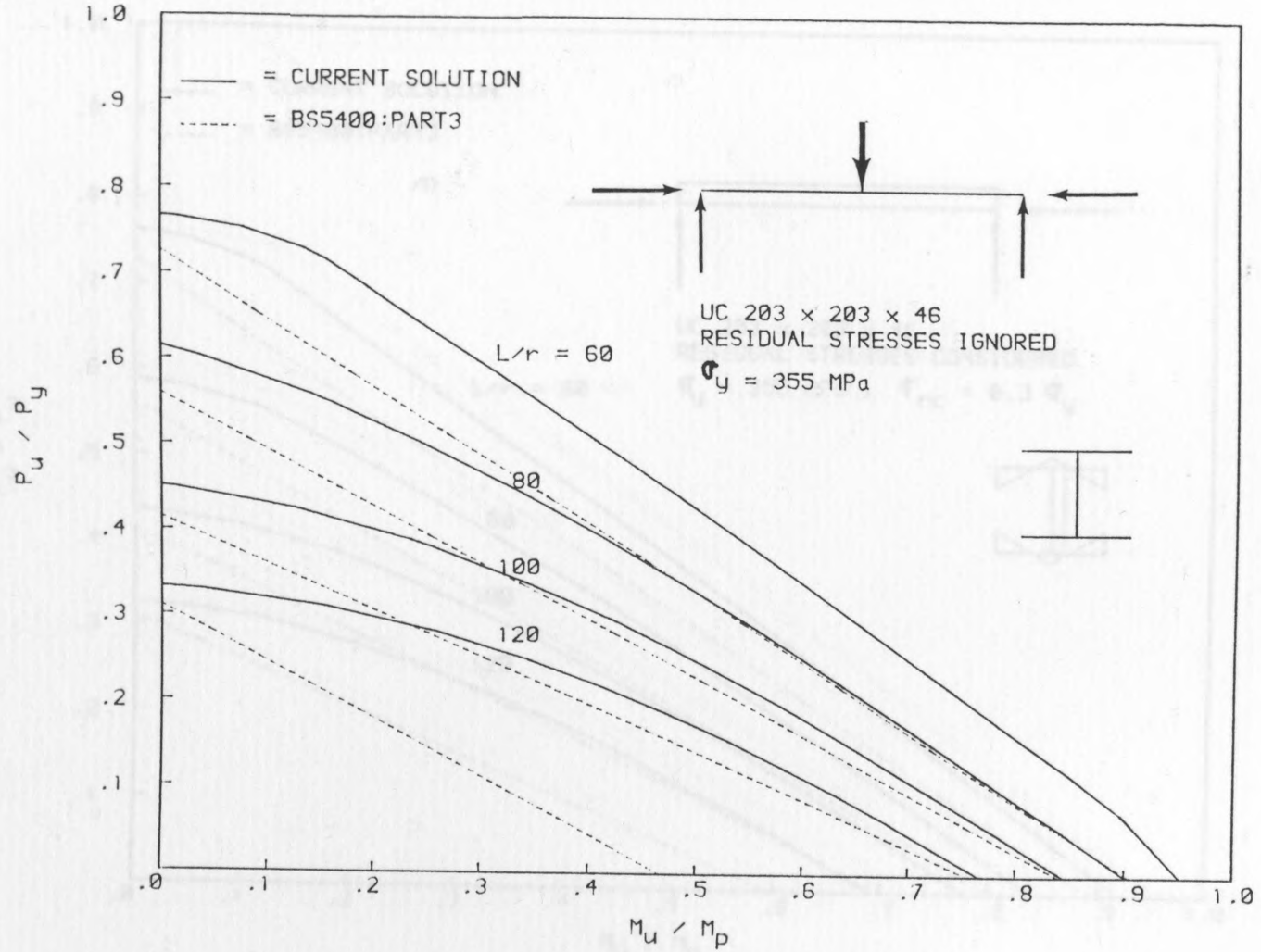

FIG. 6.4. INTERACTION CURVE OF CASE 2

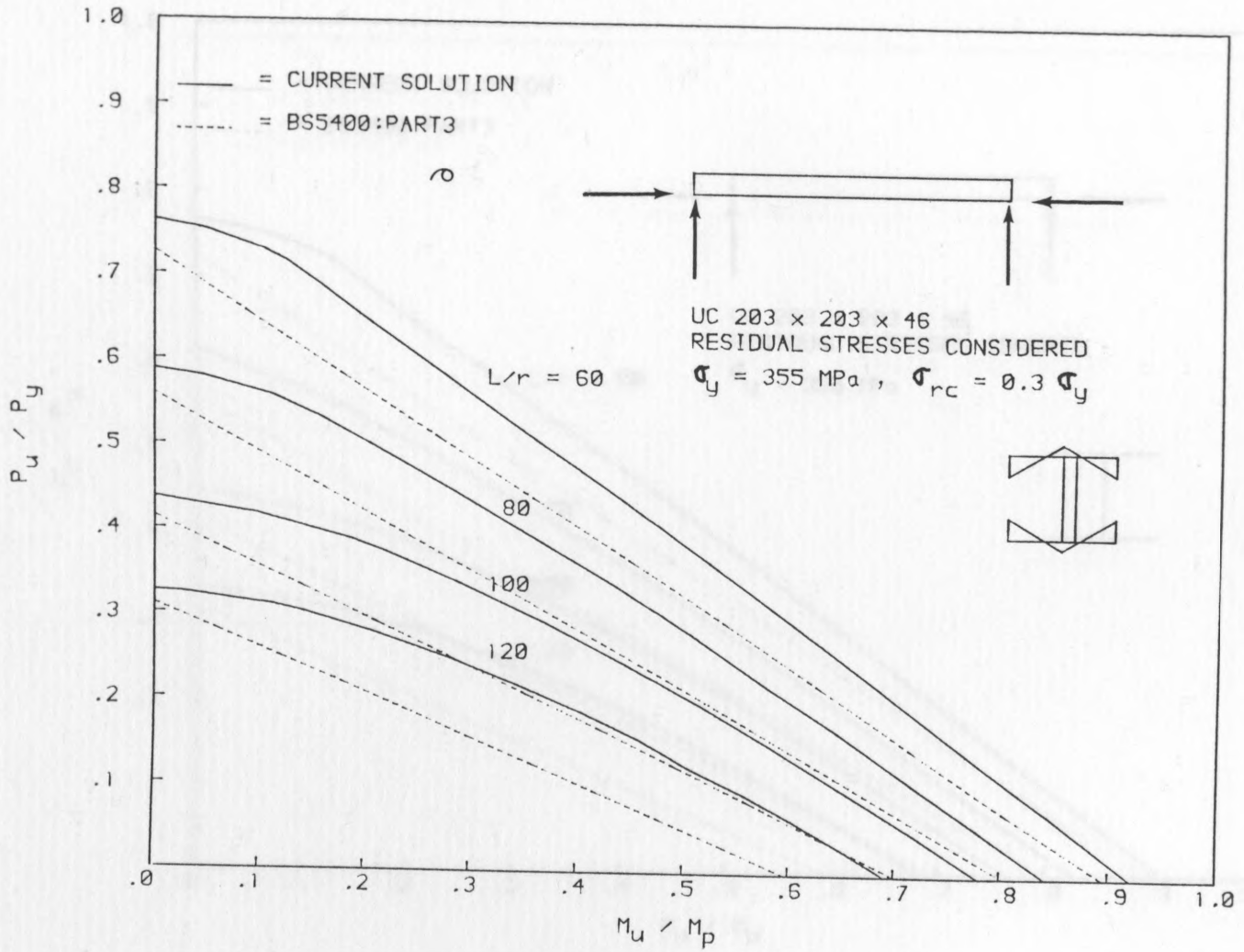

FIG. 6.5. INTERACTION CURVE OF CASE 3

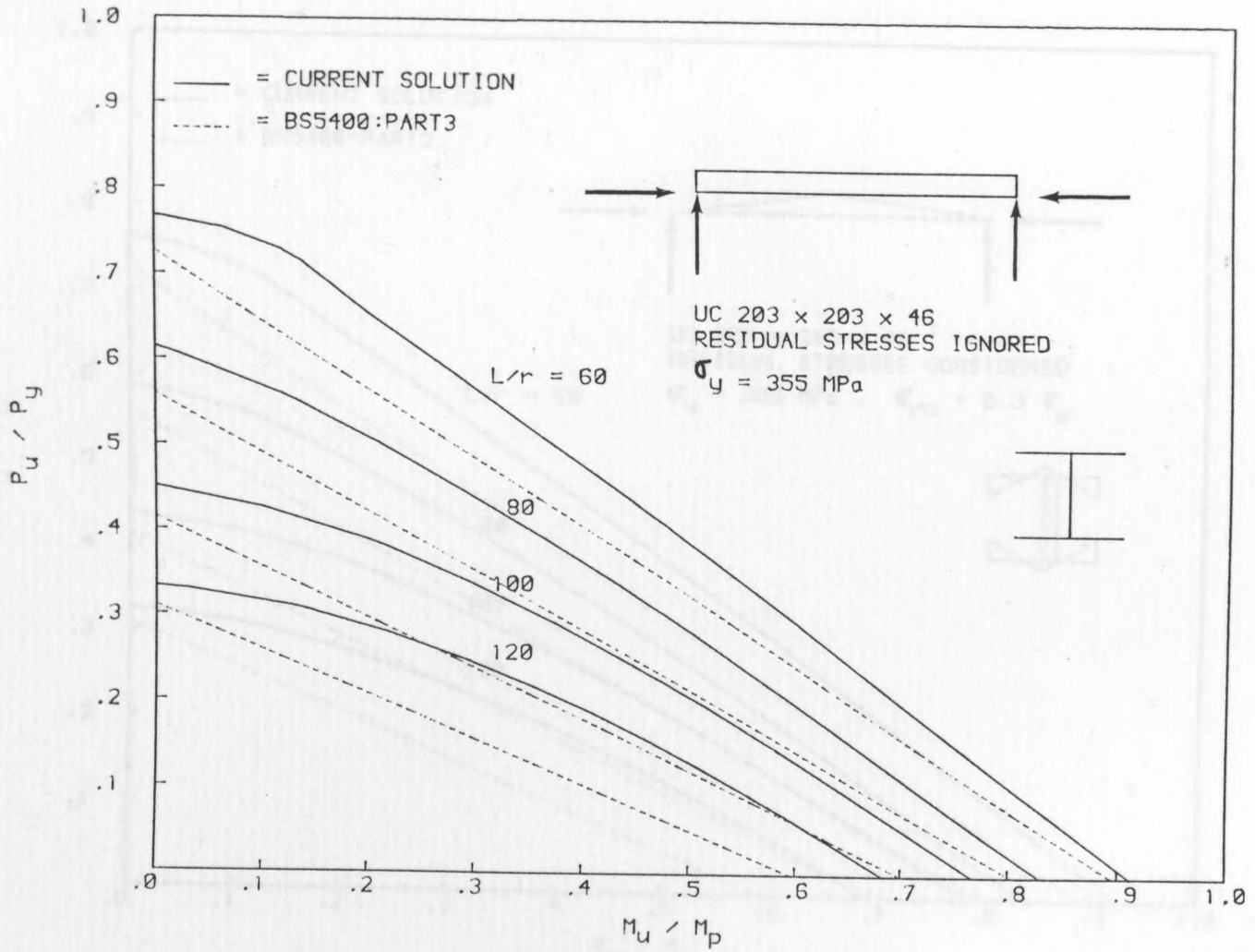

FIG. 6.6. INTERACTION CURVE OF CASE 3

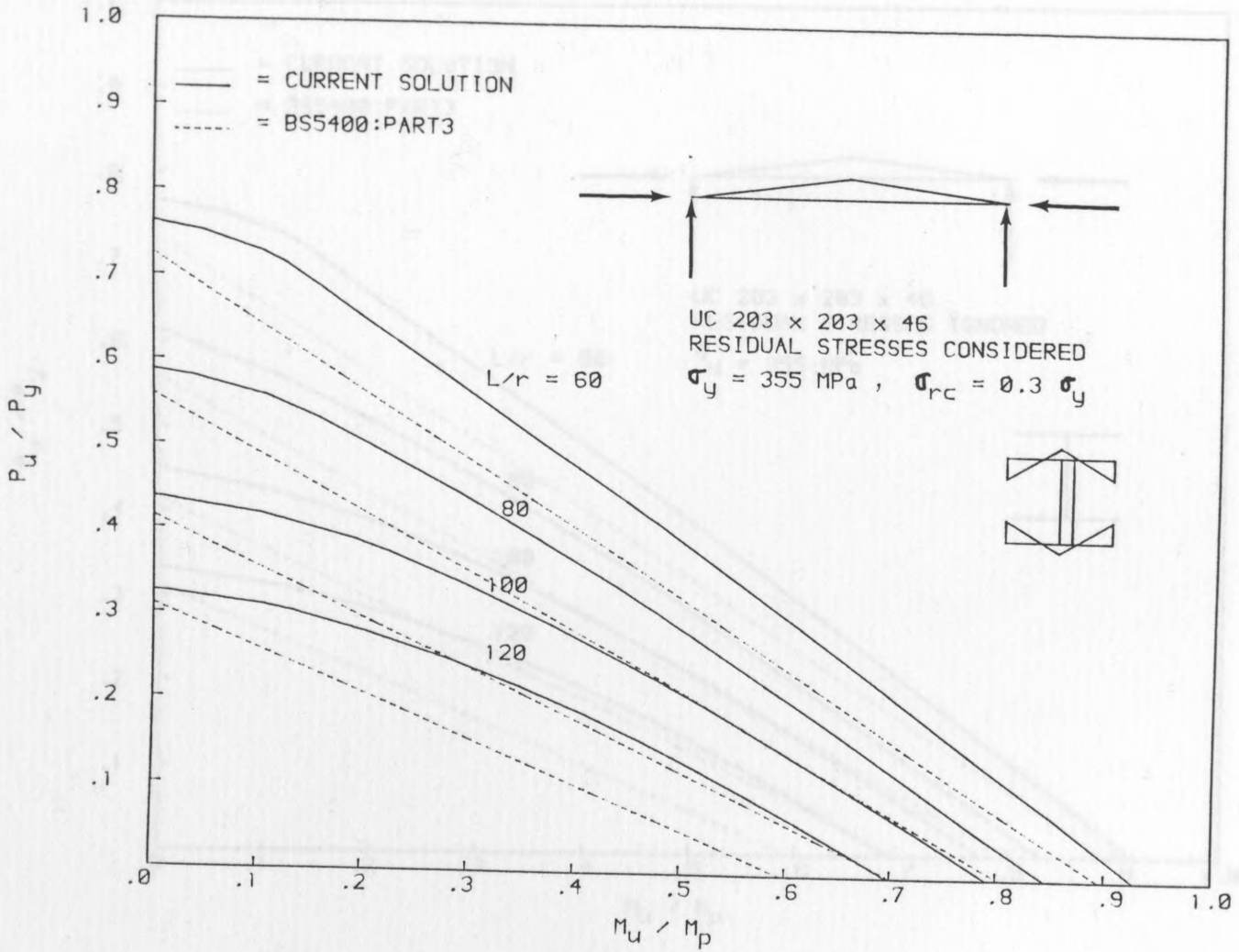

FIG. 6.7. INTERACTION CURVE OF CASE 4

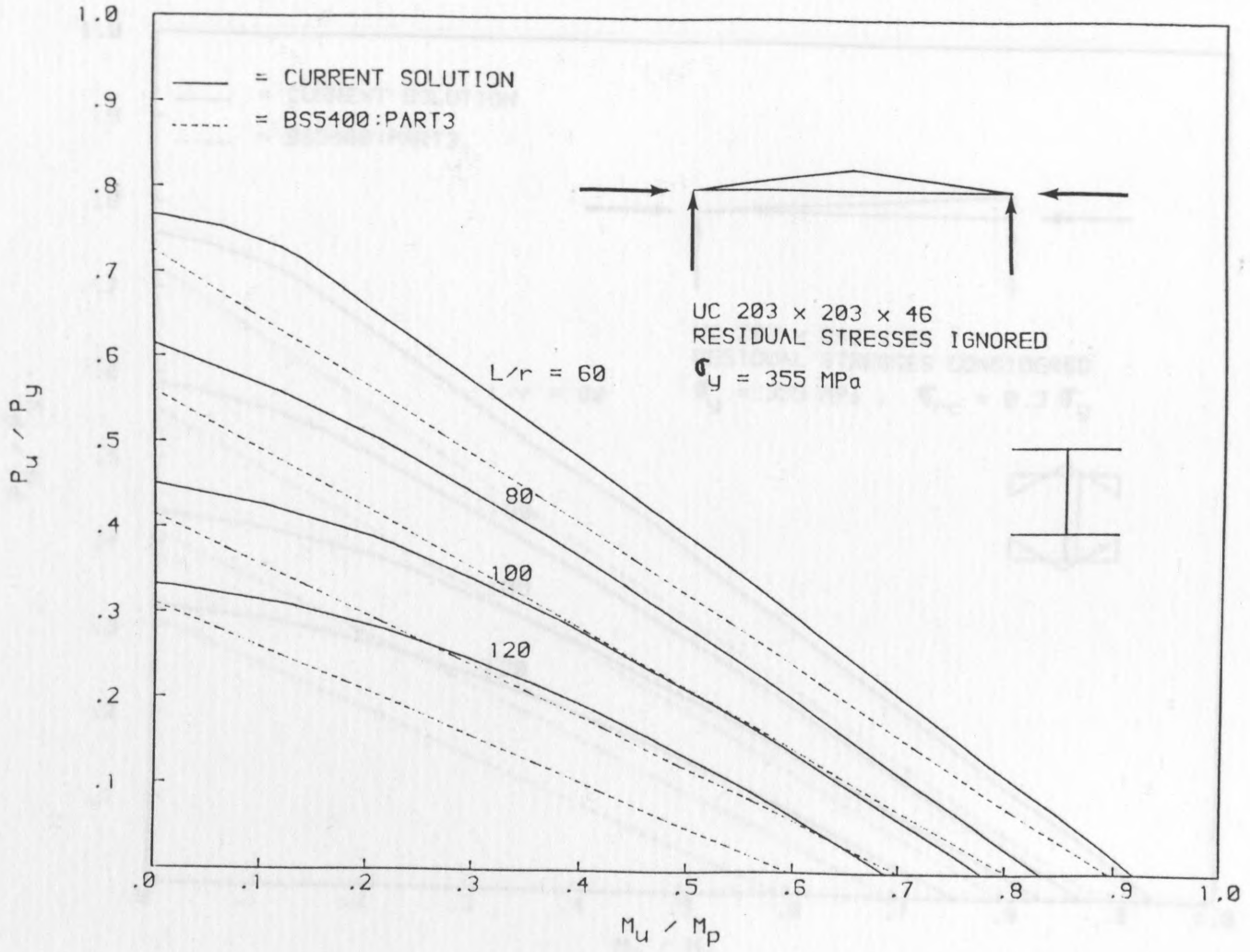

FIG. 6.8. INTERACTION CURVE OF CASE 4

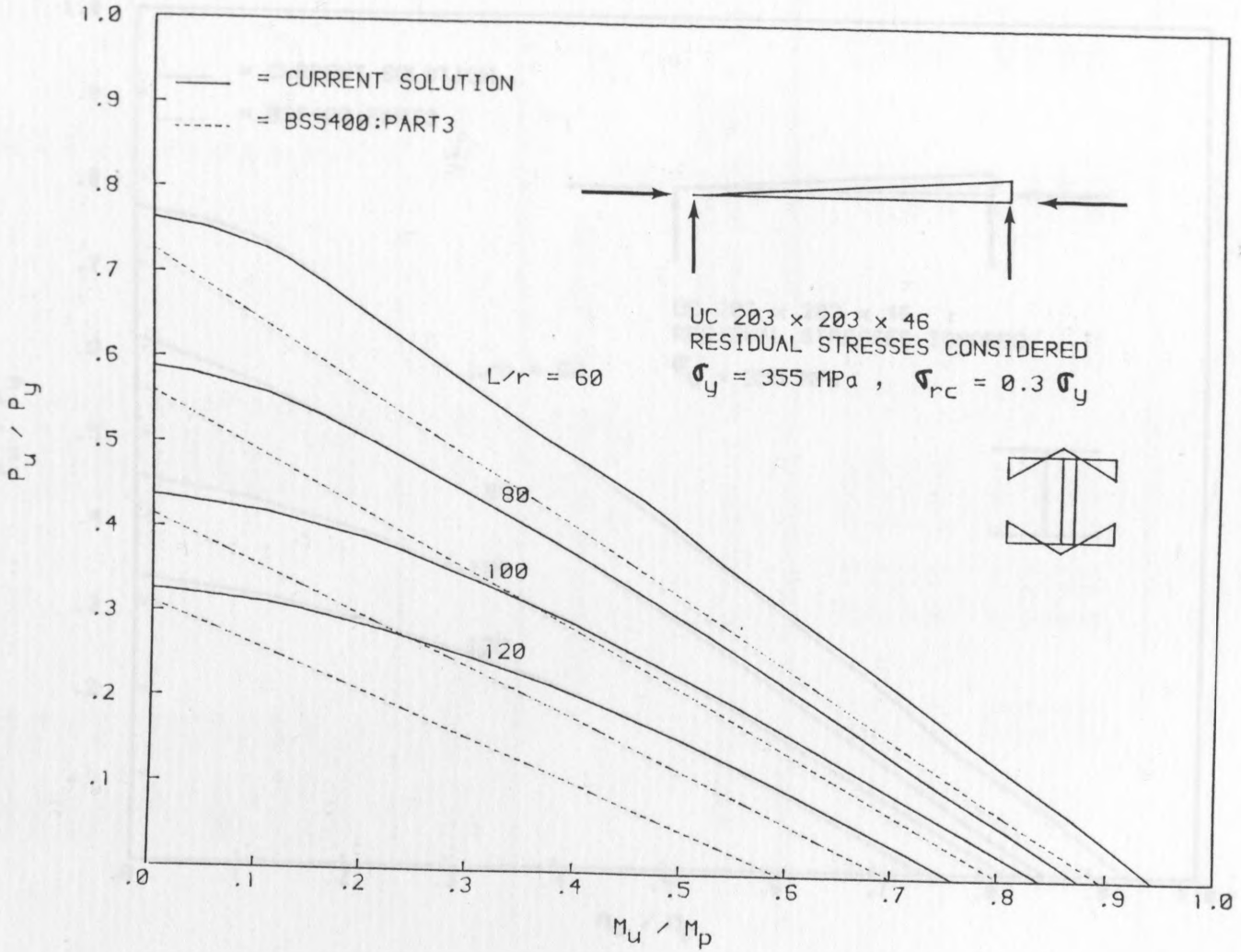

FIG. 6.9. INTERACTION CURVE OF CASE 5

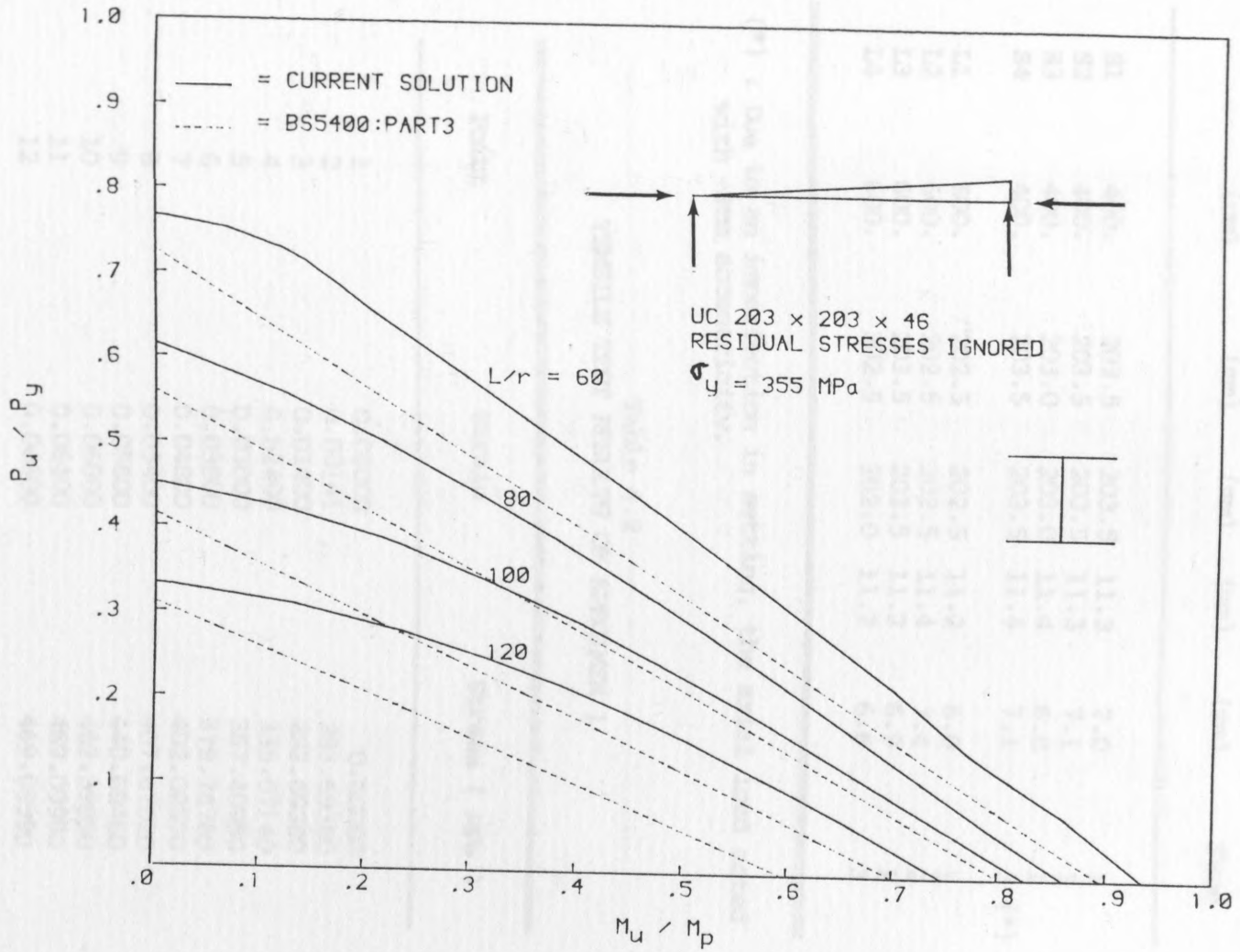

FIG. 6.10. INTERACTION CURVE OF CASE 5

Table 4.1
DETAILS OF SPECIMEN PROPERTIES AND LOADINGS

Specimen	Length (cm)	d (mm)	b (mm)	t_f (mm)	t_w (mm)	Loading Type
S1	400.	203.5	203.5	11.3	7.0	1
S2	400.	203.5	203.5	11.3	7.1	2
S3	400.	203.0	203.0	11.4	6.8	1
S4	400.	203.5	203.5	11.4	7.1	3 (*)
L1	600.	202.5	202.5	11.2	6.8	1
L2	600.	202.5	202.5	11.4	7.4	2
L3	600.	203.5	203.5	11.2	6.9	1
L4	600.	202.5	202.0	11.2	6.6	3

(*) : Due to an imperfection in setting, the axial load acted with -3mm eccentricity.

Table 4.2
TENSILE TEST RESULTS OF SPECIMEN 1

Point	Strain	Stress (MPa)
1	0.00000	0.00000
2	0.00141	283.69380
3	0.01400	283.69380
4	0.02400	335.07140
5	0.03000	357.40950
6	0.03800	379.74760
7	0.04800	402.08570
8	0.05400	407.67020
9	0.05600	440.60460
10	0.06000	462.39850
11	0.06400	469.09990
12	0.06600	469.09990

Table 4.3
TENSILE TEST RESULTS OF SPECIMEN 2

Point	Strain	Stress (MPa)
1	0.00000	0.00000
2	0.00150	332.78110
3	0.00900	332.78110
4	0.01600	342.28910
5	0.02000	370.81320
6	0.02200	380.32120
7	0.02600	399.33730
8	0.03200	418.35340
9	0.04600	456.38550
10	0.05400	475.40150
11	0.06000	486.81130
12	0.06600	486.81130

Table 4.4
TENSILE TEST RESULTS OF SPECIMEN 3

Point	Strain	Stress, in MPa
1	0.00000	0.00000
2	0.00150	330.44800
3	0.01000	330.44800
4	0.01800	376.34360
5	0.02000	385.52270
6	0.02400	403.88090
7	0.03600	440.59730
8	0.05400	468.13470
9	0.05600	486.49300

Table 5.1
COMPARISON OF RESULTS
WITH CULVER'S, THURLIMANN'S AND DABROWSKI'S RESULTS
PROBLEM 1

Load Kips	Current Results	Thurlimann [14]		Dabrowski [15]		Culver [12]	
	(a) Maximum Deflection - u						
	(in)	(in)	(*)	(in)	(*)	(in)	(*)
10.	0.0600	0.0595	0.992	0.0600	1.000	0.0600	1.000
20.	0.1212	0.1215	1.002	0.1213	1.001	0.1212	1.000
30.	0.1838	0.1835	0.998	0.1838	1.000	0.1837	0.999
40.	0.2477	0.2470	0.997	0.2476	1.000	0.2476	1.000
50.	0.3129	0.3130	1.000	0.3129	1.000	0.3128	1.000
	(b) Maximum Deflection - v						
	(in)	(in)	(*)	(in)	(*)	(in)	(*)
10.	0.0063	0.0065	1.032	0.0063	1.000	0.0063	1.000
20.	0.0127	0.0130	1.024	0.0125	0.984	0.0125	0.984
30.	0.0191	0.0185	0.969	0.0188	0.984	0.0188	0.984
40.	0.0255	0.0250	0.980	0.0251	0.984	0.0251	0.984
50.	0.0319	0.0315	0.987	0.0315	0.987	0.0314	0.984
	(c) Maximum Twist-Angle						
	(rad)	(rad)	(*)	(rad)	(*)	(rad)	(*)
10.	0.00004	0.00005	1.250	0.00005	1.250	0.00005	1.25
20.	0.00019	0.00019	1.000	0.00020	1.053	0.00020	1.05
30.	0.00044	0.00044	1.000	0.00045	1.023	0.00045	1.02
40.	0.00079	0.00079	1.000	0.00082	1.038	0.00080	1.01
50.	0.00125	0.00126	1.008	0.00130	1.040	0.00130	1.04

(*) : relative to the current results

Table 5.2
COMPARISON OF RESULTS
WITH CULVER'S, THURLIMAN'S AND DABROWSKI'S RESULTS
PROBLEM 2

Load Kips	Current Results	Thurlimann [14]		Dabrowski [15]		Culver [12]	
	(in)	(in)	(*)	(in)	(*)	(in)	(*)
(a) Maximum Deflection - u							
10.	0.3422	0.3427	1.001	0.0314	0.092	0.3420	0.999
20.	0.7276	0.7279	1.000	0.7259	0.998	0.7267	0.999
30.	1.1662	1.1690	1.002	1.1597	0.994	1.1642	0.998
40.	1.6717	1.6653	0.996	1.6594	0.993	1.6683	0.998
50.	2.2624	2.2704	1.004	2.2473	0.993	2.2579	0.998
(b) Maximum Deflection - v							
10.	0.0348	0.0340	0.977	0.0342	0.983	0.0342	0.983
20.	0.0698	0.0688	0.986	0.0686	0.983	0.0686	0.983
30.	0.1049	0.1028	0.980	0.1015	0.968	0.1031	0.983
40.	0.1395	0.1388	0.995	0.1374	0.985	0.1373	0.984
50.	0.1731	0.1716	0.991	0.1739	1.005	0.1710	0.988
(c) Maximum Twist-Angle							
	(rad)	(rad)	(*)	(rad)	(*)	(rad)	(*)
10.	0.00080	0.00075	0.938	0.00077	0.962	0.00076	0.95
20.	0.00337	0.00326	0.967	0.00335	0.994	0.00324	0.96
30.	0.00801	0.00806	1.006	0.00823	1.027	0.00818	1.02
40.	0.01514	0.01568	1.036	0.01611	1.064	0.01602	1.06
50.	0.02536	0.02750	1.084	0.02800	1.104	0.02780	1.10

(*) : relative to the current results

Table 5.3

DETAILS OF TESTS REPORTED BY BIRNSTIEL [29]

Size of Column Specimens and Eccentricities of Loading

Specimen number	Nominal size of column (in)	Length of column (ksi)	Yield stress of material	Eccentricities of Loading (in)			
				e_{ox}	e_{lx}	e_{oy}	e_{ly}
1	6 x 6H	96.0	33	1.61	1.61	2.78	2.78
2	5 x 5H	96.0	36	1.60	1.60	3.21	3.21
3	5 x 5H	120.0	36	0.80	0.80	2.63	2.63
4	6 x 6H	96.0	36	1.66	1.66	2.95	2.95
5	5 x 5H	96.0	36	2.36	2.36	3.17	3.17
6	5 x 5H	120.0	36	2.38	2.38	2.51	2.51
7	5 x 6WF	96.0	36	0.89	0.89	2.82	2.82
8	5 x 6WF	96.0	36	0.34	0.34	1.87	1.87
10	4 x 8WF	96.0	36	0.19	0.19	2.60	2.60
12	5 x 5H	120.0	36	0.77	0.77	2.78	2.78
13	4 x 4H	120.0	65	0.42	0.42	2.72	2.72
14	4 x 4H	120.0	65	0.83	0.83	2.35	2.35

Table 5.4

DETAILS OF TEST REPORTED BY BIRNSTIEL [29]

Cross-Sectional Dimensions of Column Specimens

Specimen number	Nominal size	Average Dimensions of Cross Section at Midheight (in)			
		Flange width	Flange Thickness	Depth	Web Thickness
1	6 x 6H	6.01	0.60	6.01	0.51
2	5 x 5H	5.10	0.42	5.13	0.29
3	5 x 5H	5.11	0.42	5.13	0.28
4	6 x 6H	6.11	0.45	6.45	0.33
5	5 x 5H	5.00	0.51	5.01	0.41
6	5 x 5H	5.02	0.51	5.02	0.41
7	5 x 6WF	5.01	0.48	6.29	0.33
8	5 x 6WF	5.01	0.47	6.28	0.35
10	4 x 8WF	4.00	0.45	8.00	0.34
12	5 x 5H	5.04	0.42	5.02	0.29
13	4 x 4H	4.01	0.35	4.12	0.30
14	4 x 4H	4.01	0.35	4.12	0.30

Table 5.5
COMPARISON OF RESULTS WITH PREVIOUSLY PUBLISHED RESULTS
Ultimate Loads (Kips)

No.	Experiment Birnstiel [29]	Harstead et al. [28]	Sharma and Gaylord [35]	Syal and Sharma [59]	Chen and Atsuta [60]	Current Results
1	92.80	92.80	93.40	93.10	102.70	92.50
2	54.10	52.60	49.90	50.75	49.40	51.41
3	62.70	62.80	58.30	60.84	55.30	59.84
4	86.30	83.30	83.60	84.35	84.90	82.82
5	49.60	52.70	51.40	50.20	46.20	53.01
6	47.90	49.40	49.20	47.76	39.60	49.41
7	76.60	79.30	70.40	80.16	75.70	81.72
8	109.40	110.30	98.00	110.10	110.60	112.73
10	85.00	80.50	75.70	78.70	79.50	76.22
12	51.00	55.70	51.50	56.23	53.30	56.24
13	46.10	45.00	42.70	47.24	45.60	43.59
14	38.70	41.20	37.20	40.12	44.10	38.13

Table 5.6
COMPARISON OF RESULTS WITH PREVIOUSLY PUBLISHED RESULTS
Ultimate Loads (Relative to the Current Results)

No.	Experiment Birnstiel [29]	Harstead et al. [28]	Sharma and Gaylord [35]	Syal and Sharma [59]	Chen and Atsuta [60]	Current Results
1	1.003	1.003	1.010	1.006	1.110	1.000
2	1.052	1.023	0.971	0.987	0.961	1.000
3	1.048	1.049	0.974	1.017	0.924	1.000
4	1.042	1.006	1.009	1.018	1.025	1.000
5	0.936	0.994	0.970	0.947	0.872	1.000
6	0.969	1.000	0.996	0.967	0.801	1.000
7	0.937	0.970	0.861	0.981	0.926	1.000
8	0.970	0.978	0.869	0.977	0.981	1.000
10	1.115	1.056	0.993	1.033	1.043	1.000
12	0.907	0.990	0.916	1.000	0.948	1.000
13	1.058	1.032	0.980	1.084	1.046	1.000
14	1.015	1.081	0.976	1.052	1.157	1.000

Table 5.7

STRESS-STRAIN CURVE ADOPTED BY VIRDI AND SEN [59]

Point	Curve 1 strain	Curve 1 stress (Ksi)	Curve 2 strain	Curve 2 stress (Ksi)
1	0.00000	0.00	0.00000	0.00
2	0.00130	18.00	0.00140	18.34
3	0.00160	20.50	0.00160	19.97
4	0.00181	21.75	0.00193	21.60
5	0.00197	22.40	0.00308	24.86
6	0.00230	23.70	0.00415	26.91
7	0.00258	24.60	0.00960	28.78
8	0.00415	27.75	0.01785	31.30
9	0.00725	30.00	0.02385	32.61
10	0.25000	33.80	0.25000	33.80

	Curve 3		Curve 4	
1	0.00000	0.00	0.00000	0.00
2	0.00212	29.27	0.00212	28.10
3	0.50000	29.27	0.50000	28.10

Table 5.8

DETAILS OF LOADING ADOPTED BY VIRDI AND SEN [59]

Column label	L (in)	P (tonf)	u_o (in)	v_o (in)	M_y (tonf-in)	Stress-Strain curve Flange	Web
S250	90	250	0.023	0.045	4.0	2	4
M230	123	230	0.020	0.030	4.0	1	3
M200	123	200	0.015	0.070	4.0	2	4
L200	153	200	0.000	0.077	4.0	1	1
L170	153	170	0.000	0.077	4.0	1	1
L140	153	140	0.000	0.077	4.0	1	1
L150H	153	153	0.015	0.110	0.0	1	3
L150W	153	153	0.015	0.110	0.0	1	3

Note : L150H and L150W had flexural end restraints of stiffness 20,000 tonf-in./rad and 12,000 tonf-in./rad respectively.

Table 5.9

COMPARISON OF RESULTS WITH VIRDI'S AND SEN'S [59]

COLUMN	ULTIMATE LOADS (tonf) TORSION NEGLECTED			ULTIMATE LOADS (tonf) TORSION CONSIDERED		
	VIRDI [61]	CURRENT RESULTS	(3)/(2)	SEN [61]	CURRENT RESULTS	(6)/(5)
(1)	(2)	(3)	(4)	(5)	(6)	(7)
S250	556.91	553.12	0.993	500.	518.43	1.037
M230	635.06	633.51	0.998	600.	495.23	0.825
M200	706.01	702.33	0.995	686.	579.69	0.845
L200	525.57	541.31	1.030	400.	366.02	0.915
L170	829.02	830.78	1.007	632.	570.00	0.902
L140	1022.83	1024.06	1.001	850.	755.94	0.889
L150H	1046.81	985.31	0.941	982.	960.00	0.978
L150W	1046.80	985.31	0.941	982.	950.00	0.967
		Average :	1.004			0.920
		Standard deviation :	0.014			0.071

*) L150H and L150W have minor axis flexural end restraints of stiffness 20,000 tonf-in/rad and 12,000 tonf-in/rad respectively.

Table 5.10

COMPARISON OF RESULTS WITH HO'S [46]

P/P_y

$\frac{M_o}{M_y}$	Ho [46]	Current Results	(3)/(2)
(1)	(2)	(3)	(4)
	$\bar{q} = 2.5$		
0.0	0.40	0.40	1.000
0.1	0.38	0.38	1.000
0.2	0.35	0.36	1.029
0.3	0.34	0.33	0.971
0.4	0.31	0.30	0.968
0.5	0.29	0.27	0.931
0.6	0.26	0.25	0.962
0.7	0.24	0.22	0.917
	$\bar{q} = 0.$		
0.0	0.92	0.90	0.978
0.1	0.85	0.87	1.024
0.2	0.78	0.76	0.974
0.3	0.69	0.69	1.000
0.4	0.62	0.61	0.984
0.5	0.55	0.54	0.982
0.6	0.49	0.45	0.918
0.7	0.42	0.38	0.905
		Average value :	0.972
		Standard deviation :	0.037

Table 5.11

COMPARISON OF THE EXPERIMENTAL AND THEORETICAL RESULTS

FAILURE LOADS (KN)

SPECIMEN	CASE A	CASE B	CASE C	CASE D	TEST	(6)/(2)
(1)	(2)	(3)	(4)	(5)	(6)	(7)
S1	1166.2	1156.9	991.6	989.7	1185.	1.016
S2	1447.5	1435.6	1259.8	1209.2	1570.	1.085
S3	1501.3	1463.8	1204.4	1185.6	1520.	1.012
S4	1137.2	1134.1	1313.8	1307.5	1495.	1.315
L1	935.0	860.0	592.8	581.9	1010.	1.080
L2	1320.0	1120.0	746.2	725.1	1270.	0.962
L3	1020.0	1045.0	714.9	705.5	1120.	1.098
L4	832.7	817.8	745.9	728.0	860.	1.033
			Average value			: 1.075
			Standard deviation			: 0.107

Table 6.1

RESULTS OF CASE 1

$\frac{L}{r}$	BS5400	$\frac{P}{P_y}$	$\frac{P_r}{P_y}$	$\frac{(3)}{(2)}$	$\frac{(4)}{(2)}$
(1)	(2)	(3)	(4)	(5)	(6)
30	.927	.958	.934	1.033	1.008
40	.870	.925	.894	1.063	1.028
50	.804	.867	.838	1.078	1.042
60	.727	.792	.763	1.089	1.050
70	.644	.707	.674	1.098	1.047
80	.560	.615	.588	1.098	1.050
90	.482	.527	.508	1.093	1.054
100	.415	.451	.437	1.087	1.053
110	.359	.386	.377	1.075	1.050
120	.311	.333	.326	1.071	1.048
130	.272	.289	.284	1.063	1.044
140	.239	.253	.249	1.059	1.042
150	.212	.223	.220	1.052	1.038
160	.189	.198	.195	1.048	1.032
170	.169	.177	.175	1.047	1.036
180	.152	.159	.157	1.046	1.033
190	.138	.144	.142	1.044	1.029
200	.125	.130	.129	1.040	1.032
		Average value :		1.0639	1.0398
		Standard deviation :		0.0204	0.0116

Table 6.2
RESULTS OF CASES 2-5
Ultmate Moment (M_u/M_p)
L/r = 60
Residual Stresses Ignored

$\frac{P}{P_y}$	CASE 2	CASE 3	CASE 4	CASE 5
0.000	0.951	0.911	0.919	0.934
0.073	0.895	0.834	0.844	0.860
0.146	0.817	0.755	0.764	0.770
0.219	0.734	0.676	0.685	0.698
0.292	0.650	0.598	0.605	0.616
0.365	0.567	0.518	0.526	0.535
0.438	0.482	0.439	0.445	0.453
0.510	0.397	0.359	0.364	0.371
0.584	0.313	0.279	0.283	0.288
0.656	0.226	0.198	0.202	0.205
0.729	0.134	0.117	0.119	0.121
0.763	0.000	0.000	0.000	0.000

Table 6.3
RESULTS OF CASES 2-5
Ultmate Moment (M_u/M_p)
L/r = 60
Residual Stresses Considered

$\frac{P}{P_y}$	CASE 2	CASE 3	CASE 4	CASE 5
0.000	0.955	0.920	0.927	0.943
0.073	0.897	0.843	0.851	0.867
0.146	0.819	0.762	0.770	0.784
0.219	0.734	0.681	0.689	0.702
0.292	0.647	0.600	0.608	0.618
0.365	0.561	0.518	0.525	0.533
0.438	0.475	0.436	0.442	0.459
0.510	0.389	0.354	0.359	0.365
0.584	0.303	0.273	0.277	0.281
0.656	0.215	0.191	0.194	0.198
0.729	0.116	0.103	0.104	0.106
0.763	0.000	0.000	0.000	0.000

Table 6.4
RESULTS OF CASES 2-5
Ultmate Moment (M_u/M_p)
L/r = 80
Residual Stresses Ignored

$\frac{P}{P_y}$	CASE 2	CASE 3	CASE 4	CASE 5
0.000	0.901	0.829	0.832	0.861
0.056	0.837	0.764	0.770	0.792
0.112	0.769	0.699	0.703	0.725
0.168	0.701	0.633	0.637	0.656
0.224	0.631	0.566	0.571	0.588
0.280	0.560	0.500	0.504	0.519
0.336	0.487	0.431	0.436	0.447
0.391	0.411	0.361	0.365	0.375
0.447	0.330	0.286	0.289	0.297
0.503	0.241	0.208	0.209	0.214
0.559	0.141	0.120	0.117	0.120
0.615	0.000	0.000	0.000	0.000

Table 6.5
RESULTS OF CASES 2-5
Ultmate Moment (M_u/M_p)
$L/r = 80$
Residual Stresses Considered

$\frac{P}{P_y}$	CASE 2	CASE 3	CASE 4	CASE 5
0.000	0.909	0.842	0.845	0.875
0.056	0.845	0.777	0.778	0.808
0.112	0.776	0.709	0.713	0.734
0.168	0.704	0.641	0.645	0.664
0.224	0.632	0.569	0.575	0.592
0.280	0.558	0.502	0.506	0.521
0.336	0.482	0.431	0.436	0.447
0.391	0.403	0.357	0.362	0.371
0.447	0.322	0.281	0.285	0.291
0.503	0.233	0.201	0.202	0.207
0.559	0.128	0.110	0.107	0.108
0.588	0.000	0.000	0.000	0.000

Table 6.6
RESULTS OF CASES 2-5
Ultmate Moment (M_u/M_p)
L/r = 100
Residual Stresses Ignored

$\frac{P}{P_y}$	CASE 2	CASE 3	CASE 4	CASE 5
0.000	0.844	0.767	0.779	0.826
0.049	0.781	0.706	0.717	0.759
0.097	0.716	0.644	0.654	0.691
0.146	0.649	0.579	0.589	0.621
0.195	0.579	0.513	0.522	0.550
0.243	0.505	0.444	0.452	0.476
0.292	0.425	0.371	0.379	0.399
0.340	0.336	0.291	0.298	0.313
0.389	0.232	0.198	0.203	0.214
0.451	0.000	0.000	0.000	0.000

Table 6.7
RESULTS OF CASES 2-5
Ultmate Moment (M_u/M_p)
$L/r = 100$
Residual Stresses Considered

$\frac{P}{P_y}$	CASE 2	CASE 3	CASE 4	CASE 5
0.000	0.855	0.780	0.791	0.840
0.049	0.790	0.717	0.728	0.771
0.097	0.723	0.651	0.662	0.700
0.146	0.652	0.584	0.594	0.627
0.195	0.579	0.514	0.523	0.552
0.243	0.502	0.442	0.450	0.475
0.292	0.419	0.366	0.373	0.394
0.340	0.326	0.283	0.289	0.305
0.389	0.218	0.186	0.191	0.202
0.437	0.000	0.000	0.000	0.000

Table 6.8
RESULTS OF CASES 2-5
Ultmate Moment (M_u/M_p)
L/r = 120
Residual Stresses Ignored

$\frac{P}{P_y}$	CASE 2	CASE 3	CASE 4	CASE 5
0.000	0.767	0.683	0.688	0.748
0.031	0.722	0.641	0.647	0.702
0.062	0.678	0.598	0.603	0.655
0.093	0.631	0.554	0.560	0.606
0.124	0.580	0.507	0.513	0.554
0.156	0.527	0.458	0.464	0.501
0.187	0.470	0.407	0.411	0.443
0.218	0.408	0.351	0.354	0.383
0.249	0.340	0.289	0.291	0.314
0.280	0.258	0.217	0.216	0.233
0.311	0.149	0.126	0.120	0.128
0.333	0.000	0.000	0.000	0.000

Table 6.9
RESULTS OF CASES 2-5
Ultmate Moment (M_u/M_p)
$L/r = 120$
Residual Stresses Considered

$\frac{P}{P_y}$	CASE 2	CASE 3	CASE 4	CASE 5
0.000	0.779	0.691	0.697	0.759
0.031	0.732	0.648	0.653	0.711
0.062	0.683	0.603	0.608	0.660
0.093	0.632	0.555	0.561	0.609
0.124	0.578	0.501	0.512	0.555
0.156	0.523	0.455	0.460	0.499
0.187	0.464	0.401	0.405	0.438
0.218	0.399	0.342	0.345	0.374
0.249	0.327	0.278	0.279	0.302
0.280	0.243	0.203	0.202	0.219
0.311	0.130	0.110	0.104	0.111
0.326	0.000	0.000	0.000	0.000

Table 6.10

CHECKING OF RESULTS OF CASE 2

$L/r = 60$

$\frac{P}{P_D}$	$\frac{M}{M_D}$	$\frac{P}{P_D} + \frac{M}{M_D}$	$\frac{M_r}{M_D}$	$\frac{P}{P_D} + \frac{M_r}{M_D}$
0.000	1.053	1.053	1.057	1.057
0.100	0.990	1.090	0.992	1.092
0.200	0.905	1.105	0.906	1.106
0.300	0.812	1.112	0.812	1.112
0.400	0.720	1.120	0.716	1.116
0.500	0.628	1.128	0.621	1.121
0.600	0.534	1.134	0.526	1.126
0.700	0.440	1.140	0.431	1.131
0.800	0.347	1.147	0.336	1.136
0.900	0.250	1.150	0.238	1.138
1.000	0.148	1.148	0.128	1.128
Average value	:	1.120		1.115
Standard deviation	:	0.030		0.023

Table 6.11

CHECKING OF RESULTS OF CASE 3

$L/r = 60$

$\frac{P}{P_D}$	$\frac{M}{M_D}$	$\frac{P}{P_D} + \frac{M}{M_D}$	$\frac{M_r}{M_D}$	$\frac{P}{P_D} + \frac{M_r}{M_D}$
0.000	1.018	1.018	1.028	1.028
0.100	0.932	1.032	0.942	1.042
0.200	0.843	1.043	0.852	1.052
0.300	0.755	1.055	0.761	1.061
0.400	0.668	1.068	0.670	1.070
0.500	0.579	1.079	0.579	1.079
0.600	0.490	1.090	0.487	1.087
0.700	0.401	1.101	0.396	1.096
0.800	0.311	1.111	0.305	1.105
0.900	0.221	1.121	0.213	1.113
1.000	0.131	1.131	0.115	1.115
Average value	:	1.077		1.077
Standard deviation	:	0.037		0.029

Table 6.12

CHECKING OF RESULTS OF CASE 4

$L/r = 60$

$\frac{P}{P_D}$	$\frac{M}{M_D}$	$\frac{P}{P_D} + \frac{M}{M_D}$	$\frac{M_r}{M_D}$	$\frac{P}{P_D} + \frac{M_r}{M_D}$
0.000	1.028	1.028	1.036	1.036
0.100	0.943	1.043	0.951	1.051
0.200	0.853	1.053	0.861	1.061
0.300	0.766	1.066	0.770	1.070
0.400	0.677	1.077	0.679	1.079
0.500	0.587	1.087	0.587	1.087
0.600	0.498	1.098	0.494	1.094
0.700	0.407	1.107	0.402	1.102
0.800	0.317	1.117	0.310	1.110
0.900	0.225	1.125	0.217	1.117
1.000	0.133	1.133	0.117	1.117
Average value		: 1.085		1.076
Standard deviation		: 0.035		0.035

Table 6.13

CHECKING OF RESULTS OF CASE 5

$L/r = 60$

$\frac{P}{P_D}$	$\frac{M}{M_D}$	$\frac{P}{P_D} + \frac{M}{M_D}$	$\frac{M_r}{M_D}$	$\frac{P}{P_D} + \frac{M_r}{M_D}$
0.000	1.044	1.044	1.053	1.053
0.100	0.961	1.061	0.969	1.069
0.200	0.871	1.071	0.876	1.076
0.300	0.780	1.080	0.784	1.084
0.400	0.689	1.089	0.690	1.090
0.500	0.600	1.100	0.596	1.096
0.600	0.506	1.106	0.502	1.102
0.700	0.414	1.114	0.408	1.108
0.800	0.322	1.122	0.314	1.114
0.900	0.229	1.129	0.221	1.121
1.000	0.135	1.135	0.119	1.119
Average value :		1.096		1.094
Standard deviation :		0.029		0.022

Table 6.14

CHECKING OF RESULTS OF CASE 2

$L/r = 100$

$\frac{P}{P_D}$	$\frac{M}{M_D}$	$\frac{P}{P_D} + \frac{M}{M_D}$	$\frac{M_r}{M_D}$	$\frac{P}{P_D} + \frac{M_r}{M_D}$
0.000	1.116	1.116	1.130	1.130
0.117	1.033	1.150	1.044	1.161
0.234	0.947	1.181	0.955	1.190
0.352	0.857	1.209	0.862	1.213
0.469	0.766	1.235	0.765	1.234
0.586	0.668	1.254	0.664	1.250
0.703	0.562	1.265	0.553	1.256
0.820	0.444	1.264	0.431	1.251
0.937	0.307	1.244	0.288	1.225
average value :		1.213		1.212
standard deviation :		0.053		0.044

Table 6.15

CHECKING OF RESULTS OF CASE 3

$L/r = 100$

$\frac{P}{P_D}$	$\frac{M}{M_D}$	$\frac{P}{P_D} + \frac{M}{M_D}$	$\frac{M_r}{M_D}$	$\frac{P}{P_D} + \frac{M_r}{M_D}$
0.000	1.094	1.094	1.111	1.111
0.117	1.007	1.124	1.022	1.139
0.234	0.918	1.152	0.928	1.163
0.352	0.826	1.278	0.833	1.184
0.469	0.732	1.200	0.733	1.202
0.586	0.633	1.219	0.630	1.216
0.703	0.529	1.232	0.521	1.224
0.820	0.415	1.236	0.403	1.223
0.937	0.283	1.220	0.266	1.203
Average value :		1.184		1.185
Standard deviation :		0.051		0.040

Table 6.16

CHECKING OF RESULTS OF CASE 4

$L/r = 100$

$\frac{P}{P_D}$	$\frac{M}{M_D}$	$\frac{P}{P_D} + \frac{M}{M_D}$	$\frac{M_r}{M_D}$	$\frac{P}{P_D} + \frac{M_r}{M_D}$
0.000	1.112	1.112	1.130	1.130
0.117	1.025	1.142	1.039	1.157
0.234	0.935	1.169	0.945	1.180
0.352	0.842	1.193	0.848	1.200
0.469	0.746	1.215	0.748	1.216
0.586	0.646	1.232	0.643	1.229
0.703	0.541	1.244	0.533	1.236
0.820	0.426	1.246	0.413	1.233
0.937	0.291	1.228	0.273	1.210
Average value :		1.198		1.199
Standard deviation :		0.048		0.037

Table 6.17

CHECKING OF RESULTS OF CASE 5

$L/r = 100$

$\frac{P}{P_D}$	$\frac{M}{M_D}$	$\frac{P}{P_D} + \frac{M}{M_D}$	$\frac{M_r}{M_D}$	$\frac{P}{P_D} + \frac{M_r}{M_D}$
0.000	1.117	1.117	1.198	1.198
0.117	1.082	1.199	1.100	1.217
0.234	0.985	1.220	0.999	1.233
0.352	0.886	1.238	0.895	1.246
0.469	0.784	1.253	0.788	1.256
0.586	0.679	1.265	0.677	1.263
0.703	0.568	1.271	0.561	1.264
0.820	0.447	1.267	0.435	1.255
0.937	0.306	1.243	0.288	1.225
average value		: 1.237		1.240
standard deviation		: 0.033		0.023

Table 6.18
TORSIONAL EFFECT ON CASE 2
L/r = 60

$\frac{P}{P_y}$	$\frac{M_{tn}}{M_p}$	$\frac{M}{M_p}$	$\frac{M}{M_{tn}}$	Reduction %
0.000	0.997	0.951	0.955	4.5
0.073	0.962	0.895	0.930	7.0
0.146	0.906	0.817	0.902	9.8
0.219	0.828	0.734	0.887	11.3
0.292	0.736	0.650	0.884	11.6
0.365	0.646	0.567	0.877	12.3
0.438	0.561	0.482	0.859	14.1
0.510	0.478	0.397	0.832	16.8
0.584	0.395	0.313	0.794	20.6
0.656	0.315	0.226	0.717	28.3
0.729	0.209	0.134	0.643	35.7

Table 6.19
TORSIONAL EFFECT ON CASE 3
L/r = 60

$\frac{P}{P_y}$	$\frac{M_{tn}}{M_p}$	$\frac{M}{M_p}$	$\frac{M}{M_{tn}}$	Reduction %
0.000	0.996	0.911	0.915	8.5
0.073	0.954	0.834	0.874	12.6
0.146	0.902	0.755	0.847	15.3
0.219	0.798	0.676	0.847	15.3
0.292	0.703	0.598	0.850	14.5
0.365	0.615	0.518	0.843	15.7
0.438	0.530	0.439	0.827	17.3
0.510	0.449	0.359	0.799	20.1
0.584	0.369	0.279	0.756	24.4
0.656	0.286	0.198	0.690	31.0
0.729	0.175	0.117	0.668	33.2

Table 6.20
TORSIONAL EFFECT ON CASE 4
L/r = 60

$\frac{P}{P_y}$	$\frac{M_{tn}}{M_p}$	$\frac{M}{M_p}$	$\frac{M}{M_{tn}}$	Reduction %
0.000	0.997	0.919	0.922	7.8
0.073	0.954	0.844	0.885	11.5
0.146	0.894	0.764	0.854	14.6
0.219	0.804	0.685	0.852	14.8
0.292	0.711	0.605	0.852	14.8
0.365	0.620	0.526	0.848	15.2
0.438	0.535	0.445	0.833	16.7
0.510	0.454	0.364	0.803	19.7
0.584	0.373	0.283	0.760	24.0
0.656	0.292	0.202	0.700	30.0
0.729	0.180	0.119	0.662	33.8

Table 6.21
TORSIONAL EFFECT ON CASE 5
L/r = 60

$\frac{P}{P_y}$	$\frac{M_{tn}}{M_p}$	$\frac{M}{M_p}$	$\frac{M}{M_{tn}}$	Reduction %
0.000	0.999	0.934	0.935	6.5
0.073	0.953	0.860	0.902	9.8
0.146	0.861	0.780	0.906	9.4
0.219	0.803	0.698	0.870	13.0
0.292	0.707	0.616	0.872	12.8
0.365	0.619	0.535	0.865	13.5
0.438	0.534	0.453	0.848	15.2
0.510	0.452	0.371	0.820	18.0
0.584	0.372	0.288	0.774	22.6
0.656	0.291	0.205	0.705	29.5
0.729	0.178	0.121	0.677	32.3

Table 6.22
TORSIONAL EFFECT ON CASE 2
L/r = 100

$\frac{P}{P_y}$	$\frac{M_{tn}}{M_p}$	$\frac{M}{M_p}$	$\frac{M}{M_{tn}}$	Reduction %
0.000	0.996	0.844	0.847	15.3
0.049	0.950	0.781	0.822	17.8
0.097	0.900	0.716	0.795	20.5
0.146	0.845	0.649	0.767	23.3
0.195	0.776	0.579	0.746	25.4
0.243	0.704	0.505	0.718	28.2
0.292	0.622	0.425	0.683	31.7
0.340	0.508	0.336	0.662	33.8
0.389	0.349	0.232	0.665	33.5

Table 6.23
TORSIONAL EFFECT ON CASE 3
L/r = 100

$\frac{P}{P_y}$	$\frac{M_{tn}}{M_p}$	$\frac{M}{M_p}$	$\frac{M}{M_{tn}}$	Reduction %
0.000	0.997	0.767	0.770	23.0
0.049	0.938	0.706	0.755	24.5
0.097	0.880	0.644	0.731	26.9
0.146	0.808	0.579	0.716	28.4
0.195	0.730	0.513	0.703	29.7
0.243	0.649	0.444	0.684	31.6
0.292	0.552	0.371	0.673	32.7
0.340	0.435	0.291	0.669	33.1
0.389	0.293	0.198	0.678	32.2

Table 6.24
TORSIONAL EFFECT ON CASE 4
L/r = 100

$\frac{P}{P_y}$	$\frac{M_{tn}}{M_p}$	$\frac{M}{M_p}$	$\frac{M}{M_{tn}}$	Reduction %
0.000	0.997	0.779	0.781	21.9
0.049	0.941	0.717	0.762	23.8
0.097	0.884	0.654	0.740	26.0
0.146	0.816	0.589	0.722	27.8
0.195	0.738	0.522	0.707	29.3
0.243	0.659	0.452	0.686	31.4
0.292	0.562	0.379	0.673	32.7
0.340	0.446	0.298	0.668	33.2
0.389	0.300	0.203	0.678	32.2

Table 6.25
TORSIONAL EFFECT ON CASE 5
L/r = 100

$\frac{P}{P_y}$	$\frac{M_{tn}}{M_p}$	$\frac{M}{M_p}$	$\frac{M}{M_{tn}}$	Reduction %
0.000	0.998	0.826	0.827	19.3
0.049	0.941	0.759	0.806	19.4
0.097	0.883	0.691	0.782	21.8
0.146	0.814	0.621	0.763	23.7
0.195	0.736	0.550	0.747	25.3
0.243	0.657	0.476	0.725	27.5
0.292	0.560	0.399	0.712	28.8
0.340	0.443	0.313	0.707	29.3
0.389	0.299	0.214	0.717	28.3

Table 6.26

STRENGTH REDUCTION DUE TO LACK OF STRAIGHTNESS

(%)

Maximum Bow	S1 L/r = 78	L3 L/r = 117
L/20,000	1.6	16.2
L/10,000	2.4	17.4
L/5,000	3.9	19.5
L/1,000	15.0	29.9

Table 6.27
COMPARISON OF THE RESULTS
OBTAINED WITH DIFFERENT INITIAL BOW
LOADING CASE 1, RESIDUAL STRESSES CONSIDERED

Slenderness ratio	u_{o1} (cm)	$\frac{P_1}{P_y}$	u_{o2} (cm)	$\frac{P_2}{P_y}$	$\frac{(3)}{(5)}$
(1)	(2)	(3)	(4)	(5)	(6)
30	0.235	0.934	0.176	0.944	0.989
40	0.314	0.894	0.294	0.898	0.996
50	0.392	0.838	0.412	0.833	1.006
60	0.471	0.763	0.529	0.750	1.017
70	0.549	0.674	0.647	0.655	1.029
80	0.627	0.588	0.765	0.566	1.039
90	0.706	0.508	0.882	0.487	1.043
100	0.784	0.437	1.000	0.418	1.045
110	0.863	0.377	1.118	0.360	1.047
120	0.941	0.326	1.235	0.312	1.045
130	1.020	0.284	1.353	0.273	1.040
140	1.098	0.249	1.471	0.240	1.038
150	1.177	0.220	1.588	0.212	1.038
160	1.255	0.195	1.706	0.189	1.032
170	1.333	0.175	1.824	0.169	1.036
180	1.412	0.157	1.941	0.152	1.033
190	1.490	0.142	2.059	0.137	1.036
200	1.569	0.129	2.177	0.125	1.032
				Average value :	1.030
				Standard deviation :	0.017

Note : u_{o1} initial bow in accordance with BS153.

u_{o2} initial bow in accordance with BS5400.

P_1 and P_2 are the computed results, corresponding to u_{o1} and u_{o2}, respectively.